

Magnus Mar Gudnason
s072205

Characterization of Potassium Nitrate - Sugar Alcohol Based Solid Rocket Propellants

Bachelor Thesis, August 2010

Magnus Mar Gudnason
s072205

Characterization of Potassium Nitrate - Sugar Alcohol Based Solid Rocket Propellants

Bachelor Thesis, August 2010

This report was prepared by

Magnus Mar Gudnason
s072205

Supervisor

Niels Bjerrum

Department of Chemistry
Kemitorvet
Technical University of Denmark
Building 207
DK-2800 Kgs. Lyngby
Denmark

www.kemi.dtu.dk

Tel: (+45) 45 25 24 19

Fax: (+45) 45 88 31 36

E-mail: isc@kemi.dtu.dk

Release date: July 1st 2010

Category: 1 (public)

Edition: First

Comments: This report is part of the requirements to achieve the Bachelor of Science in Engineering (B.Sc.Eng.) at the Technical University of Denmark. This report represents 20 ECTS points.

Rights: ©Magnus Mar Gudnason, 2010

Acknowledgements

I wish to take this opportunity to express my gratitude to my supervisor Dr. Niels I. Bjerrum for giving me the opportunity of working at this project.

Special thanks for always helping out goes to the laboratory assistant Claus Burke Mortensen and Steen Blichfeldt.

I would specially like to thank Richard Nakka for his contribution to the field of experimental rocketry and the motivation that lead to this project.

I would like to thank

- Scott Fintel for his work on KN-Erythritol propellant and his support and encouragement.
- the members of Danish Amateur Rocketry Club (DARK) for their help and especially Hans Olaf Toft for his help with the data acquisition system and Henrik Nissen for supplying a burst disc and help with hydrostatic testing of the firing vessel.
- CCP (Developer of EVE-Online) for their support and a fund of 50.000 ISK.
- Kevin Swingler of Incite Technology Ltd. at Stirling University for his contribution of one Linux USBDUX-fast DAQ board for data recording.
- Gunnar Ingi at Malmtaekni for supplying polycarbonate and polyethylene plates.
- Sonja Hansen at Cargill for supplying free samples of sugar alcohols.

Preface

This thesis is submitted as partial fulfillment of the requirements for a degree of Bachelor of Science in Engineering (B.Sc.Eng.) at the Technical University of Denmark. This report represent 20 ECTS points. It was written by Magnus Mar Gudnason under the supervision of professor Niels J. Bjerrum.

The thesis is based upon studies conducted during March 2010 to August 2010 at the Department of Chemistry, Technical University of Denmark.

Abstract

Standard KN-Sorbitol, KN-Erythritol and KN-Mannitol propellants with 65/35 oxidizer/fuel ratio were casted into 8x8x100 mm sized strands for strand burner tests at pressures of 0 to 10 MPa. The use of a pressure relief valve for release of combustion gases was studied. Burn rate coefficient a and pressure exponent n for KN-Sorbitol, KN-Erythritol and KN-Mannitol solid propellants were determined as 5.132 mm/s/MPa and 0.222, 2.903 mm/s/MPa and 0.395, and 5.126 mm/s/MPa and 0.224, respectively.

The primary objective of these studies is to provide information on the burning rate of sugar alcohol propellants. The report presents a design and structure of a strand burner, raw data and a method of calculations for burning rate.

Nomenclature

χ	Mass fraction, page 20
\dot{m}	Mass flow rate of exhaust gases, page 8
γ	Specific heat ratio, page 8
γ_{2ph}	Ratio of specific heat capacities of two phase flow products, page 20
γ_{gas}	Ratio of specific heat capacities of gaseous products, page 20
γ_{mix}	Ratio of specific heat capacities of mixed (gaseous + condensed) products, page 20
ψ	Mass fraction relation $\chi/(1-\chi)$, page 20
ρ_P	Propellant density, page 13
v_e	Exhaust velocity, page 8
A	Surface area, page 9
a	Burn rate coefficient, page 14
A_b	Burning area of propellant, page 13
A_e	Cross-sectional area at the exit plane of nozzle, page 9
A_t	Cross-sectional area at nozzle throat, page 9
c^*	Characteristic velocity, page 10
C_F	Thrust coefficient, page 9
C_P	Specific heat capacity, page 20
C_S	Specific heat capacity of a solid, page 20

$C_{P,gas}$	Specific heat capacity of a gas, page 20
F	Thrust, page 8
g	Gravitational force, page 11
I_t	Total impulse, page 11
I_{sp}	Specific impulse, page 11
Kn	Ratio of propellant burning area to nozzle cross-sectional throat area, page 14
M	Mean (effective) molecular weight of exhaust gases, page 8
m	Mass, page 13
m_{mix}	Mass of propellant mix, page 20
n	Burn rate pressure exponent, page 14
n_s	Number of moles of condensed component, page 20
n_{gas}	Number of gas moles, page 19
P	Pressure, page 9
P_a	Ambient pressure, page 8
P_c	Chamber pressure, page 8
P_e	Pressure at the exit plane of the nozzle, page 8
R	Universal gas constant, page 8
r	Burning rate of propellant, page 13
T_c	Temperature in the combustion chamber, page 8
V_c	Free volume within a combustion chamber, page 15
w_p	Total weight of propellant, page 11

Contents

Nomenclature	v
List of Figures	xiii
List of Tables	xviii
1 Introduction	1
2 Background	3
2.1 Motivation	3
2.2 Objectives	3
2.3 Former studies	4
2.3.1 History of sugar propellant	4
3 Definition and fundamentals of rocket propulsion	7
3.1 Basic assumptions of an ideal rocket	7
3.2 Thermodynamic relations	8
3.2.1 Exhaust velocity	8
3.2.2 Thrust	8
3.2.3 Thrust coefficient	9
3.2.4 Characteristic velocity	10
3.2.5 Total and specific impulse	11

4	Burning rate of solid propellant	13
4.1	Pressure sensitivity of burning rate	13
4.1.1	Mass flow rate	13
4.1.2	Burning rate	13
4.1.3	Steady-state chamber pressure	14
4.2	Empirical determination of burning rate	15
4.2.1	Crawford strand burner	15
4.2.2	Ballistic evaluation motor	16
4.2.3	Full-scale motor	16
5	Chemistry and combustion of sugar rocket propellants	17
5.1	Sugar chemistry	17
5.2	Combustion	19
6	Apparatus and experimental preparation	21
6.1	Preparation of propellant	21
6.1.1	Propellant mixes	21
6.1.2	Casting mold	22
6.1.3	Casting procedure	23
6.1.4	Propellant strands	25
6.2	Strand Burner	27
6.2.1	Firing vessel	29
6.2.2	Strand holder	30
6.2.3	Fill and exhaust line	32
6.2.4	Structural frame	36
6.3	Electronic devices	37
6.3.1	Ignition box	37
6.3.2	Burning rate measurement	37
6.3.3	Data recording and acquisition	37
6.4	Experimental Technique	39

6.5	Analysis	39
7	Experimental results	41
8	Performance estimation of solid rocket motors	49
8.1	Ideal performance	49
8.2	Comparison of a rocket motor performance	50
8.3	Comparison of burning rate	51
9	Discussion	53
9.1	Technical obstacles	54
9.1.1	Casting mold	54
9.1.2	Ignition of strands	54
9.1.3	Inhibiting of propellant strands	54
10	Conclusion	55
10.1	Conclusions	55
10.2	Contribution	55
10.3	Future work	56
	References	57
	Appendix	A-1
A	Matlab scripts and functions	A-1
A.1	Power law fitting	A-1
A.2	Experimental data analysis	A-3
A.3	Combustion of sugar rocket propellant	A-6
A.4	Ideal performance calculations	A-9
A.5	Pressure-time trace	A-14
B	Particle distribution	B-1

C Propellant batches	C-1
C.1 KN-Sorbitol propellant batches	C-1
C.2 KN-Erythritol propellant batches	C-1
C.3 KN-Mannitol propellant batches	C-2
D Propellant Density	D-1
D.1 Example	D-2
E Ideal performance calculations using PROPEP	E-1
E.1 PROPEP results	E-1
E.1.1 KN-Sorbitol ideal performace calculations	E-2
E.1.2 KN-Erythritol ideal performace calculations	E-3
E.1.3 KN-Mannitol ideal performace calculations	E-4
F Propellant strand burns	F-1
F.1 Analysis of KN-Sorbitol strand burns	F-1
F.2 Analysis of KN-Erythritol strand burns	F-25
F.3 Analysis of KN-Mannitol strand burns	F-48

List of Figures

3.1	Schematic showing the forces acted upon the combustion chamber and the nozzle (1).	10
4.1	Dependence of burning rate as a function of pressure (6). . .	14
4.2	Burn rate evaluation motor (15).	16
5.1	Chemical structure of three sugar alcohols.	18
6.1	Sieved particles showing the particle distribution. Note that the markings indicates the particle size that was retained on each screen.	22
6.2	Polyethylene jar and ball mill.	22
6.3	PTFE casting mold with 8x8 mm grooves for propellant and M3x20 bolts for attachment to the strand holder.	23
6.4	From left to right: Casting mold prior to heating on a hot plate, PTFE coated pot with sorbitol based propellant and a multimeter for measuring mold and slurry temperature as well as relative humidity.	24
6.5	Sorbitol cooling down and curing in the casting mold.	25
6.6	From top to bottom: Strands of fully cured KN-Sorbitol, KN-Erythritol, KN-Mannitol and painted KN-Erythritol.	25
6.7	KN-Sorbitol immersed in ethanol in a burette.	26
6.8	Propellant strands prior to painting.	26

6.9	Strand burner setup.	27
6.10	Main components of the strand burner. (1) Needle valve, (2) Particle filter, (3,4) Pressure transducers, (5) Pressure gauge, (6) Proportional pressure relief valve, (7) Ball valve, (8) Structural frame, (9) Firing vessel, (10) Propellant strand, (11) Stainless steel rod.	28
6.11	Cooling system.	29
6.12	Hydraulic piston pump used for hydrostatic tests.	29
6.13	Stainless steel rods fixed in place by epoxy.	30
6.14	Strand holder where KN-Sorbitol propellant strand is fixed in place.	31
6.15	Schematic of the strand holder. (1) Stainless steel closure. (2) POM insulating disc. (3) Fixture bolt for propellant strand. (4) O-ring. (5) Propellant strand. (6) Stainless steel rod. (7) Epoxy joint.	31
6.16	Burst disc housing with nickel diaphragm.	32
6.17	Needle valve for restriction of flow rate.	32
6.18	Particle filter for stopping unwanted particles of the combustion gases. The 100 μm stainless steel element is marked as number 8.	33
6.19	Pressure transducers for recording pressure during strands firing. Particle filter in between.	33
6.20	Pressure gauge for visual inspection of firing vessel pressure.	34
6.21	Schematic of proportional relief valve and the manual override handle.	35
6.22	Ball valve for releasing of nitrogen and combustion gases.	35
6.23	Structural frame where the polycarbonate and MDF plates are connected to the aluminum strut profiles.	36
6.24	Ignition box with attached ignition lead wire.	37
6.25	Linux USB DUX-FAST DAQ board connected to an electrical housing box.	38
6.26	Electrical crocodile clips attached to the stainless steel rods.	38
6.27	KN-Erythritol. Set pressure 6 MPa.	40

7.1	Experimental results for KN-Sorbitol propellant.	43
7.2	Experimental results for KN-Erythritol propellant.	43
7.3	Experimental results for KN-Mannitol propellant.	44
7.4	Comparison of experimental results for KN-Sorbitol, KN-Erythritol and KN-Mannitol propellants.	44
7.5	Log-log plot of experimental results for KN-Sorbitol.	45
7.6	Log-log plot of experimental results for KN-Erythritol.	45
7.7	Log-log plot of experimental results for KN-Mannitol.	46
7.8	Experimental results for KN-Sorbitol with a fitted power law curve.	46
7.9	Experimental results for KN-Erythritol with a fitted power law curve.	47
7.10	Experimental results for KN-Mannitol with a fitted power law curve.	47
8.1	Comparison of recorded and ideal chamber pressure of the KN-Erythritol Globos flight motor.	50
8.2	Estimation of burn rate of KN-Erythritol Globos flight motor using the pressure-time trace method.	51
8.3	Comparison of burn rate results from strand burner and the KN-Erythritol Globos flight motor.	52
B.1	Particle distribution of potassium nitrate	B-2
B.2	Particle distribution of potassium nitrate where particle size is shown as the log of the particle size.	B-2
E.1	Propep results for KN-Sorbitol propellant.	E-2
E.2	Propep results for KN-Erythritol propellant.	E-3
E.3	Propep results for KN-Mannitol propellant.	E-4
F.1	KN-Sorbitol. Set pressure 10 MPa.	F-2
F.2	KN-Sorbitol. Set pressure 10 MPa.	F-3
F.3	KN-Sorbitol. Set pressure 9 MPa.	F-4
F.4	KN-Sorbitol. Set pressure 9 MPa.	F-5

F.5	KN-Sorbitol. Set pressure 9 MPa.	F-6
F.6	KN-Sorbitol. Set pressure 9 MPa.	F-7
F.7	KN-Sorbitol. Set pressure 8 MPa.	F-8
F.8	KN-Sorbitol. Set pressure 8 MPa.	F-9
F.9	KN-Sorbitol. Set pressure 7 MPa.	F-10
F.10	KN-Sorbitol. Set pressure 7 MPa.	F-11
F.11	KN-Sorbitol. Set pressure 6 MPa	F-12
F.12	KN-Sorbitol. Set pressure 6 MPa.	F-13
F.13	KN-Sorbitol. Set pressure 5 MPa.	F-14
F.14	KN-Sorbitol. Set pressure 5 MPa.	F-15
F.15	KN-Sorbitol. Set pressure 4 MPa.	F-16
F.16	KN-Sorbitol. Set pressure 4 MPa.	F-17
F.17	KN-Sorbitol. Set pressure 3 MPa.	F-18
F.18	KN-Sorbitol. Set pressure 3 MPa.	F-19
F.19	KN-Sorbitol. Set pressure 2 MPa.	F-20
F.20	KN-Sorbitol. Set pressure 2 MPa.	F-21
F.21	KN-Sorbitol. Set pressure 1 MPa.	F-22
F.22	KN-Sorbitol. Set pressure 1 MPa.	F-23
F.23	KN-Sorbitol. Atmospheric pressure	F-24
F.24	KN-Erythritol. Set pressure 10 MPa.	F-26
F.25	KN-Erythritol. Set pressure 10 MPa.	F-27
F.26	KN-Erythritol. Set pressure 9 MPa.	F-28
F.27	KN-Erythritol. Set pressure 9 MPa.	F-29
F.28	KN-Erythritol. Set pressure 9 MPa.	F-30
F.29	KN-Erythritol. Set pressure 8 MPa.	F-31
F.30	KN-Erythritol. Set pressure 8 MPa.	F-32
F.31	KN-Erythritol. Set pressure 7 MPa.	F-33
F.32	KN-Erythritol. Set pressure 7 MPa.	F-34
F.33	KN-Erythritol. Set pressure 6 MPa	F-35

F.34 KN-Erythritol. Set pressure 6 MPa.	F-36
F.35 KN-Erythritol. Set pressure 5 MPa.	F-37
F.36 KN-Erythritol. Set pressure 5 MPa.	F-38
F.37 KN-Erythritol. Set pressure 4 MPa.	F-39
F.38 KN-Erythritol. Set pressure 4 MPa.	F-40
F.39 KN-Erythritol. Set pressure 3 MPa.	F-41
F.40 KN-Erythritol. Set pressure 3 MPa.	F-42
F.41 KN-Erythritol. Set pressure 2 MPa.	F-43
F.42 KN-Erythritol. Set pressure 2 MPa.	F-44
F.43 KN-Erythritol. Set pressure 1 MPa.	F-45
F.44 KN-Erythritol. Set pressure 1 MPa.	F-46
F.45 KN-Erythritol. Atmospheric pressure	F-47
F.46 KN-Mannitol. Set pressure 10 MPa.	F-49
F.47 KN-Mannitol. Set pressure 10 MPa.	F-50
F.48 KN-Mannitol. Set pressure 9 MPa.	F-51
F.49 KN-Mannitol. Set pressure 9 MPa.	F-52
F.50 KN-Mannitol. Set pressure 8 MPa.	F-53
F.51 KN-Mannitol. Set pressure 8 MPa.	F-54
F.52 KN-Mannitol. Set pressure 7 MPa.	F-55
F.53 KN-Mannitol. Set pressure 7 MPa.	F-56
F.54 KN-Mannitol. Set pressure 7 MPa.	F-57
F.55 KN-Mannitol. Set pressure 6 MPa	F-58
F.56 KN-Mannitol. Set pressure 6 MPa.	F-59
F.57 KN-Mannitol. Set pressure 5 MPa.	F-60
F.58 KN-Mannitol. Set pressure 5 MPa.	F-61
F.59 KN-Mannitol. Set pressure 4 MPa.	F-62
F.60 KN-Mannitol. Set pressure 4 MPa.	F-63
F.61 KN-Mannitol. Set pressure 3 MPa.	F-64
F.62 KN-Mannitol. Set pressure 3 MPa.	F-65

F.63 KN-Mannitol. Set pressure 2 MPa.	F-66
F.64 KN-Mannitol. Set pressure 2 MPa.	F-67
F.65 KN-Mannitol. Set pressure 1 MPa.	F-68
F.66 KN-Mannitol. Set pressure 1 MPa.	F-69
F.67 KN-Mannitol. Set pressure 1 MPa.	F-70
F.68 KN-Mannitol. Set pressure 1 MPa.	F-71
F.69 KN-Mannitol. Atmospheric pressure	i

List of Tables

5.1	Physical constants of sorbitol, erythritol and mannitol (12). . .	18
7.1	Experimental results for KN-Sorbitol, KN-Erythritol and KN-Mannitol propellants. Vessel pressure shown as gauge and absolute pressures.	42
7.2	Burn rate coefficient (a) and pressure exponent (n) for KN-Sorbitol, KN-Erythritol and KN-Mannitol propellant.	48
8.1	Ideal performance estimation of KN-Sorbitol, KN-Erythritol and KN-Mannitol at 6.89 MPa.	49
8.2	Geometrical parameters of the Globos flight motor.	51
B.1	Particle distribution of potassium nitrate.	B-1
C.1	Slurry and mold temperature of casting batches of KN-Sorbitol.	C-1
C.2	Slurry and mold temperature of casting batches of KN-Erythritol.	C-1
C.3	Slurry and mold temperature of casting batches of KN-Mannitol.	C-2
D.1	Ideal and recorded densities of 65/35 O/F ratio for KN-Sorbitol, KN-Erythritol and KN-Mannitol propellants	D-1
F.1	KN-Sorbitol. Set pressure 10 MPa.	F-2
F.2	KN-Sorbitol. Set pressure 10 MPa.	F-3
F.3	KN-Sorbitol. Set pressure 9 MPa.	F-4

F.4	KN-Sorbitol. Set pressure 9 MPa.	F-5
F.5	KN-Sorbitol. Set pressure 9 MPa.	F-6
F.6	KN-Sorbitol. Set pressure 9 MPa.	F-7
F.7	KN-Sorbitol. Set pressure 8 MPa.	F-8
F.8	KN-Sorbitol. Set pressure 8 MPa.	F-9
F.9	KN-Sorbitol. Set pressure 7 MPa.	F-10
F.10	KN-Sorbitol. Set pressure 7 MPa.	F-11
F.11	KN-Sorbitol. Set pressure 6 MPa.	F-12
F.12	KN-Sorbitol. Set pressure 6 MPa.	F-13
F.13	KN-Sorbitol. Set pressure 5 MPa.	F-14
F.14	KN-Sorbitol. Set pressure 5 MPa.	F-15
F.15	KN-Sorbitol. Set pressure 4 MPa.	F-16
F.16	KN-Sorbitol. Set pressure 4 MPa.	F-17
F.17	KN-Sorbitol. Set pressure 3 MPa.	F-18
F.18	KN-Sorbitol. Set pressure 3 MPa.	F-19
F.19	KN-Sorbitol. Set pressure 2 MPa.	F-20
F.20	KN-Sorbitol. Set pressure 2 MPa.	F-21
F.21	KN-Sorbitol. Set pressure 1 MPa.	F-22
F.22	KN-Sorbitol. Set pressure 1 MPa.	F-23
F.23	KN-Sorbitol. Atmospheric pressure	F-24
F.24	KN-Erythritol. Set pressure 10 MPa.	F-26
F.25	KN-Erythritol. Set pressure 10 MPa.	F-27
F.26	KN-Erythritol. Set pressure 9 MPa.	F-28
F.27	KN-Erythritol. Set pressure 9 MPa.	F-29
F.28	KN-Erythritol. Set pressure 9 MPa.	F-30
F.29	KN-Erythritol. Set pressure 8 MPa.	F-31
F.30	KN-Erythritol. Set pressure 8 MPa.	F-32
F.31	KN-Erythritol. Set pressure 7 MPa.	F-33
F.32	KN-Erythritol. Set pressure 7 MPa.	F-34

F.33 KN-Erythritol. Set pressure 6 MPa.	F-35
F.34 KN-Erythritol. Set pressure 6 MPa.	F-36
F.35 KN-Erythritol. Set pressure 5 MPa.	F-37
F.36 KN-Erythritol. Set pressure 5 MPa.	F-38
F.37 KN-Erythritol. Set pressure 4 MPa.	F-39
F.38 KN-Erythritol. Set pressure 4 MPa.	F-40
F.39 KN-Erythritol. Set pressure 3 MPa.	F-41
F.40 KN-Erythritol. Set pressure 3 MPa.	F-42
F.41 KN-Erythritol. Set pressure 2 MPa.	F-43
F.42 KN-Erythritol. Set pressure 2 MPa.	F-44
F.43 KN-Erythritol. Set pressure 1 MPa.	F-45
F.44 KN-Erythritol. Set pressure 1 MPa.	F-46
F.45 KN-Erythritol. Atmospheric pressure	F-47
F.46 KN-Mannitol. Set pressure 10 MPa.	F-49
F.47 KN-Mannitol. Set pressure 10 MPa.	F-50
F.48 KN-Mannitol. Set pressure 9 MPa.	F-51
F.49 KN-Mannitol. Set pressure 9 MPa.	F-52
F.50 KN-Mannitol. Set pressure 8 MPa.	F-53
F.51 KN-Mannitol. Set pressure 8 MPa.	F-54
F.52 KN-Mannitol. Set pressure 7 MPa.	F-55
F.53 KN-Mannitol. Set pressure 7 MPa.	F-56
F.54 KN-Mannitol. Set pressure 7 MPa.	F-57
F.55 KN-Mannitol. Set pressure 6 MPa.	F-58
F.56 KN-Mannitol. Set pressure 6 MPa.	F-59
F.57 KN-Mannitol. Set pressure 5 MPa.	F-60
F.58 KN-Mannitol. Set pressure 5 MPa.	F-61
F.59 KN-Mannitol. Set pressure 4 MPa.	F-62
F.60 KN-Mannitol. Set pressure 4 MPa.	F-63
F.61 KN-Mannitol. Set pressure 3 MPa.	F-64

F.62 KN-Mannitol. Set pressure 3 MPa.	F-65
F.63 KN-Mannitol. Set pressure 2 MPa.	F-66
F.64 KN-Mannitol. Set pressure 2 MPa.	F-67
F.65 KN-Mannitol. Set pressure 1 MPa.	F-68
F.66 KN-Mannitol. Set pressure 1 MPa.	F-69
F.67 KN-Mannitol. Set pressure 1 MPa.	F-70
F.68 KN-Mannitol. Set pressure 1 MPa.	F-71
F.69 KN-Mannitol. Atmospheric pressure	i

CHAPTER 1

Introduction

Design, fabrication and the use of a strand burner, where potassium nitrate sugar alcohol based solid propellant were burned under pressure, is examined in this project thesis. Strand burners (3; 5; 6; 9; 10) are used to estimate the burning rate of solid propellants.

Three types of propellants were burned in the strand burner in the pressure range of 0 to 10 MPa. The types of propellants were KN-Sorbitol, KN-Erythritol and KN-Mannitol, where KN stands for potassium nitrate. The burn rate behavior was estimated by using Vieille's (Saint Roberts) empirical law.

Objectives and motivation for this study is presented in chapter 2. Former studies of strand burners, burning rates and the history of sugar propellants are given in the same chapter.

In chapter 3 the fundamental laws of rocket propulsion is explained. Thermodynamic thrust, impulse, exhaust and characteristic velocity and the nozzle coefficient are given in the chapter.

The expression of the burning behavior of solid propellants is given in chapter 4. The empirical Vieille's law is explained and the steady state chamber pressure for a given rocket motor is expressed as a function of burning rate behavior. The three methods of empirical determination of burn rates is explained.

In chapter 5 the chemical and physical constants of sugar alcohols are given. This includes molecular weight, density, melting point, enthalpy of formation and the glass transition temperature. The chemical structures of the sor-

bitol, erythritol and mannitol are shown. The production of sugar alcohols is briefly described and listed.

The ideal combustion reaction of KN-Sorbitol, KN-Erythritol and KN-Mannitol propellants are estimated and given in section 5.2. Knowing the combustion reactions, estimation of the thermodynamic properties, such as combustion chamber temperature, effective molecular weight of gaseous products and the specific heat capacities, were made. The specific heat capacities was used to estimate the ratio of specific heat capacities for gaseous and mixed products as well as for the two phase flow through a nozzle.

Apparatus and experimental preparation is described in details in chapter 6. Preparation of the propellant such as mixing, melting, casting and analysis is explained in section 6.1. The construction of the strand burner and it's components is explained in section 6.2. The electronic devices needed for recording and analysis of the burn rate is explained in section 6.3. The experimental technique of the strand firings are explained and given in section 6.4

Results of the burn rates of KN-Sorbitol, KN-Erythritol and KN-Mannitol are given in chapter 7. The burning rates of the types of propellants are graphically shown where burn rate is a function of pressure.

Results of the burn rate data was used to estimate the ideal performance of a solid rocket motor in chapter 8. The ideal chamber pressure and burning rate was compared with a full-scale rocket motor.

Discussion of the results and the technical obstacles are detailed in chapter 9.

Conclusion of the work is given in chapter 10.

CHAPTER 2

Background

2.1 Motivation

Experimental rocketry is an activity in where participants experiment with wide variety of rocket propellants, rocket motors and engine designs, aviation electronics and rocket body structures. The goal is thus to design, build, test and launch rockets in a safe way.

The author has been involved in experimental rocketry since early 2006 and has designed, built and launched several rockets. The rockets have all been launched with potassium nitrate sugar based propellants.

The process of designing, building and launching experimental rockets involves a wide spectrum of scientific laws and theories that are related to chemistry, physics, math and engineering.

The learning curve that is provided in an undergraduate level of any science and engineering study can be easily related to experimental rocketry. The author thus believes that this project is well suited for a partial fulfillment of a bachelor degree in science and engineering.

2.2 Objectives

Empirical estimation of the burning rate behavior of solid propellant is needed to effectively design and construct a rocket motor.

The main objective is to design and construct a small one liter strand burner that can be used to effectively estimate the burning rate of KN-Sorbitol, KN-Erythritol and KN-Mannitol solid rocket propellants.

The approach of using a proportional relief valve to release combustion gases, of burning propellant strands, from the strand burner is investigated.

The results of the burning rates were used to estimate the ideal performance of a rocket motor and compared to empirical values of a full-scale motor firing.

2.3 Former studies

Numerous studies (3; 5; 6; 9; 10) have been conducted to estimate the burning rate of solid propellants. These studies are though all related to ammonium perchlorate or double base propellants and not sugar propellants.

Few studies have been published related to sugar propellants. “*Effect of chamber pressure on burning rate for the potassium nitrate-dextrose and potassium nitrate-sorbitol rocket propellants*” (13) was published by Richard Nakka in 1999. In this report, burn rate data are estimated using a strand burner for KN-Sorbitol and KN-Dextrose propellants.

Tony Vyverman published “*The potassium nitrate-sugar propellant*” (18) in 1980. In this booklet the sucrose based propellant is explained and characterized.

2.3.1 History of sugar propellant

The following is the history of development of sugar propellant (11).

1944 *First experiments with KN/sucrose by William Colburn of the Rocket Missile Research Society (later Rocket Motor Research Group) followed by first launch of a sugar rocket in 1947. The first propellant, designated TF-1 was dry-mixed KN/sucrose moistened with water and pressed into the motor tube. (from Bill Colburn via Richard Nakka’s website)*

1950 *Melting of KN/sucrose by Dirk Thyse allows casting of propellant grains, thus different configurations are available and larger motors can be produced. (Colburn via Nakka)*

1957 *First use of hydraulic press to make grains by Bill Colburn allows creation of Bates-type grains without the need to melt propellant components.*

- 1960** Publication of “*Rocket Manual for Amateurs*” by B. R. Brinley includes a brief description of KN/sucrose propellant. This book has inspired many amateurs (notably Richard Nakka) to try sugar propellants, as well as serving as a manual for many high-school rocketry clubs, which often favored sugar propellant (John Wickman, personal correspondence.)
- 1975** BVRO (Flemish Rocketry Organization) begins first scientific investigation of this KN/sucrose propellant and its performance characteristics. Culminates in the 1980 publication of “*The Potassium Nitrate - Sugar Propellant*” by Antoon Vyverman. This group recognized problems of case-bonding in large sugar motors. Contains first mention of KN/sorbitol and KN/mannitol, first used by this group in 1977. (Vyverman 1980, Vyverman, personal correspondence)
- 1983** David Sleeter of Teleflite Corporation, releases the book “*Building Your own Rocket Motors*“, and a booklet entitled: “*The Incredible Five-Cent Sugar Rocket*“ using KN/sucrose and sulfur. These publications were advertised in magazines such as *Popular Science*, and so presumably found wide audience.
- 1993** NERO performs substantial tests of KN/sorbitol, which allows melting and casting at lower temperature than sucrose, perceived to be safer. (Vyverman, personal correspondence)
- 1996** First use of KN/dextrose by Richard Nakka. KN/DX offers a melting point only a little higher than KN/sorbitol, with a more predictable burn rate. Also, a Rocket discussion group opens, facilitating discussion of amateur/experimental rocketry in general. Sugar propellants are a common topic on this list.
- 1997** Richard Nakka opens his website on experimental rocketry, devoted primarily to the use of sugar propellants. His creative and careful technical work provides a scientific foundation for experimenters working with sugar propellants. It includes substantial treatments of rocketry theory in general, so as to be commendable to users of other propellants as well. Also, Al Bradley uses hydraulic press to compress sugar propellant moistened with 60/40 water/ethanol, resulting in grains which air-dry to a very hard consistency.
- 1998** Publication of *Rocket Boys* by Homer Hickam and subsequent movie *October Sky* (1999) stirs new interest in rocketry, creating a distinct class of “*Born-Again Rocketeers*”. KN/sucrose was one of the propellants used by the “*Rocket Boys*”, ostensibly co-invented by them independent of knowledge of previous experimenters. (Hickam 1998)

-
- 2000** *Invention of the “Candymatic,” by Paul Kelly allows automated, remote melting of propellants. It is a bread machine modified to heat and stir propellant to the melting point, allowing the operator to remain at a distance. (2001 Jay Ward places a photo of the Candymatic on the Web).*
- 2001** *Publication of the recrystallization process by Jimmy Yawn resolves some limitations of KN/sucrose.*
- 2002** *Substantial dialogue regarding sugar propellants on the Arocket discussion list prompts formation of the SugPro list, specifically for the discussion of sugar based propellants. List owners are Dave McCue and David Muesing. SugPro currently has 100 members (September 2002).*
- 2002** *“Yuw“ reports melting of KN/sorbitol in a boiling-water bath. The propellant mix is enclosed in a plastic bag and immersed in hot water. This may be the safest method yet of melting sugar propellants.*
- 2002** *Two different companies produce and market kits for making sugar-propelled rocket engines. Woody Stanford of Stanford Systems and Jon Drayna of October Science each produce such kits. Sugar propellant knocks at the door of consumer rocketry.*
- 2004** *Scott Fintel introduce the use of KN-Erythritol propellant followed by the launch of his rocket Defiance (2006) to just under 9 km.*
- 2005** *Sugar Shot to Space project is started. The underlying goal of the project is to loft a rocket powered by sugar propellant into space, officially defined as 100 km above the earth’s surface.*

CHAPTER 3

Definition and fundamentals of rocket propulsion

Rocket propulsion is an exact but not a fundamental subject, and there are no basic scientific laws of nature peculiar to propulsion. The basic principles are essentially those of mechanics, thermodynamics and chemistry (7).

3.1 Basic assumptions of an ideal rocket

A number of basic assumptions must be taken into account when deriving the needed relations of thermodynamics for a chemical rocket motor. These assumptions are the following (7):

- *The working substance (or chemical reaction products) is homogeneous.*
- *The working substance obeys the perfect gas law.*
- *There is no heat transfer across the rocket walls; therefore, the flow is adiabatic.*
- *There is no appreciable friction and all boundary layer effects are neglected.*
- *There are no shock waves or discontinuities in the nozzle flow.*
- *The propellant flow is steady and constant. The expansion effects (i.e., start up and shut down) are of very short duration and may be neglected.*

- *All exhaust gases leaving the rocket have an axially directed velocity.*
- *The gas velocity, pressure, temperature and density are all uniform across any section normal to the nozzle axis.*
- *Chemical equilibrium is established within the rocket chamber and the gas composition does not change in the nozzle (frozen flow).*
- *Stored propellant are at room temperature.*

3.2 Thermodynamic relations

3.2.1 Exhaust velocity

Exhaust velocity, or sometimes referred to as the nozzle exit velocity, is the velocity of the combustion gases that flow through the nozzle. It is related to the thermodynamics constants of the propellant and the pressure inside the motor chamber. The exhaust velocity can be expressed as

$$v_e = \sqrt{\frac{2\gamma}{\gamma-1} \frac{RT_c}{M} \left[1 - \left(\frac{P_e}{P_c} \right)^{\frac{\gamma-1}{\gamma}} \right]} \quad (3.1)$$

where γ is the ratio of specific heats for the exhaust gases, R is the universal gas constant, T_c is the temperature inside the chamber, M is the effective molecular weight of the exhaust gases, P_e is the pressure at the exit plane of the nozzle and P_c is the pressure inside the chamber.

The expression for exhaust velocity is an important one, since it is a significant performance indicator for a rocket motor. It determines the final velocity of the rocket and it is the major contributor to the thrust development as can be expressed by using Newton's second law

$$F = \dot{m}v_e \quad (3.2)$$

where F is the thrust generated and \dot{m} is the mass flow rate of the exhaust gases.

3.2.2 Thrust

Thrust is a measure of force that propels a rocket. It is the result of the pressures that is exerted on the wall of the combustion chamber. It is generated

by the exhaust gases flowing through the nozzle. Thrust can be expressed as

$$F = \int PdA = \dot{m}v_e + (P_e - P_a)A_e \quad (3.3)$$

where the left hand term is represented by the surface (A) integral of the pressure (P) over the walls of the combustion chamber and the nozzle. In the right hand term, \dot{m} is the mass flow rate of the exhaust products, P_a is the ambient pressure and A_e is the cross-sectional area at the exit plane of the nozzle.

The term $(P_e - P_a)$ is a so-called pressure thrust. The maximum thrust is generated when the nozzle is optimized so that the exit pressure is equal to the ambient pressure or $P_e = P_a$.

Equation 3.3 can be extended by substituting expression for the velocity v_e and the mass flow rate \dot{m} into what is normally referred to as the full thermodynamic thrust equation

$$F = A_t P_c \sqrt{\frac{2\gamma^2}{\gamma-1} \left(\frac{2}{\gamma+1}\right)^{\frac{\gamma+1}{\gamma-1}} \left[1 - \left(\frac{P_e}{P_c}\right)^{\frac{\gamma-1}{\gamma}}\right]} + (P_e - P_c)A_e \quad (3.4)$$

This is the so-called ideal thrust equation. This equation shows that the thrust is proportional to the nozzle throat area A_t and the chamber pressure P_c and is a function of the pressure ratio across the nozzle $\frac{P_e}{P_c}$, the specific heat ratio γ and of the pressure thrust.

The forces acted upon the combustion chamber and the nozzle is shown in Figure 3.1

3.2.3 Thrust coefficient

The thrust coefficient represent the performance of a nozzle. It is the measure of the efficiency of the extracted energy from the hot gases in the combustion chamber that is acted upon the nozzle. The thrust coefficient is defined in terms of the chamber pressure and the throat area

$$C_F = \frac{F}{P_c A_t} \quad (3.5)$$

The ideal thrust coefficient is derived from equation 3.4 and can be written

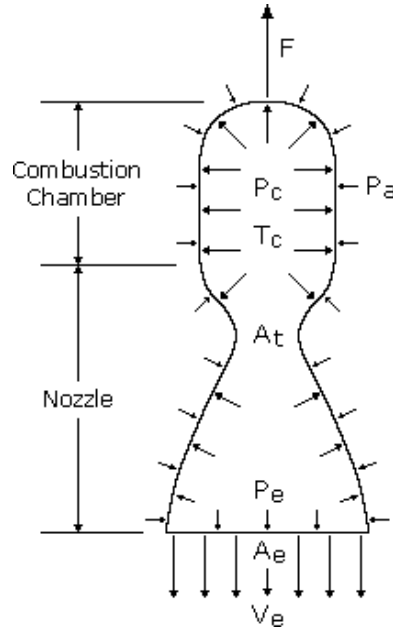


Figure 3.1: Schematic showing the forces acted upon the combustion chamber and the nozzle (1).

as

$$C_F = \sqrt{\frac{2\gamma^2}{\gamma-1} \left(\frac{2}{\gamma+1}\right)^{\frac{\gamma+1}{\gamma-1}} \left[1 - \left(\frac{P_e}{P_c}\right)^{\frac{\gamma-1}{\gamma}}\right]} + \left(\frac{P_e}{P_c} - \frac{P_a}{P_c}\right) \frac{A_e}{A_t} \quad (3.6)$$

3.2.4 Characteristic velocity

The characteristic velocity is the measure of efficiency of conversion of thermal energy in the combustion chamber into high-velocity exhaust gas (17). The characteristic velocity, which is independent of nozzle performance, is usually denoted, c^* , and is thus referred to as c -star. It can be expressed as

$$c^* = \frac{P_c A_t}{\dot{m}} \quad (3.7)$$

The thermodynamic form is given by the ideal expression

$$c^* = \sqrt{\frac{\frac{RT_c}{M}}{\left(\frac{2\gamma}{\gamma+1}\right)^{\frac{\gamma+1}{\gamma-1}}}} \quad (3.8)$$

The characteristic velocity depends on the temperature and on the molecular weight.

The performance of a motor firing can be estimated by comparing the ideal characteristic velocity, using equation 3.8, with the empirical value found from equation 3.7.

3.2.5 Total and specific impulse

The total impulse is defined as the average thrust multiplied by the total time of a motor firing or in other words, the integral of the thrust over the operating duration of a motor

$$I_t = \int F dt \quad (3.9)$$

Specific impulse can be expressed as the efficiency of a propellant per unit weight

$$I_{sp} = \frac{I_t}{w_p} \quad (3.10)$$

where w_p is the total weight of a propellant. The specific impulse is related to the characteristic velocity as:

$$I_{sp} = c^* \frac{C_F}{g} \quad (3.11)$$

where g is the gravitational force.

The ideal specific impulse can be expressed as

$$I_{sp} = \frac{1}{g} \sqrt{\left(\frac{RT_c}{M}\right) \left(\frac{2\gamma}{\gamma-1}\right) \left[1 - \frac{P_e}{P_c}\right]^{\frac{\gamma-1}{\gamma}}} \quad (3.12)$$

CHAPTER 4

Burning rate of solid propellant

4.1 Pressure sensitivity of burning rate

4.1.1 Mass flow rate

The generation of combustion gases in the chamber can be expressed as

$$\dot{m} = A_b \rho_P r \quad (4.1)$$

where A_b is the propellant burning area, ρ_P is the propellant density and r is the propellant burning rate.

Integration of the mass flow over time yields the total effective mass of propellant burned and can thus be expressed as

$$m = \int \dot{m} dt = \rho_P \int A_b r dt \quad (4.2)$$

4.1.2 Burning rate

The empirical equation for burning rate as a function of pressure can be expressed as

$$\frac{dx}{dt} = r = aP^n \quad (4.3)$$

where a is the burn rate coefficient, P is the burning pressure and n is the pressure exponent. This is often referred to as Vieille's law or Saint Robert's law.

Vieille's law is an empirical, dimensional non-homogeneous law named after the French combustion engineer and scientist Paul Vieille (1854-1934), and used to describe the dependence of steady-state burning rate of solid propellants on pressure, at fixed initial temperature of the propellant (2).

The law can be characterized by a straight-line relationship between the log-burning rate and log-pressure as shown in Figure 4.1.

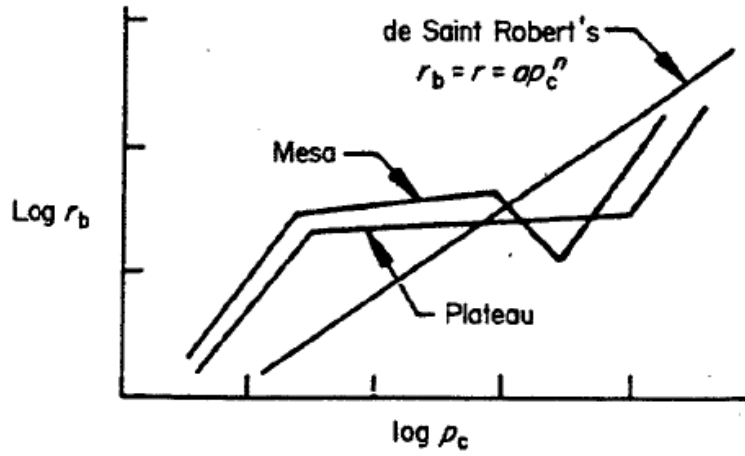


Figure 4.1: Dependence of burning rate as a function of pressure (6).

4.1.3 Steady-state chamber pressure

When the production of propellant consumption gases and the mass flow of exhaust gases are in equilibrium, the term steady-state chamber pressure can be expressed as

$$P_c = \left[\frac{A_b}{A_t} \frac{a \rho P}{\sqrt{\frac{\gamma}{RT_c} \left(\frac{2}{\gamma+1} \right)^{\frac{\gamma+1}{\gamma-1}}}} \right]^{\frac{1}{1-n}} \quad (4.4)$$

This expression can be simplified by using equation 3.8 and by denoting that

$$Kn = \frac{A_b}{A_t} \quad (4.5)$$

thus

$$P_c = Kn\rho_Prc^* \quad (4.6)$$

where Kn is the so-called Klemmung constant. This is the simplified expression for steady-state pressure.

Equations 4.4 and 4.6 is the all important expressions for estimating the chamber pressure of a given motor design.

4.2 Empirical determination of burning rate

The values of the burn rate coefficient and the burn rate pressure exponent can be determined empirically by means of three different well know techniques

- Standard strand burner, often called Crawford strand burner.
- Small-scale ballistic evaluation motor.
- Full-scale motor.

The actual burning rate can be determined from using the equation of mass conversation and is expressed as

$$r = \frac{1}{\rho_P A_b} \left(\frac{P_c}{RT_c} \frac{dV_c}{dt} + \frac{V_c}{RT_c} \frac{dP_c}{dt} + \frac{P_c A_b}{c^*} \right) \quad (4.7)$$

where V_c is the free volume within the combustion chamber.

4.2.1 Crawford strand burner

A strand burner is a pressure vessel (often referred to as firing vessel) in which a strand of propellant is burned. The firing vessel is pressurized with inert gas, typically nitrogen, prior to ignition of the strand.

The strand is ignited electrically at one end and burns along its length. The duration of the time is measured by the aid of two or more thermocouples, by ultrasonic waves, or by optical means. The pressure is recorded by means of a pressure gauge or a pressure transducer.

By knowing the length between the thermocouples and the burn time at certain pressure, the burn rate can be found.

4.2.2 Ballistic evaluation motor

A ballistic evaluation motor is a closed vessel in one end with a nozzle in the other end. It is usually a single segment motor i.e. with only one propellant segment that burns along its web length as shown in Figure 4.2.

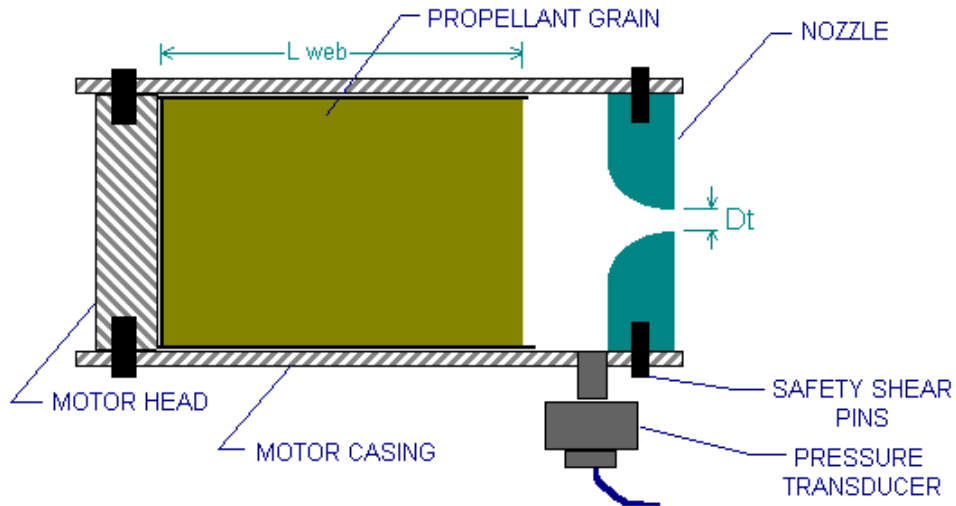


Figure 4.2: Burn rate evaluation motor (15).

The burning area is constant and thus the vessel pressure is at steady-state. By this configuration it is possible to estimate the burning rate from the web length divided by the motor burn time. The pressure is recorded by a pressure transducer.

4.2.3 Full-scale motor

Full scale motor firing is the final proof of burning rate behavior. This is the real life scenario where every thermodynamic parameters and forces come into play.

The method of pressure time-trace (16) can be used to estimate the instantaneous burning rate from a motor firing.

This can be done since the motor chamber pressure and burn rate are directly related in terms of K_n , characteristic velocity and the propellant density as described in equation 4.6.

CHAPTER 5

Chemistry and combustion of sugar rocket propellants

5.1 Sugar chemistry

Polyols are reduced-calorie, sugar-free bulk sweeteners. They are sugar alcohols or polyhydric alcohols that are derived from saccharides by the reduction of the aldehyde or ketone group to an alcohol group through chemical or biochemical process. A majority of polyols are naturally occurring substances. Erythritol, sorbitol, and mannitol can be found in plants (4).

The chemical structure of sorbitol, erythritol and mannitol is shown in Figure 5.1.

Sorbitol is a reduced form of dextrose and the most available polyol. Sorbitol is industrially produced either by catalytic hydrogenation of dextrose, which produces less than 2 % mannitol, or by catalytic hydrogenation of sucrose as a mixture with mannitol.

Erythritol is a four-carbon symmetrical polyol and exists only in the meso form. Unlike other polyols of the hydrogenation process, the industrial production of erythritol uses a fermentation process.(19)

Mannitol is obtained from hydrogenation of fructose, which is from either sucrose or starch. Sucrose, after hydrolysis, can be hydrogenated to produce a mixture of sorbitol and mannitol (8).

The physical constants of sorbitol, erythritol and mannitol are given in Table 5.1

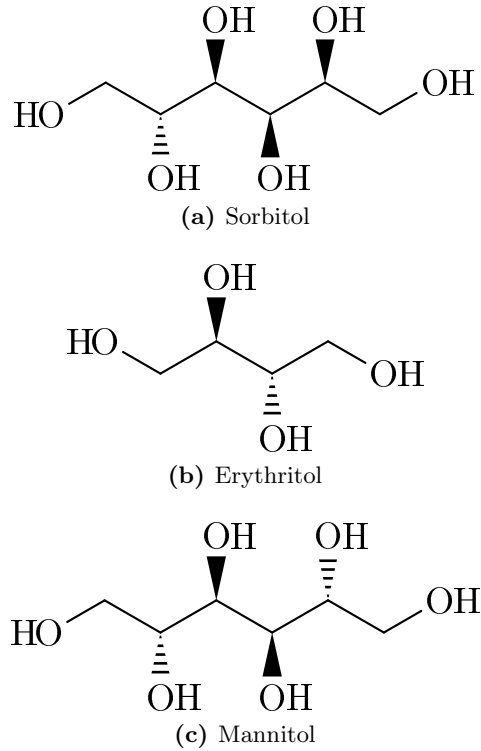


Figure 5.1: Chemical structure of three sugar alcohols.

	Sorbitol	Erythritol	Mannitol	
Molecular form	$C_6H_{14}O_6$	$C_4H_{10}O_4$	$C_6H_{14}O_6$	
Density ²⁰	1.489	1.451	1.489	g/cm ³
Melting point	101	121.5	166-168	°C
Molecular weight	182.172	122.120	182.172	g/mol
Enthalpy of formation	-1353.7	-885.6	-1314.5	kJ/mol
Enthalpy of formation	7.431	7.284	7.216	kJ/g
Glass transition	-43.5	-53.5	-40.0	°C

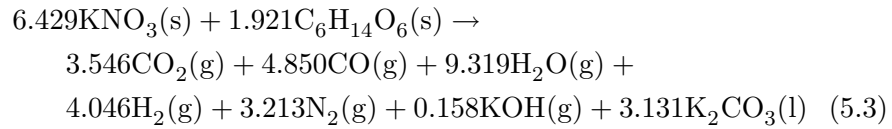
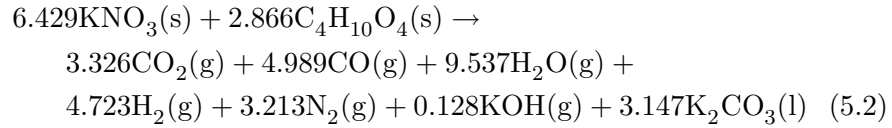
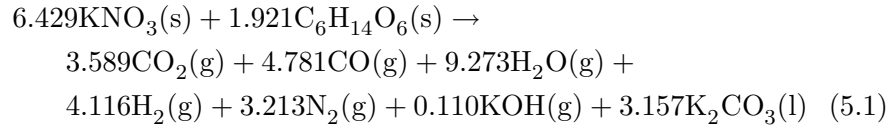
Table 5.1: Physical constants of sorbitol, erythritol and mannitol (12).

5.2 Combustion

Combustion is the sequence of exothermic chemical reactions between a fuel and an oxidant accompanied by the production of heat and conversion of chemical species.

The combustion of a propellant is given by a chemical equation. With the aid of a combustion simulation software such as PROPEP¹ the ideal combustion equation of sugar propellant can be estimated. The PROPEP runs of KN-Sorbitol, KN-Erythritol and KN-Mannitol are given in Appendix E.

Combustion equations for a 65/35 O/F ratio of KN-Sorbitol, KN-Erythritol and KN-Mannitol propellants are given in equations 5.1, 5.2 and 5.3, respectively. The number of moles represent a mixture of 1 kg



where CO_2 is carbon dioxide, CO is carbon monoxide, H_2O is water, H_2 is hydrogen, N_2 , is nitrogen, KOH is potassium hydroxide and K_2CO_3 is potassium carbonate.

The number of gas moles n_{gas} can be estimated using the chemical combustion equations 5.1, 5.2 and 5.3. It is the total number of gas moles

$$n_{gas} = \sum_i n_i \quad (5.4)$$

where n_i is the number of moles of gas components i .

The effective molecular weight can be found by the expression

$$M = \frac{m_{mix}}{n_{gas}} \quad (5.5)$$

¹PROPEP is a combustion simulation software, that estimates the specific impulse and thermodynamical constants for a propellant composition

where m_{mix} is the mass of the propellant mix.

The mass fraction of the condensed phase can be expressed by

$$\chi = \frac{n_s MW_s}{100} \quad (5.6)$$

where n_s is the number of moles of the condensed components, the liquid phase of the potassium carbonate.

The specific heat capacity of gaseous products and the mixture products (gas + condensed) is expressed as

$$C_{P,gas} = \frac{1}{n} \sum_i n_i C_{P,i} \quad (5.7)$$

and

$$C_{P,mix} = \frac{1}{n} \sum_i (n_i C_{P,i} + n_s C_s) \quad (5.8)$$

where C_P and C_s is the specific heat capacity of gas and solids at constant pressure, respectively.

The ratio of specific heat capacities for the mixture, gas and two-phase flow² can now be expressed as

$$\gamma_{gas} = \frac{C_{P,gas}}{C_{P,gas} - R} \quad (5.9)$$

$$\gamma_{mix} = \frac{C_{P,mix}}{C_{P,mix} - R} \quad (5.10)$$

$$\gamma_{2ph} = \gamma_{gas} * \left(\frac{1 + \frac{C_s}{C_{P,gas}}}{1 + \gamma_{gas} \psi \frac{C_s}{C_{P,gas}}} \right) \quad (5.11)$$

where ψ is equal to $\frac{\chi}{1-\chi}$

²In fluid mechanics, two-phase flow occurs in a system containing gas and liquid with a meniscus separating the two phases

CHAPTER 6

Apparatus and experimental preparation

6.1 Preparation of propellant

6.1.1 Propellant mixes

Three different types of propellants were made, KN-Sorbitol, KN-Erythritol and KN-Mannitol. The oxidizer/fuel mass ratio was 65 % potassium nitrate and 35 % sugar alcohol. This mass ratio was utilized exclusively.

The potassium nitrate (Riedel.de Haen, puriss p.a. Reag. ACS) was screened through a sieve to break up any clumps that had formed. The sorbitol (Cargill Sorbidex) was also screened since it had a tendency of caking but the erythritol (Cargill Zerose) and the mannitol (Cargill Mannidex) were used straight out of the purchased container since it showed no sign of caking.

The potassium nitrate was sieved through different sized mesh screens to estimate the particle distribution. The sieved potassium nitrate particles is shown in Figure 6.1. The particle distribution is shown in Table B.1 and as a curve in Figure B.1 in Appendix B.

After screening, the constituents were carefully weighed out using an analytical scale with accuracy and resolution of 1 mg. Typical prepared batch size was around 100-160 g depending on the type of propellant.

After weighing, the constituents were placed into a 80 by 120 mm polyethy-



Figure 6.1: Sieved particles showing the particle distribution. Note that the markings indicates the particle size that was retained on each screen.

lene jar and closed with screwed cap and then shaken for about 10 seconds. The jar was placed in a rotating device, namely a ball mill, and rotated at 60 rpm to facilitate mixing. The mixing occurred for a minimum of 1 hour. A detailed record of the propellant batches is given in Appendix C.

The ball mill is shown in Figure 6.2.



Figure 6.2: Polyethylene jar and ball mill.

6.1.2 Casting mold

Rectangular grooves of 8x8 mm and 100 mm in length were milled in a PTFE (Teflon) plate using a milling machine with carbide end mill. A total of 13 grooves were milled with 5 mm spacing between each groove in a 200x100x22

mm PTFE plate.

A 5 mm thick aluminum plate (Aluminum alloy 6083) was attached to the bottom side with six M4x10 mm countersunk screws. The purpose of this plate was to stiffen the PTFE plate and conduct heat to the PTFE plate when heated on a hot plate.

Two 3 mm thick plates were cut to length and attached with M3x10 mm socket head bolts on each longitudinal side of the PTFE plate. A number of 13 holes with 3.2 mm in diameter were drilled through one of the aluminum plates with a 13 mm spacing. Through these holes M3x20 mm bolts were attached with nuts on both sides of the aluminum plate. The bolts act as a fixture for the propellant strands to the strand holder.

The casting mold is shown in Figure 6.3.



Figure 6.3: PTFE casting mold with 8x8 mm grooves for propellant and M3x20 bolts for attachment to the strand holder.

6.1.3 Casting procedure

The propellant mixtures were slowly heated in a PTFE coated pot (Raadvad 1.5 L) that was placed on a thermostatically controlled hot plate (Heidolph MR 3001 K). A thermocouple (type K) connected to a multimeter (Velleman DVM601) was used to monitor the temperature of the slurry (melted propellant). The casting equipment is shown in Figure 6.4.

The slurry temperature was kept between 110-120 °C for the KN-Sorbitol, between 145-150 °C for the KN-Erythritol and between 170-175 °C for the KN-Mannitol.

The slurry was typically fully melted in about 15 - 20 minutes and showing



Figure 6.4: From left to right: Casting mold prior to heating on a hot plate, PTFE coated pot with sorbitol based propellant and a multimeter for measuring mold and slurry temperature as well as relative humidity.

no signs of non-melted lumps of propellant mixture. The slurry was kept at constant temperature for another 25-30 minutes to allow the dissolved gases to be released. This was done to limit the amount of gas bubbles in the propellant when fully cured.

The propellant slurry was poured into the casting mold after it had been fully heated and melted. A tapping knife was used to scrape the slurry into the grooves of the casting mold. It was found necessary to preheat the tapping knife on a hot plate to prevent the propellant slurry to “freeze up“ on the knife.

It was also necessary to preheat the casting mold prior to casting (pouring of the propellant into the mold) of the propellants. This extended the working time of the propellant and eliminated trapped air bubbles. The casting mold was heated up to 90-105 °C for the KN-Sorbitol, 100-110 °C for the KN-Erythritol and 130-140 °C for the KN-Mannitol.

The propellant slurry was let to cool down and cure before it was taken out of the casting mold. KN-Erythritol and KN-Mannitol propellant strands were removed from the molds about 1-2 hours after casting had taken place. KN-Sorbitol was let to cure for 24 hours before taken out of the mold. This was found to be necessary since it had a tendency to stick to the casting mold within 24 hours from casting. It was also noted that KN-Sorbitol strands were pliable if taken out before 24 hours had passed.

Curing of KN-Sorbitol propellant is shown in Figure 6.5.

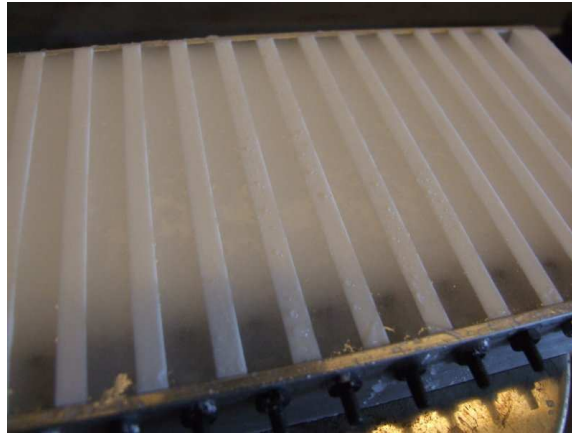


Figure 6.5: Sorbitol cooling down and curing in the casting mold.

6.1.4 Propellant strands

Fully cured propellant strands were inspected for flaws such as air bubbles. Strands with any sign of flaws were discarded. Strands were measured 100 mm in length and 8.0 ± 0.1 mm x 8.2 ± 0.5 mm in depth and width.



Figure 6.6: From top to bottom: Strands of fully cured KN-Sorbitol, KN-Erythritol, KN-Mannitol and painted KN-Erythritol.

Sample strands were density approved by filling a burette (a vertical cylindrical glass ware with volumetric graduation) with ethanol. Weighted strands were immersed in ethanol and the volume increase was recorded. The density of the strands showed good correlation to the theoretical density as shown in Appendix D. An acceptable density was chosen to be 95 % of the theoretical density. Density apparatus setup is shown in Figure 6.7



Figure 6.7: KN-Sorbitol immersed in ethanol in a burette.

Prior to burning of the propellant strands, the surfaces of the strands were inhibited due to the fact that liquid products of combustion could drool or shoot down the strands, causing ignition along the sides, thus increasing the relative burn rate. High heat spray paint (Plasti-Kote, BBQ) used for painting barbecues was used to paint the strands. Two layers/coats were applied and allowed to dry for a minimum of twenty-four hours in a drying rack as shown in Figure 6.8.

A pyrotechnic mixture of potassium chlorate and air float charcoal in the oxidizer/fuel mass ratio of 75/25 was coated on the ignition end of the strands. The dry mixture was added to a nitrocellulose liquid in the form of a table tennis balls dissolved in acetone. The strands were then dipped into the wet mixture and let dry for minimum of 12 hours. This coating was believed to help in ignition of the propellant surface to eliminate non-parallel burn of the strands.

Fully cured strands, one which is also coated, are shown in Figure 6.6.

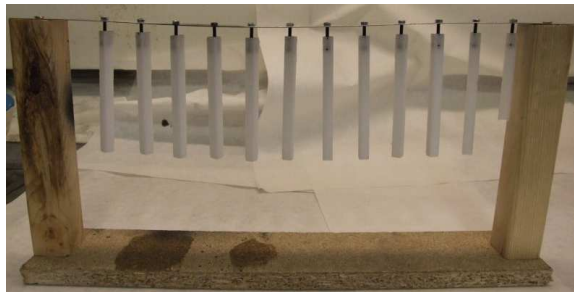


Figure 6.8: Propellant strands prior to painting.

6.2 Strand Burner

The strand burner, shown in Figures 6.9 and 6.10, consist of several major components. Those components are, a firing vessel, a closure on both ends where the front end closure holds the propellant strands in place and the aft end allows both intake of nitrogen gases and exhaust gases to flow through, a burst disc, a particle filter, a needle valve, two pressure transducers, a pressure gauge, a proportional pressure relief valve and a ball valve.

Other components shown in Figure 6.9 are a data acquisition board, a box for housing electrical circuits for pressure transducers and thermocouple inputs, an ignition box, a laptop and a multimeter.

Individual components are described in details in following sections.

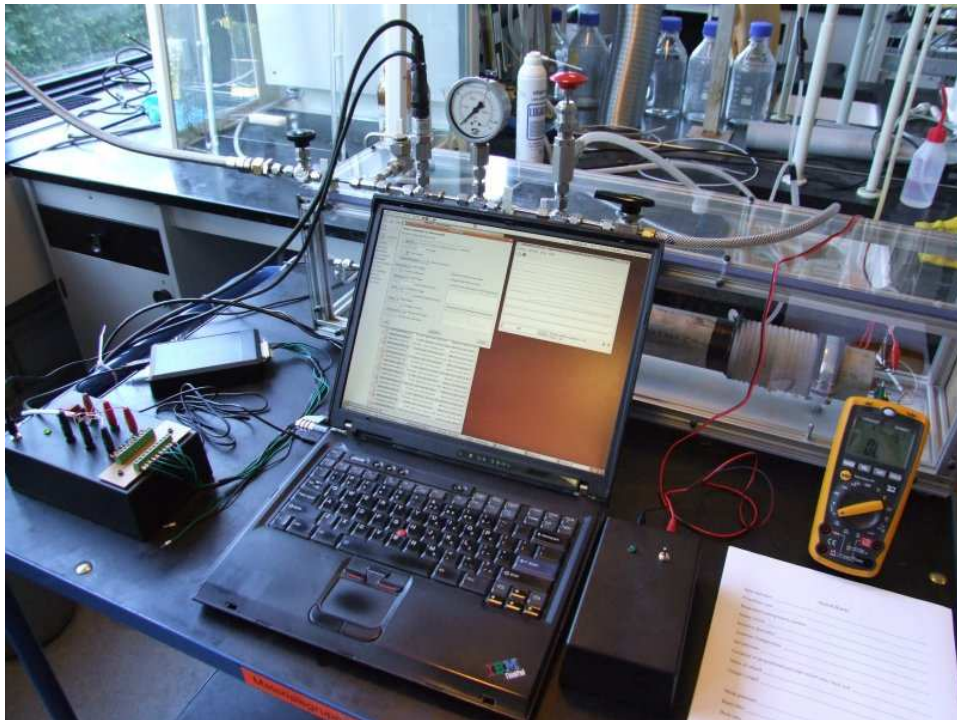


Figure 6.9: Strand burner setup.

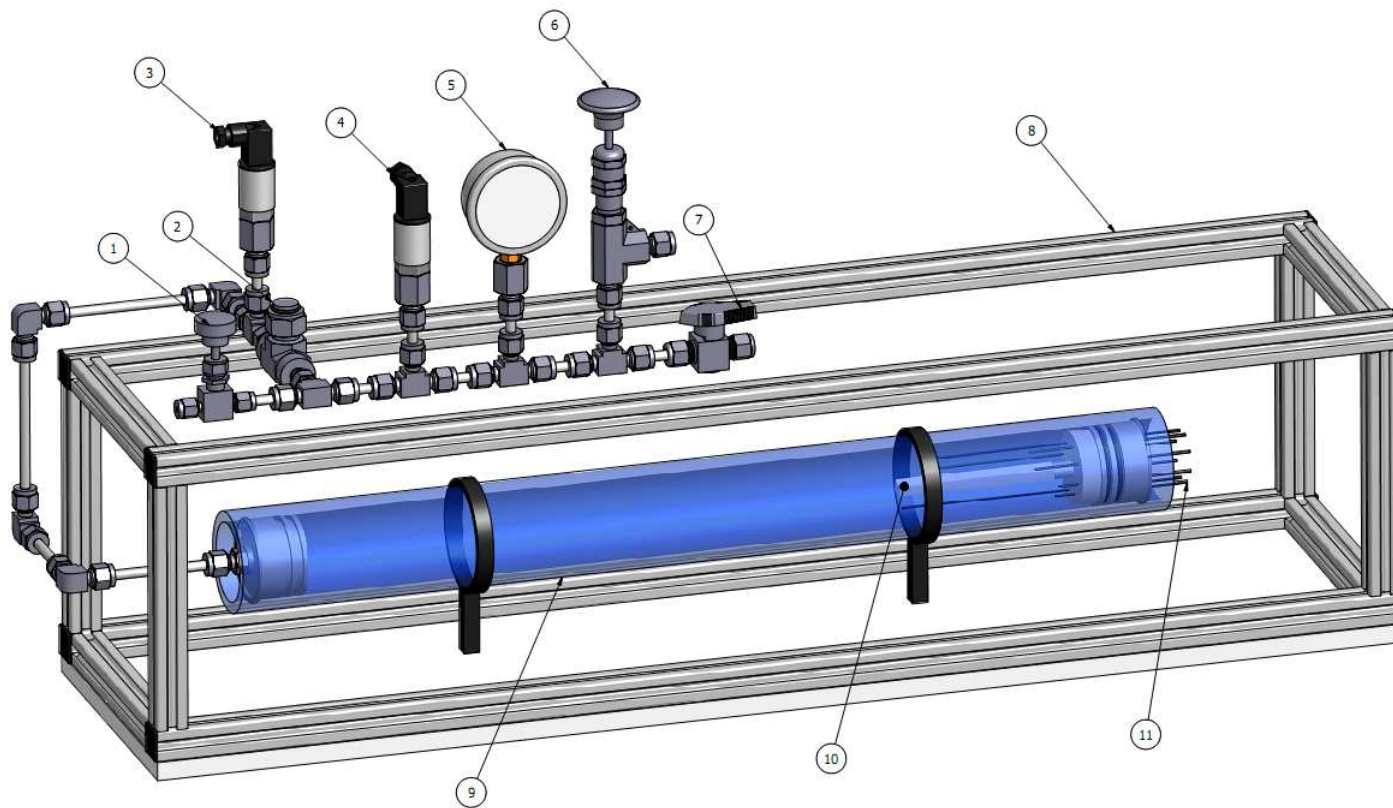


Figure 6.10: Main components of the strand burner. (1) Needle valve, (2) Particle filter, (3,4) Pressure transducers, (5) Pressure gauge, (6) Proportional pressure relief valve, (7) Ball valve, (8) Structural frame, (9) Firing vessel, (10) Propellant strand, (11) Stainless steel rod.

6.2.1 Firing vessel

The firing vessel was fabricated using a seamless stainless steel tube (304, 1.4301S C2, DIN 17456) with inner diameter of 50 mm and a wall thickness of 6.5 mm. The length of the firing vessel is 600 mm where the internal usable volume is 1.0 L. Calculated burst pressure is over 50 MPa which is 3.5 times more than the maximum expected operational pressure (MEOP).

A groove with 2.15 mm in width and 1.5 mm in depth was machined for placement of a snap ring for a bore diameter of 50 mm (DIN 472, Code no. INT0500) that holds the closures in place. The grooves were machined 15 mm from both ends of the tubes.

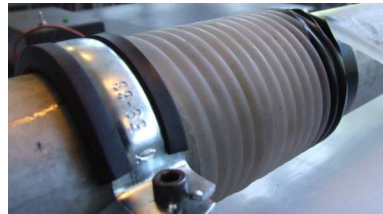


Figure 6.11: Cooling system.

A plastic hose was wrapped around the firing vessel and connected to a water outtake to cool the firing vessel down to ambient temperature after each firing. This was done to minimize the time interval between each firing since the burning of the propellant strands generates hot combustion gases, thus increasing the temperature of the firing vessel tube. The cooling system is shown in Figure 6.11

The firing vessel was filled with water and hydrostatically tested to 240 bars. A hydraulic piston pump as shown in Figure 6.12 was used to pressurize the system.



Figure 6.12: Hydraulic piston pump used for hydrostatic tests.

6.2.2 Strand holder

The front end closure was fabricated using a stainless steel round bar (304L, 1.4307 K12, BS EN10088-2). The round bar was turned down to 30 mm lengthwise and two grooves were machined for placement of o-rings (NBR-70 no. 223). Eight 3 mm diameter equally spaced holes were drilled through the closure. Stainless steel rods (SS 316 1/16 inch welding electrodes) were cut to length ranging from 80 mm to 180 mm and firmly placed and fixed by epoxy (Casco Strong Epoxy) through the eight drilled holes. This provided insulated electrical connections for thermocouples and an igniter. Electrical shrinking tubes were put around the stainless rods, which provided insulation to prevent heat generated from combustion gases to soften the epoxy in place. The epoxy joints are shown in Figure 6.13

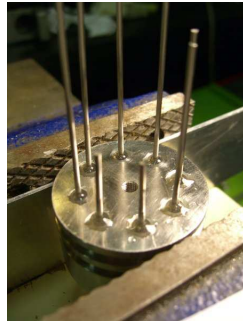


Figure 6.13: Stainless steel rods fixed in place by epoxy.

The thermocouples (K-type, 0.020 inch, OMEGA CHAL-20) were attached to the stainless steel rods by an electrical screw terminal blocks. The igniter was made of a nichrome wire (0.350 mm diameter, 14.7 Ω /m) that glows red hot when a supply voltage of 12 volts is applied. The igniter wire was attached to the stainless steel rods by electrical screw terminal blocks.

A 20 mm thick round bar of POM plastic was attached to the aft end of the strand holder closure by using M5x10 mm Allen bolt. Eight 4 mm equally spaced holes were drilled through the POM disc so it could slide through the stainless steel rods. The purpose of the POM disc was to inhibit heat from the combustion gases that could soften or melted the epoxy that was used to fasten the stainless steel rods. A M10 hole was drilled and tapped concentric of the POM round bar and to this hole a M10x40 mm Allen bolt was attached. A M3 hole was drilled and tapped at the head end of the bolt for placement of propellant strands. The strand holder was secured to the firing vessel by means of a snap ring.

The strand holder is shown in Figure 6.14 and 6.15

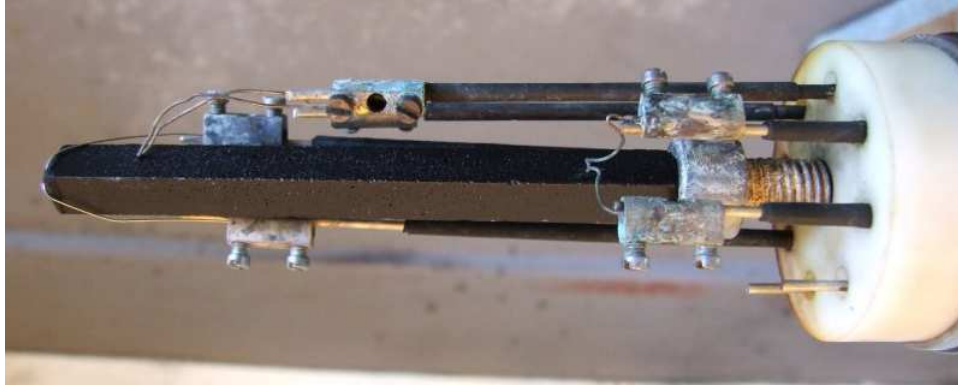


Figure 6.14: Strand holder where KN-Sorbitol propellant strand is fixed in place.

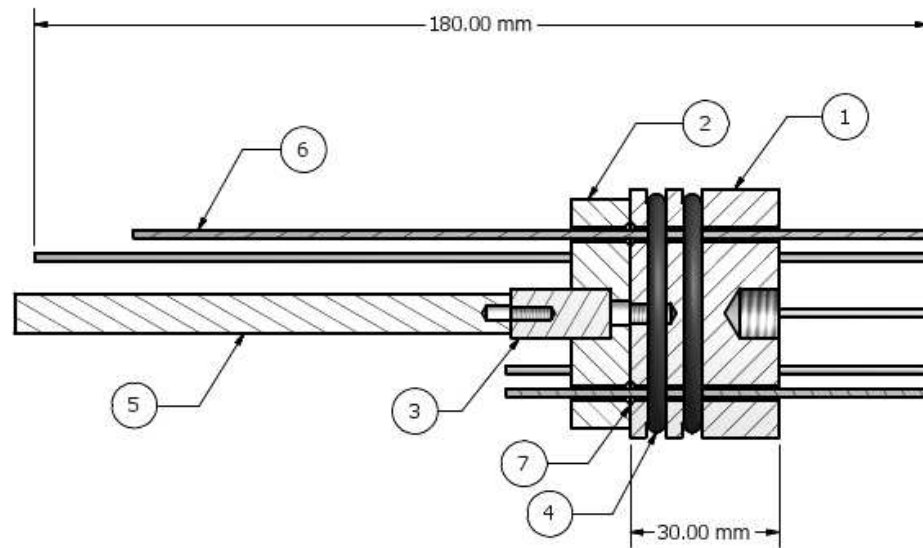


Figure 6.15: Schematic of the strand holder. (1) Stainless steel closure. (2) POM insulating disc. (3) Fixture bolt for propellant strand. (4) O-ring. (5) Propellant strand. (6) Stainless steel rod. (7) Epoxy joint.

6.2.3 Fill and exhaust line

A burst disc was added to the aft end closure coupler. A nickel diaphragm (10/6 M150W 04-05) was calibrated to burst at 15 ± 1 MPa which was 1.5 of the MEOP. This diaphragm was installed in the burst disc housing which was made of a brass round bar with minimum opening of 4.5 mm in diameter. The burst disc is shown in Figure 6.16



Figure 6.16: Burst disc housing with nickel diaphragm.

A needle valve (Swagelok SS-1RS6MM) rated to 345 bar was used to restrict the flow rate of nitrogen gas during pressurization. The needle valve is shown in Figure 6.17



Figure 6.17: Needle valve for restriction of flow rate.

A particle filter (Parker, 4A-FT4-100-BN-SS) rated to 414 bar with $100 \mu\text{m}$ 316 stainless steel filter element was used to filter or stop unwanted particles from the combustion gases of the burning propellant strands. The filter is shown in Figure 6.18.

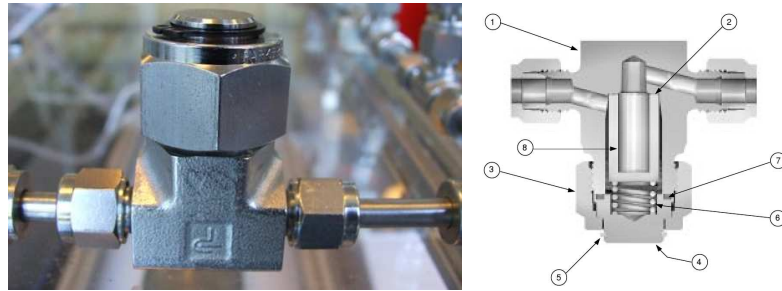


Figure 6.18: Particle filter for stopping unwanted particles of the combustion gases. The 100 μm stainless steel element is marked as number 8.

A pressure transducer (Parker, ASIC Performer, 0-100 bar) was installed on both sides of the particle filter. The purpose of having two on each side was to record any pressure drop across the filter. Measurement of the firing vessel pressure during burn was done with these pressure transducers. The pressure transducers are shown in Figure 6.19.



Figure 6.19: Pressure transducers for recording pressure during strands firing. Particle filter in between.

Visual measurement of the firing vessel pressure was done with a pressure gauge (Fimet, 0-160 bar). The accuracy of the pressure gauge was believed to be ± 2 bar and thus it was only used for measuring the pressure when

filling of the firing vessel took place and not for actual pressure recording. The pressure gauge is shown in Figure 6.20.



Figure 6.20: Pressure gauge for visual inspection of firing vessel pressure.

A proportional pressure relief valve (Swagelok SS-6R3A-MM) was used to maintain the pressure level while burning of the propellant strands took place. The relief valve opens gradually as the pressure increases by mechanical compression of a spring. The desired set pressure is adjusted by fasten or loosen the cap nut thus changing the deflection of the spring. Three springs with different compression strengths were used and rated for set pressures ranging from 3.4 to 24.1, 24.1 to 51.7 and 51.7 to 103 bars of pressure. A manual override handle was used to open the valve without changing the set pressure. A nylon hose was connected to the output port of the relief valve for escaping of gases to a fume hood. The relief valve is shown in Figure 6.21.

Releasing of nitrogen gas and combustion gases was done with an ordinary ball valve (Swagelok SS-43S6MM), rated to 207 bars of pressure. A nylon hose was connected to the output port of the relief valve for escaping of gases to a fume hood. The ball valve is shown in Figure 6.22.

Stainless steel tubes (Swagelok SS-T6M-S-1.0M-6ME) with inner diameter of 4 mm and wall thickness of 1 mm were used extensively for the fill and exhaust line. These tubes are rated to 420 bars. Stainless steel tees (Swagelok SS-6M0-3) were used when needed between individual components.

Stainless steel convoluted PTFE hose (Swagelok SS-CT8SSL8SSL8-18) was connected in between the needle valve and a nitrogen pressurized cylinder. The pressurizing gas was Instrumental nitrogen 5.0 (minimum purity 99.999%), supplied from a standard 50 L cylinder.

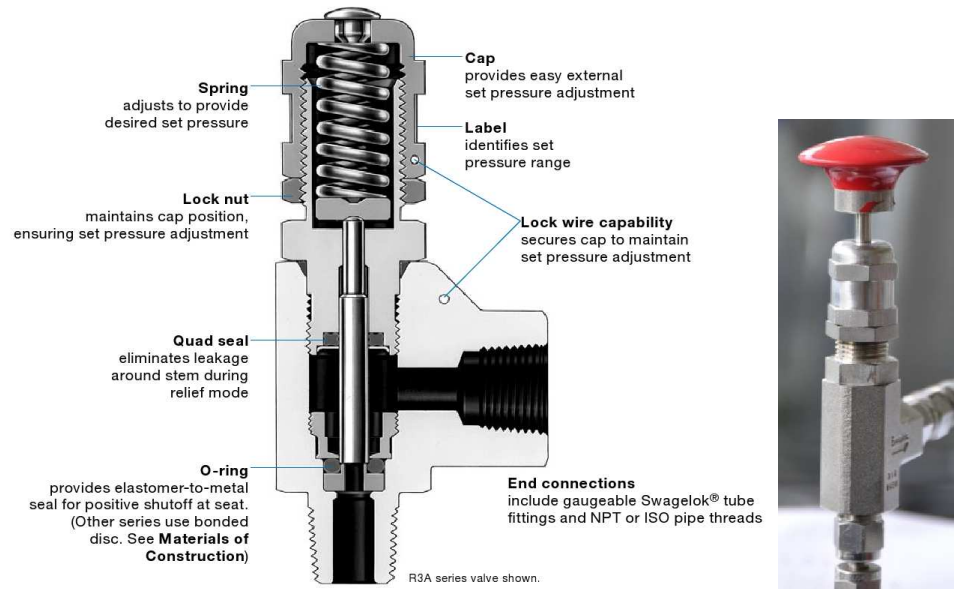


Figure 6.21: Schematic of proportional relief valve and the manual override handle.



Figure 6.22: Ball valve for releasing of nitrogen and combustion gases.

6.2.4 Structural frame

A blast proof frame was built around the firing vessel for added safety when working next to the system.

Aluminum strut profiles (BoschRexroth 3 842 517 179) were cut to sizes and connected with M6 hexagonal star socket screws (BoschRexroth 3 842 528 593) on the corners. The frame measured 60 cm in length and 20x20 cm in width and height.

Polycarbonate plates of 8 mm in thickness were cut to sizes and attached to the front and top side of the aluminum frame. The plates are blast resistant and were used for added safety.

A white polyethylene (PE300) of 10 mm in thickness was attached to the bottom side of the aluminum frame. Pipe clamps (53-65 mm) were bolted (M10x20 mm) to the polyethylene plate and the pipe clamps were firmly tighten around the firing vessel.

A MDF plate of 16 mm in thickness was cut to sizes and attached to the front end side of the aluminum frame. The purpose of having this plate was to stop the stainless steel rods from shooting across the room at high speed if the epoxy joints would suddenly give away.

The three different types of safety plates were bolted to the groove of the aluminum struts with M4x16mm 12.9 Allen bolts and a T-nut (BoschRexroth 3 842 501 751).

The bolted connections and the structural frame is shown in Figure 6.23.



Figure 6.23: Structural frame where the polycarbonate and MDF plates are connected to the aluminum strut profiles.

6.3 Electronic devices

6.3.1 Ignition box

An ignition box was made using an ordinary electrical plastic box for housing batteries, a LED, a spring back switch and two banana plugs. A total of eight rechargeable 1.2V AA NiMH batteries were used as the power source for the igniter. An ignition lead wire was connected between the ignition box and the stainless steel rods on the strand holder with the aid of crocodile clips as shown in Figure 6.26. The ignition box is shown in Figure 6.24.

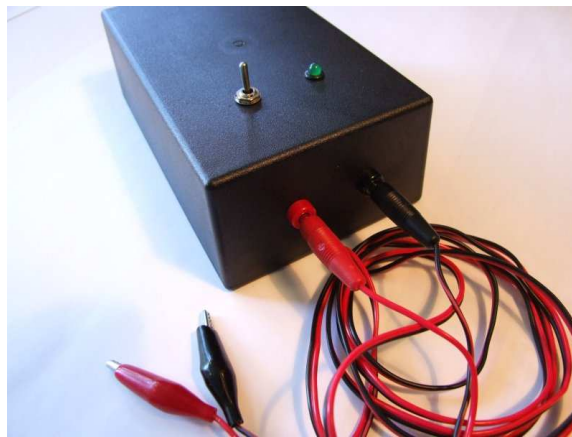


Figure 6.24: Ignition box with attached ignition lead wire.

6.3.2 Burning rate measurement

Measurement of the burning rate was done using the two thermocouples connected to the strand holder. One was attached to the strand with its bead near the upper end (nearest the igniter) and the other near the bottom end. The thermocouples lasted for approximately 20 firings and were then replaced by a new one of identical size and length.

The distance between the two thermocouples beads was measured using a digital caliber with accuracy and resolution of .01 mm. This length was recorded as the gauge length.

6.3.3 Data recording and acquisition

Data acquisition was done with the aid of a DAQ board (Linux USB-DUX-FAST) connected to a laptop (IBM ThinkPad T42p) via USB. An interface

box was made that housed the needed electrical connections for the pressure transducers and the thermocouples as shown in Figure 6.25.

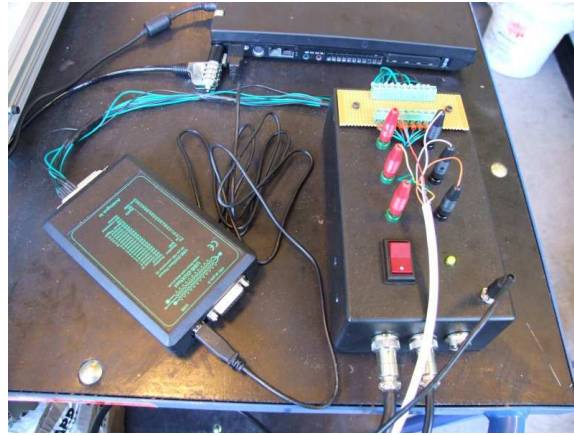


Figure 6.25: Linux USB-DUX-FAST DAQ board connected to an electrical housing box.

Connections between the stainless steel rods and the box was done with an Ethernet cable that banana plugs and crocodile clips had been attached to as shown in Figure 6.26.

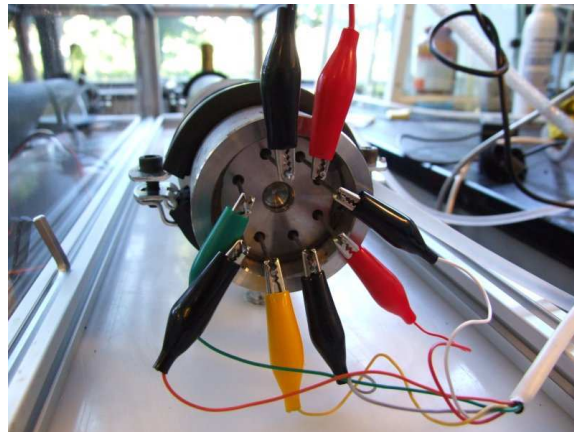


Figure 6.26: Electrical crocodile clips attached to the stainless steel rods.

Data recording was done with the aid of an open source program kTime-Trace. The program sampled the output emf (electromagnetic force) of the thermocouples and the voltage output of the pressure transducers at 3750.15 S/s.

6.4 Experimental Technique

All in all, a total of 69 strand burns were conducted, 23 KN-Sorbitol burns, 22 KN-Erythritol burns and 24 KN-Mannitol burns over the pressure range of 0 to 10 MPa. A detail listing of the usable strand burns is given in Appendix F.

Prior to burning of a strand a series of steps were followed:

- Mounting of the strand in the strand holder by screwing it in place.
- Attachment of thermocouples and igniter by carefully bending the thermocouples and igniter in place.
- Pushing the strand holder in the firing vessel and locking it in place with the snap ring.
- Attaching the crocodile clips of the thermocouples and ignition lead wires to the stainless steel rods.
- Fastening the MDF safety plate to the side of the structural frame.
- Adjusting the proportional pressure relief valve to decided set pressure.
- Pressurizing the firing vessel between two to three bars and purge. This was done two times to reduced the oxygen content inside the firing vessel.
- Pressurizing the firing vessel to the set pressure or until the proportional valve opened.
- Recording of ambient temperature and relative humidity using the multimeter.
- Data recording initiated in KTimeTrace
- Ignition of propellant strand.
- Data recording stopped.
- Ball valved opened to release nitrogen and combustion gases from the firing vessel.

6.5 Analysis

Data analysis was done with the aid of a script written in Matlab. The Matlab script is shown in Appendix A.

The voltage output recorded from the thermocouples were loaded and plotted in the form of a line graph. The graph indicates where the burn of the propellant strands reaches the two thermocouples. This was in the form of two voltage spikes, which represent the flame front reaching the first, then the second thermocouple. The time period between the spikes was taken as the time required to burn the gauge length.

Burn rate was taken as gauge length divided by the burn time.

The pressure recording of the two pressure transducer were loaded and plotted in the form of a line graph. The pressure at which burning was considered to occur was taken as the average of the recorded data points between two thermocouple spikes.

An example of a strand burn is shown in Figure 6.27. Plotted graphs of all of the strand burns are given in Appendix F.

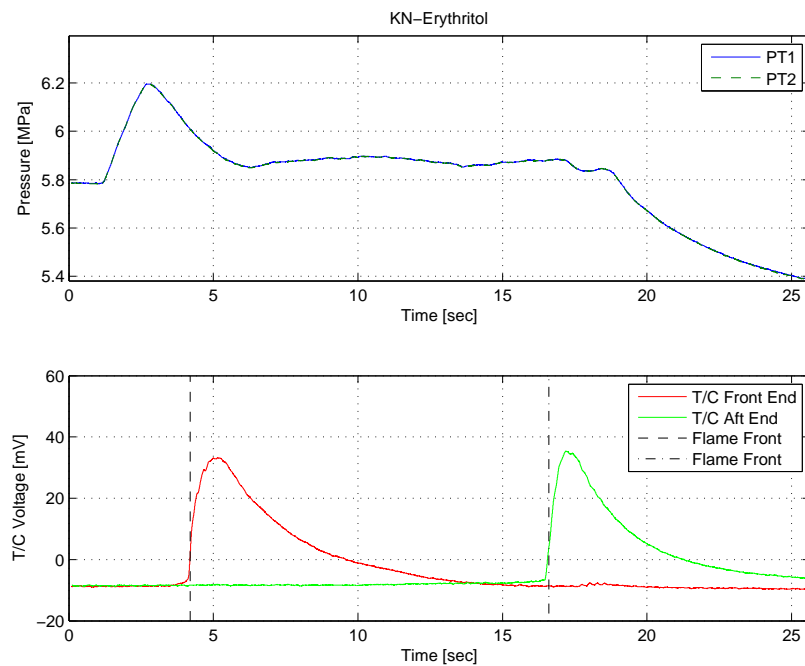


Figure 6.27: KN-Erythritol. Set pressure 6 MPa.

CHAPTER 7

Experimental results

Experimental burn rate results are given in Table 7.1 for KN-Sorbitol, KN-Erythritol and KN-Mannitol propellants.

A plot of the experimental results for KN-Sorbitol is given in Figure 7.1, for KN-Erythritol in Figure 7.2 and for KN-Mannitol in Figure 7.3.

A comparison of experimental results of the three propellant types is plotted and shown in Figure 7.4.

Log-pressure log-burn rate plots of the experimental results of the three propellant types are shown in Figures 7.5, 7.6 and 7.7.

Power law fitted curves are shown in Figures 7.8, 7.9 and 7.10, for KN-Sorbitol, KN-Erythritol and KN-Mannitol, respectively.

Burn rate coefficient a and pressure exponent n are given in Table 7.2 for KN-Sorbitol, KN-Erythritol and KN-Mannitol propellants.

The burn rate law, expressed as Vieille's law, for KN-Sorbitol, KN-Erythritol and KN-Mannitol is given in equations 7.1, 7.2 and 7.3, respectively.

KN-Sorbitol			KN-Erythritol			KN-Mannitol		
Vessel Pressure MPag	Burn Rate MPaa	Burn Rate mm/sec	Vessel Pressure MPag	Burn Rate MPaa	Burn Rate mm/sec	Vessel Pressure MPag	Burn Rate MPaa	Burn Rate mm/sec
0	0.10	3.08	0	0.10	NA	0	0.10	3.18
0.88	0.98	5.37	1.16	1.26	2.92	0.87	0.97	5.62
0.90	1.00	5.73	1.28	1.38	3.24	0.94	1.04	5.60
1.89	1.99	5.77	2.14	2.24	3.88	0.99	1.09	5.47
2.05	2.15	5.77	2.30	2.40	4.04	1.41	1.51	5.56
2.88	2.98	6.32	2.92	3.02	4.39	1.93	2.03	5.56
2.96	3.06	6.10	2.99	3.09	4.38	2.07	2.17	5.77
3.80	3.90	6.65	3.80	3.90	5.02	2.92	3.02	6.07
3.95	4.05	6.66	3.93	4.03	4.95	2.99	3.09	6.12
5.00	5.10	7.25	5.01	5.11	5.72	3.83	3.93	6.29
5.02	5.12	7.64	5.09	5.19	6.27	3.85	3.95	7.00
5.89	5.99	7.40	5.88	5.98	5.49	4.69	4.79	7.33
6.01	6.11	7.74	5.92	6.02	6.02	4.77	4.87	6.70
7.02	7.12	7.22	6.87	6.97	6.08	5.87	5.97	7.48
7.05	7.15	7.87	6.90	7.00	5.82	5.97	6.07	7.61
7.78	7.88	8.27	7.87	7.97	6.57	6.88	6.98	7.44
7.83	7.93	7.99	7.88	7.98	6.19	6.88	6.98	8.30
9.05	9.15	8.56	8.73	7.83	6.73	6.91	7.01	8.11
9.07	9.17	8.68	9.66	9.76	6.94	7.74	7.84	7.96
9.59	9.69	8.76	9.16	9.26	7.47	7.78	7.88	8.25
9.65	9.75	8.41	9.98	10.08	7.30	8.98	9.08	8.61
10.08	10.18	8.87	10.05	10.15	7.22	9.01	9.11	8.85
10.28	10.38	8.76				10.18	10.28	8.60
						10.19	10.29	8.93

Table 7.1: Experimental results for KN-Sorbitol, KN-Erythritol and KN-Mannitol propellants. Vessel pressure shown as gauge and absolute pressures.

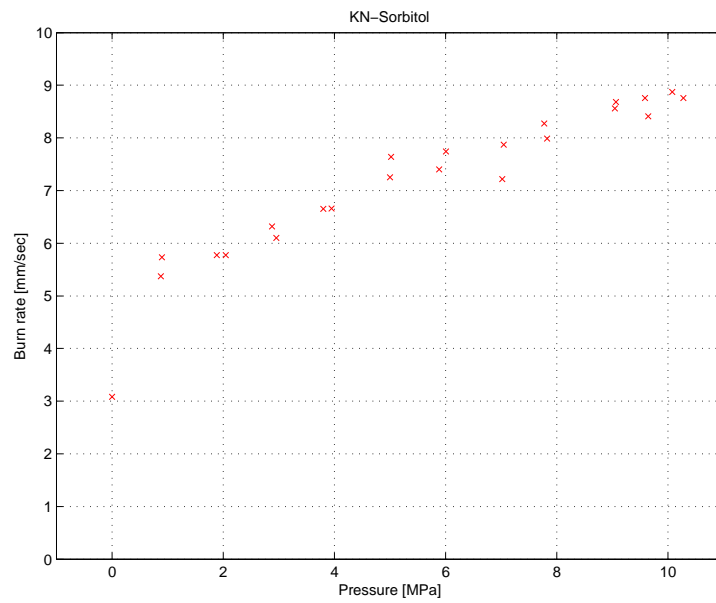


Figure 7.1: Experimental results for KN-Sorbitol propellant.

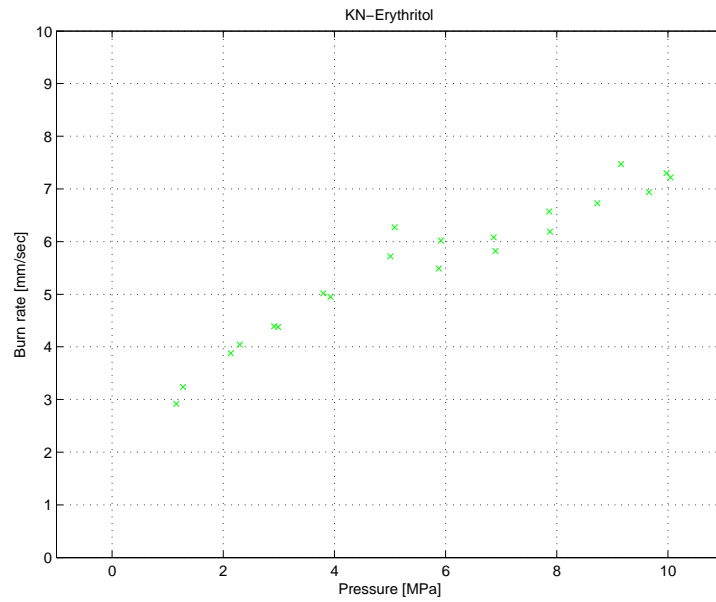


Figure 7.2: Experimental results for KN-Erythritol propellant.

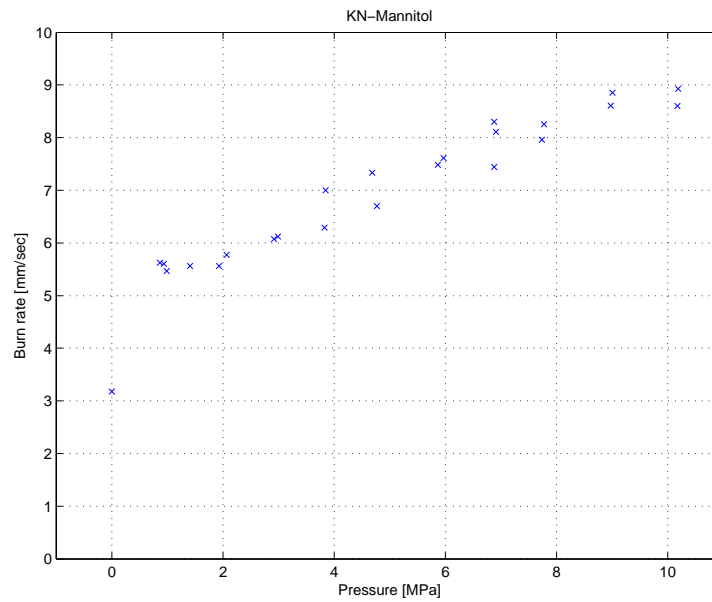


Figure 7.3: Experimental results for KN-Mannitol propellant.

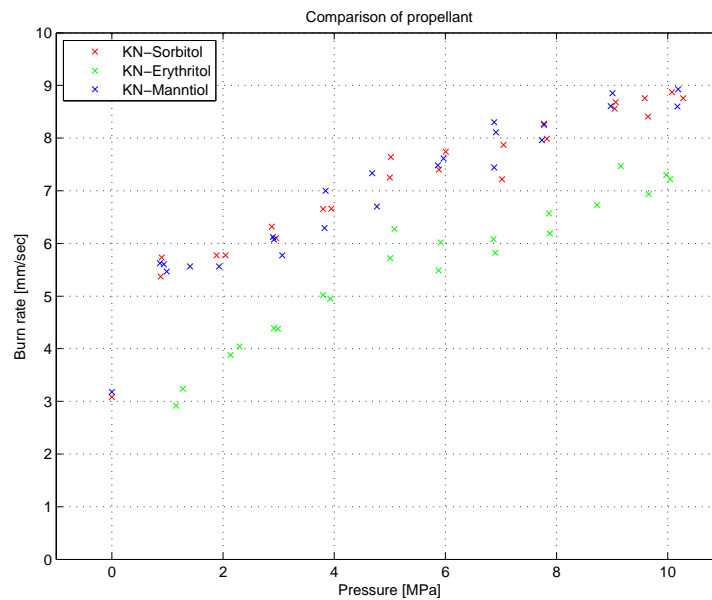


Figure 7.4: Comparison of experimental results for KN-Sorbitol, KN-Erythritol and KN-Mannitol propellants.

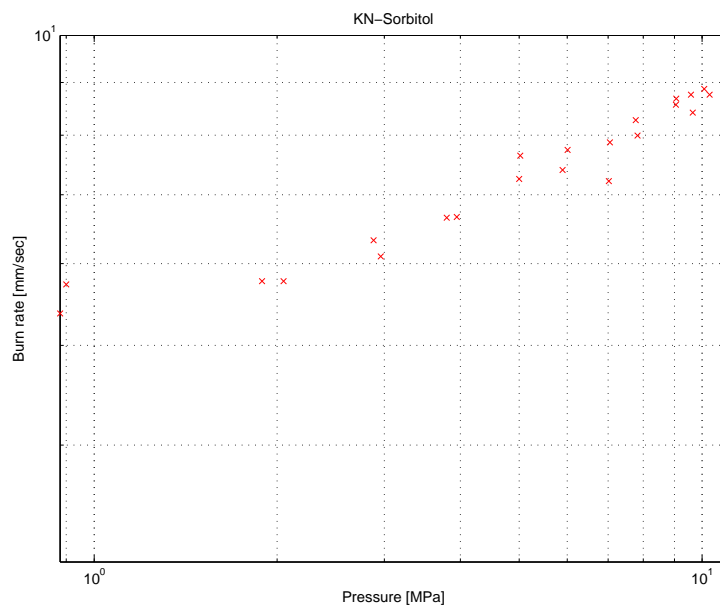


Figure 7.5: Log-log plot of experimental results for KN-Sorbitol.

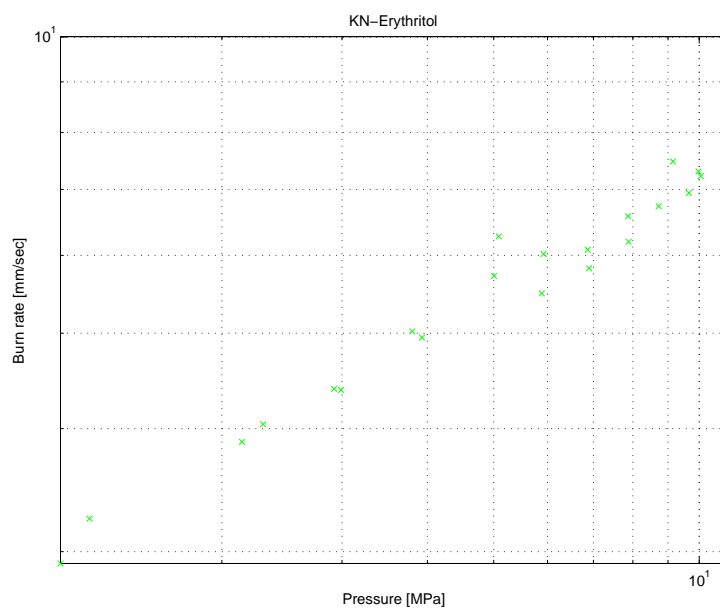


Figure 7.6: Log-log plot of experimental results for KN-Erythritol.

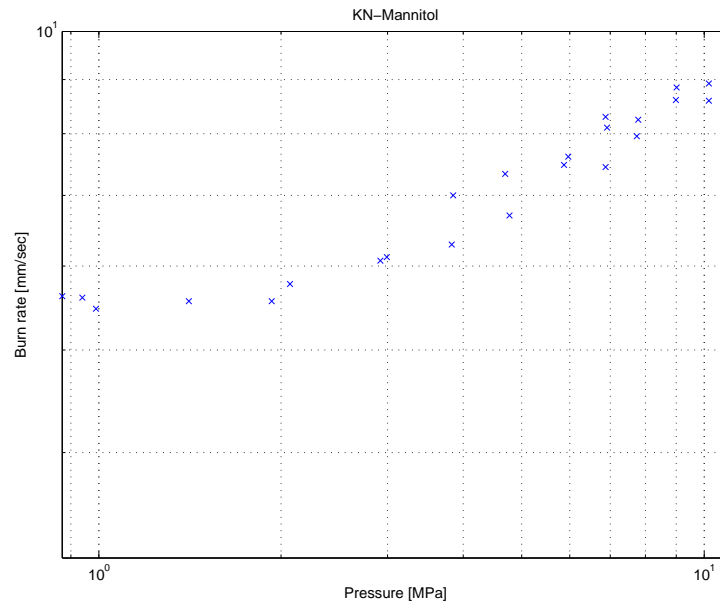


Figure 7.7: Log-log plot of experimental results for KN-Mannitol.

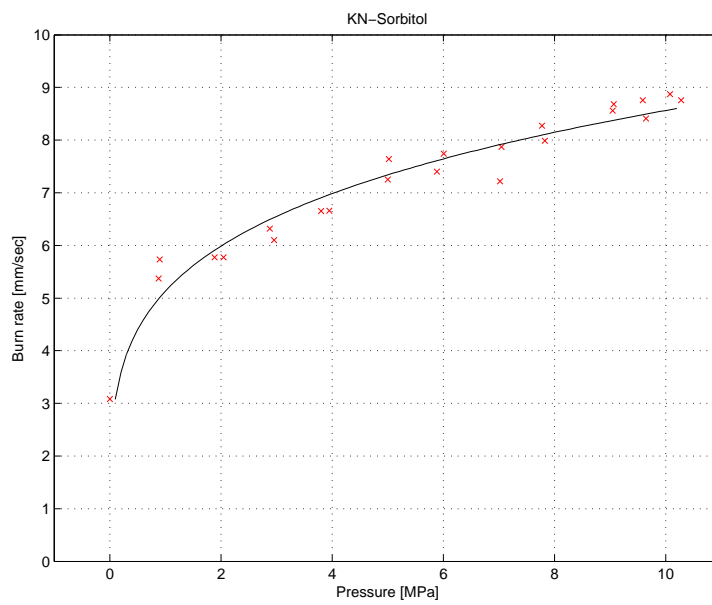


Figure 7.8: Experimental results for KN-Sorbitol with a fitted power law curve.

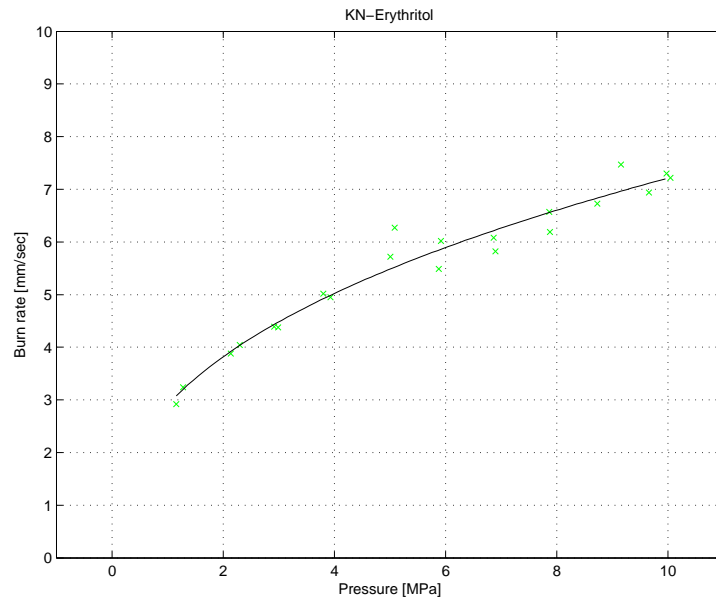


Figure 7.9: Experimental results for KN-Erythritol with a fitted power law curve.

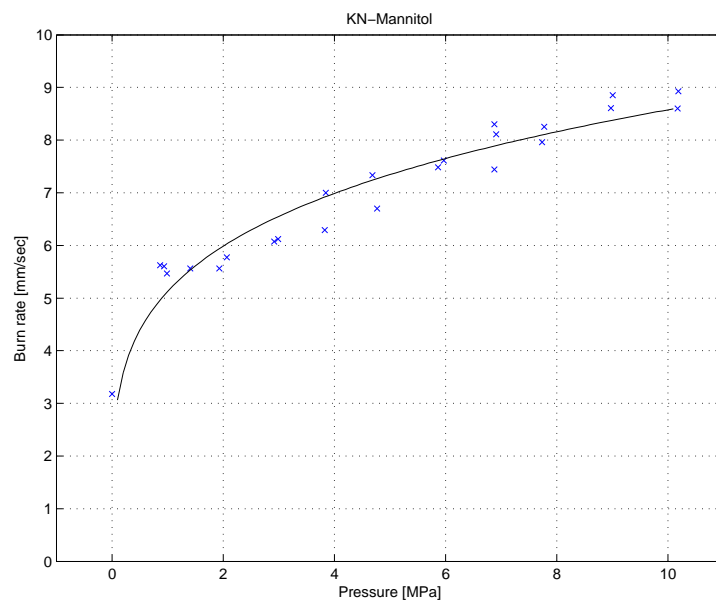


Figure 7.10: Experimental results for KN-Mannitol with a fitted power law curve.

	a	n
	mm/sec/MPa	
KN-Sorbitol	5.132	0.222
KN-Erythritol	2.903	0.395
KN-Mannitol	5.126	0.224

Table 7.2: Burn rate coefficient (a) and pressure exponent (n) for KN-Sorbitol, KN-Erythritol and KN-Mannitol propellant.

$$r = 5.132P^{0.222} \quad \text{KN-Sorbitol} \quad (7.1)$$

$$r = 2.903P^{0.395} \quad \text{KN-Erythritol} \quad (7.2)$$

$$r = 5.126P^{0.224} \quad \text{KN-Mannitol} \quad (7.3)$$

CHAPTER 8

Performance estimation of solid rocket motors

8.1 Ideal performance

Exhaust and characteristic velocity as well as the specific impulse of an ideal rocket motor can be estimated using the results of the thermodynamic properties described in chapter 3 and 5. The specific heat ratios, exhaust and characteristic velocity, and the specific impulse are given in Table 8.1.

The ideal performance calculations are given in Appendix A in the form of a Matlab script.

	KN-Sorbitol	KN-Erythritol	KN-Mannitol	
T_c	1600	1608	1637	K
γ_{gas}	1.2391	1.2416	1.2376	
γ_{mix}	1.1361	1.1390	1.1362	
γ_{2ph}	1.0423	1.0425	1.0427	
v_e	1609	1639	1628	m/s
I_{sp}	164	167	166	s
c^*	908	925	920	m/s

Table 8.1: Ideal performance estimation of KN-Sorbitol, KN-Erythritol and KN-Mannitol at 6.89 MPa.

8.2 Comparison of a rocket motor performance

Estimation of the ideal steady state chamber pressure for a given motor can be found by using equation 4.4. A comparison of the chamber pressure from an actual motor firing and the ideal chamber pressure is shown in Figure 8.1. Recorded chamber pressure of the Globos flight motor was used as a reference. The rocket Globos was launched in 2009 by the author to 2700 meters and 1000 km/h using KN-Erythritol propellant. Details of the rocket are not explained since it is beyond the scope of this report. The parameters of the rocket are though given in Appendix A in the form of a Matlab script. The geometrical parameters are given in Table 8.2

Estimation of the ideal chamber pressure of the Globos flight motor is detailed in Appendix A in the form of a Matlab script. The script was generated with the aid of the Solid Rocket Motor (SRM) spreadsheet published by Richard Nakka (14).

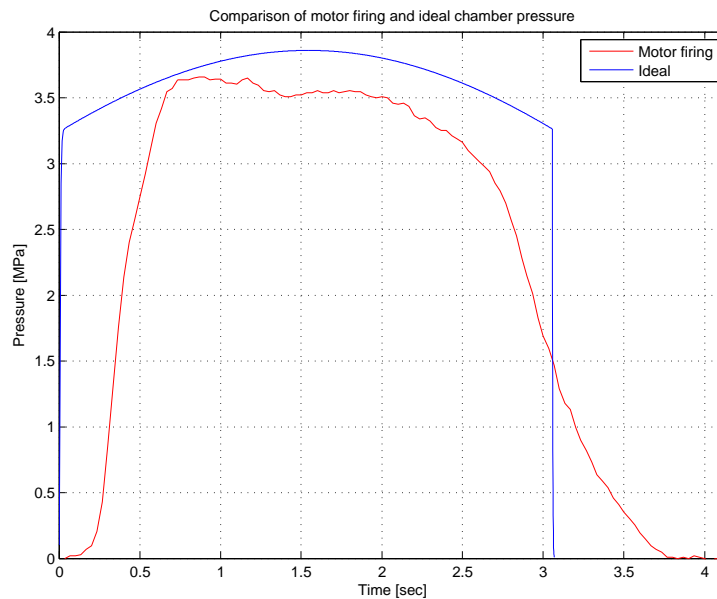


Figure 8.1: Comparison of recorded and ideal chamber pressure of the KN-Erythritol Globos flight motor.

8.3 Comparison of burning rate

The method of pressure-time trace (16) was used to estimate the burning rate of the KN-Erythritol propellant of the Globos flight motor firing. The estimated burning rate is shown in Figure 8.2.

The estimated burning rate of the Globos flight motor was compared with the strand burn measurements. This comparison is shown in Figure 8.3.

Pressure-time trace calculations are given in Appendix A.

Globos flight motor		
Segment diameter	50	mm
Segment core diameter	20.5	mm
Segment length	85	mm
No. segments	9	
Mass of propellant	2.057	kg
Nozzle throat diameter	15.3	mm
Nozzle exit diameter	39.0	mm
Nozzle expansion ratio	6.5	

Table 8.2: Geometrical parameters of the Globos flight motor.

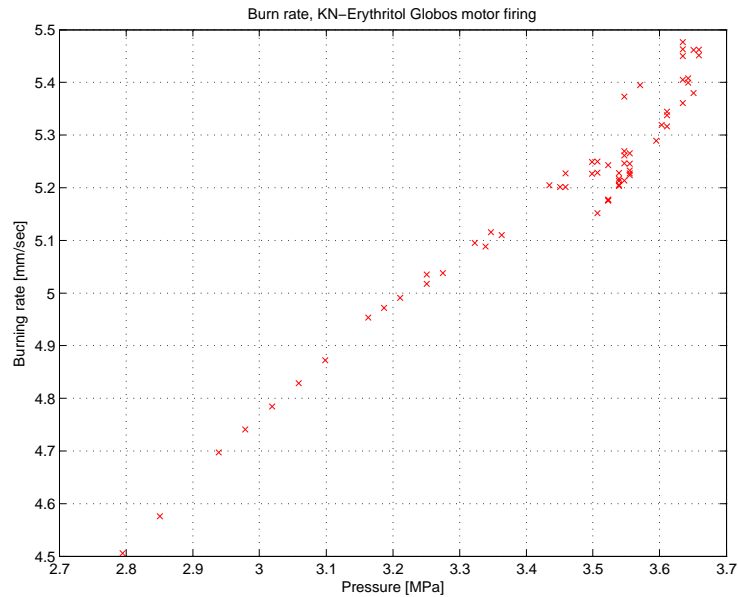


Figure 8.2: Estimation of burn rate of KN-Erythritol Globos flight motor using the pressure-time trace method.

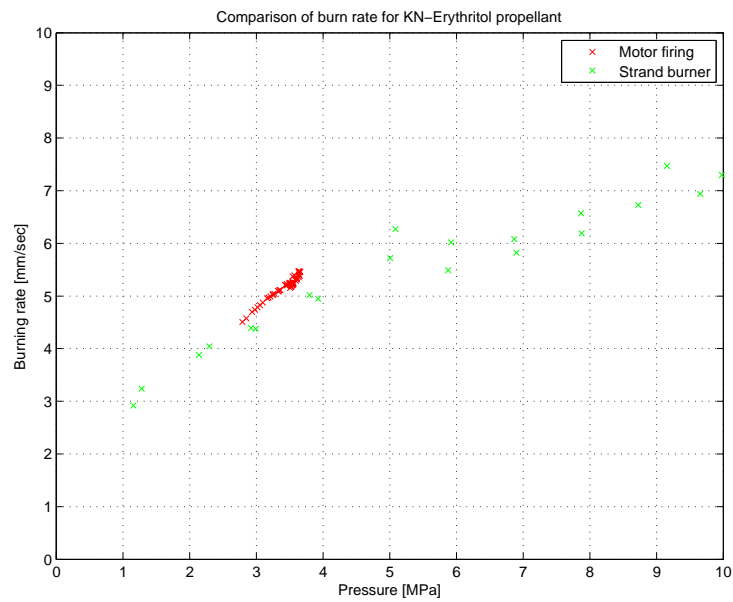


Figure 8.3: Comparison of burn rate results from strand burner and the KN-Erythritol Globos flight motor.

CHAPTER 9

Discussion

Burning rates of KN-Erythritol is about 20-25 % lower than burning rates of KN-Sorbitol and KN-Mannitol propellants. The burn rate of KN-Sorbitol and KN-Mannitol is near to identical at pressures ranging from 0 to 10 MPa. The explanation of the difference in burning rate can be related to the fact that Erythritol has a lower molecular weight and is short of two carbon atoms, four hydrogen atoms and two oxygen atoms. This behavior is though not understood.

KN-Sorbitol burning rates published by Nakka (13) indicates a faster rate of burning than the experimental results shown in chapter 7. It is believed that the smaller particle size of 60 to 125 microns, used by Nakka, is the main factor. The dessicated potassium nitrate might also affect of the burn rate.

A pressure drop was noticed at the particle filter when strands were burned at pressures ranging from 0-30 bar. Incomplete combustion at lower pressure and thus resulting in solid particles traveling to the particle filter can possibly explain the pressure drop. Condensation at the particle filter element of denser gaseous combustion products at lower pressures might also explain the pressure drop.

Some inconsistency was noticeable when comparing strand burns at the same pressure. Up to 10 % deviation was recorded. It is believed that the deviation was a results of non-perpendicular burn of the propellant strand thus leading to a default in burn time reading.

Burn rate measurement of KN-Erythritol at ambient pressure failed due to

self-extinguishing of the propellant strand. This combustion behavior at ambient pressure is not yet known.

9.1 Technical obstacles

A number of technical obstacles had to be addressed and are given below.

9.1.1 Casting mold

Prior to the successful construction and use of the PTFE casting mold a casting mold was fabricated using POM plastic. The sugar propellants had tendency to stick to the POM plastic and thus this approach was discontinued.

9.1.2 Ignition of strands

A Different method was carried out of igniting the propellant strands prior to the successful H3 coating of the tip. A nichrome wire was placed to the bare tip of a propellant strand. This method ignited the propellant but it was later discovered that the burn was not perpendicular to the long axis of the strands but rather in a diagonal way. This lead to a default reading of the burn rate due to the fact that the flame front reached the bead of the T/C wire in a wrong way.

9.1.3 Inhibiting of propellant strands

Investigations of three different coatings of inhibitor were performed. A low viscosity epoxy (West system 205) was coated with paint brush on the propellant strands and let dry for minimum of 24 hours. Ignition of the strands were successful but due to extensive amount of soot in the firing vessel this approach was discontinued.

Propellant strands were dipped into sodium silicate solution and let dry for 24 hours. The cured sodium silicate coating had low bonding effect to the propellant strands and thus the use of it was discontinued.

The coating of high temperature BBQ spray paint was found to be the best of the three and was used solely after trials and errors of the two inhibiting substances.

CHAPTER 10

Conclusion

10.1 Conclusions

Burn rate coefficient a and pressure exponent n have been determined for the KN-Sorbitol, KN-Erythritol and KN-Mannitol solid rocket propellants.

The burn rate r for the KN-Erythritol propellant showed strong relations to a full-scale motor firing.

The design and construction of the strand burner was a success and can be used further to estimate the burning behavior of all types of sugar propellants.

Using a pressure relief valve to effectively release the combustion gases was carried out.

Inhibiting of the propellant strands showed strong consistency to controlled burn rate.

10.2 Contribution

The author believes that the results of this study can be used to extend the knowledge of sugar alcohol propellants in the field of experimental rocketry.

10.3 Future work

Ballistic evaluation motor and/or full-scale motor firings has to be performed for KN-Sorbitol and KN-Mannitol propellants to characterize the burning rates even further.

Using smaller particle size of potassium nitrate could have a noticeable effect in increasing the burn rate.

Using different composition ratios of oxidizer and fuel can give higher or lower burn rates and it would be a viable experiment to follow through.

It was sought out to measure the burn rate of KN-Isomalt and KN-Maltitol in addition to KN-Sorbitol, KN-Erythritol and KN-Mannitol but due to time restraints that was discontinued.

Bibliography

- [1] Robert A. Braeunig. Basics of space flight: Rocket propulsion. Website, 1997-2009. <http://www.braeunig.us/space/propuls.htm>.
- [2] P. Carnevalheira, G.M.H.J.L. Gadiot, and W.P.C. de Klerk. Thermal decomposition of phase-stabilised ammonium nitrate (psan), hydroxyl-terminated polybutadiene (htpb) based propellants. the effect of iron(iii) oxide burning-rate catalyst. *Thermochimica Acta*, 269-270:273–293, 1995.
- [3] David Downs Donald Chiu, Aaron Grabowsky. Closed vessel combustion of stick propellant. Technical report, U.S. Army Armament Research and Development Center, 1984.
- [4] M. E. Embuscado. *Optimizing Sweet Taste in Foods*, chapter 8, Polyols. CRC Press, 2006.
- [5] Franz R. Lynn Frederick W. Robbins. Analytic solutions to the closed bomb. Technical report, U.S. Army Laboratory Command, Ballistic Research Laboratory, 1988.
- [6] R. S. Fry. Solid propellant subscale burning rate analysis methods for us and selected nato facilities. Technical report, The Johns Hopkins University, Januar 2002.
- [7] Oscar Biblarz George P. Sutton. *Rocket Propulsion Elements*. A Wiley-Interscience Publication, 7th edition, 2001.
- [8] T. H. Grenby, K. J. Parker, M. G. Lindley, P. J. Sicard, P. Leroy, C. A. Williams, I. S. Menzies, J. D. Higginbotham, D. J. Snodin, J. W. Daniel, and A. G. Renwick. Developments in sweeteners. ii. *Developments in Sweeteners*, 2, 1983.

-
- [9] Bertram B. Grollman. Carl w. nelson. Technical report, USA Armament Research and Development Command, USA Ballistic Research Laboratory, 1977.
- [10] E. Karl Bastress Kimball P. Hall. Burning rate control factors in solid propellants. Technical report, Department of the Navy Office of Naval Research, 1960.
- [11] Stuart Leslie and James Yawn. Proposal of the inclusion of kno_3 /sugar propellants in the tra experimental rocketry program. This is, October 4th.
- [12] David R. Lide, editor. *CRC Handbook of Chemistry and Physics*. CRC Press, 2009.
- [13] Richard Nakka. Effect of chamber pressure on burning rate for the potassium nitrate-dextrose and potassium nitrate-sorbitol rocket propellants. http://www.nakka-rocketry.net/soft/ds_burn.pdf, June 1991.
- [14] Richard Nakka. Solid rocket motor design. Website, 2000. <http://www.nakka-rocketry.net/soft/SRM.zip>.
- [15] Richard Nakka. Ballistic evaluation motor. Website, 2003. <http://www.nakka-rocketry.net/burn/evmot1.gif>.
- [16] Henrik Ditlev Nissen. Non parametric burn rate estimation. Technical report, DARK, 2000.
- [17] Martin J. L. Turner. *Rocket and Spacecraft Propulsion. Principles, Practice and New Developments*. Praxis Publishing Ltd, 2nd edition, 2006.
- [18] Antoon Vyverman. The potassium nitrate-sugar propellant.
- [19] Ya-Jane Wang. *Chemical and Functional Properties of Food Saccharides*, chapter 3, Saccharides Modifications and Applications. CRC Press, 2003.

APPENDIX A

Matlab scripts and functions

A.1 Power law fitting

```
1 % Function for extrapolating a power law curve
2 function r = KNSOfun(x,P)
3 a=x(1);
4 n=x(2);
5
6 %st. Roberts law.
7 r=a*P.^n;
```

```
1 % Script for calling the extrapolating a power law curve ...
  function
2 clear all, close all, clc
3
4 % Loading of experimental results
5 load KNSO.txt
6 Pdata = KNSO(:,1); % Pressure [MPa]
7 rdata = KNSO(:,2); % Burn rate [mm/sec]
8
9 % Initial conditions
10 a0=0.1;
11 n0=0.1;
12
13 % Least square curve fit method
14 x0 = [a0,n0] % Starting guess
15 [x,resnorm] = lsqcurvefit(@KNSOfun,x0,Pdata,rdata) % ...
  Extrapolating
```

```
16
17 % Assigning a and n results
18 afit = x(1)
19 nfit = x(2)
20
21 % Making the fitted curve
22 Pfit = [min(Pdata+0.1):0.1:max(Pdata)];
23 rfit = afit*Pfit.^nfit;
24
25 % Plotting experimental results
26 figure
27 plot(Pdata,rdata,'xr')
28 hold on
29 % Plotting fitted curve
30 plot(Pfit,rfit, 'k')
31 grid
32 axis([-1 11 0 10])
33 title('KN-Sorbitol')
34 xlabel('Pressure [MPa]')
35 ylabel('Burn rate [mm/sec]')
36 print -depsc -tiff -r300 PowerKNSO
```


A.2 Experimental data analysis

```

1 % Script for analysing experimental strand burn firing
2 clear all, close all, clc
3
4 % Loading of recorded data
5 load KNSO90barH3004.txt;
6
7 % Assigning channels
8 PT1 = (KNSO90barH3004(:,1)*225.66+3.5924)*0.1; % Pressure ...
    transducer no. 1
9 PT2 = (KNSO90barH3004(:,2)*224.91+3.6697)*0.1; % Pressure ...
    transducer no. 2
10 EMF1 = KNSO90barH3004(:,3)*1000; % T/C front end
11 EMF2 = KNSO90barH3004(:,4)*1000; % T/C aft end
12
13 % Assigning sample rate and time
14 sample_rate = 3750.15; % S/s
15 samples = length(PT1); % Number of samples
16 tot_time = samples/sample_rate; % seconds
17 time = (linspace(1/sample_rate,tot_time,samples))'; % ...
    seconds
18 timeP = time; % timeP to be used later
19
20 % Filtering noise with moving average method
21 PT1 = tsmovavg(PT1, 's', 375, 1);
22 PT2 = tsmovavg(PT2, 's', 375, 1);
23 EMF1 = tsmovavg(EMF1, 's', 375, 1);
24 EMF2 = tsmovavg(EMF2, 's', 375, 1);
25 time = tsmovavg(time, 's', 375, 1);
26
27 % Adding an offset of 10 mV for minimizing problems when ...
    estimating flame front start since T/C value has often a...
    negative value
28 EMF1H = KNSO90barH3004(:,3)*1000+10;
29 EMF2H = KNSO90barH3004(:,4)*1000+10;
30 EMF1H = tsmovavg(EMF1H, 's', 375, 1);
31 EMF2H = tsmovavg(EMF2H, 's', 375, 1);
32
33 % For statement for estimating the time of when flame front ...
    reaches the front end T/C. Every 375 data point is ...
    looked at and if that data point is 1.5 times larger ...
    than the previous one then execute start point.
34 i=1;
35 j=1;
36 k=375;
37 V1 = zeros(1000,2);
38 for i=(k+1):k:length(EMF1H)-(k+1)
39     if EMF1H(i+k)>1.5*EMF1H(i)
40         V1(j,1) = (i+k)/sample_rate;
41         V1(j,2) = EMF1H(i+k);
42         j=j+1;

```

```

43     end
44 end
45 xstartTC1= V1(1,1)
46
47 % Flame front of the aft end T/C.
48 i=1;
49 j=1;
50 V2 = zeros(1000,2);
51 for i=(k+1):k:length(EMF2H)-(k+1)
52     if EMF2H(i+k)>1.5*EMF2H(i)
53         V2(j,1) = (i+k)/sample_rate;
54         V(j,2) = EMF2H(i+k);
55         j=j+1;
56     end
57 end
58 xstartTC2= V2(1,1)
59
60 % Plotting
61 figure
62 subplot(2,1,1)
63 plot(timeP, PT1, timeP, PT2,'--')
64 axis([0 max(time) min(PT2) max(PT1)+0.2])
65 grid
66 title('KN-Sorbitol')
67 xlabel('Time [sec]')
68 ylabel('Pressure [MPa]')
69 legend('PT1','PT2')
70 subplot(2,1,2)
71 plot(timeP, EMF1, 'r')
72 grid
73 hold on
74 plot(timeP,EMF2, 'g')
75 axis([0 max(time) -20 60])
76 xlabel('Time [sec]')
77 ylabel('T/C Voltage [mV]')
78 plot([xstartTC1,xstartTC1],[-20,60],'k--')
79 hold on
80 plot([xstartTC2,xstartTC2],[-20,60],'k-.')
81 legend('T/C Front End','T/C Aft End','Flame Front', 'Flame ...
      Front')
82 hold off
83 print -depsc -tiff -r300 KNSO90barH3004
84
85 % Mean value of pressure
86 xstart1PT1 = xstartTC1*sample_rate;
87 xstart2PT1 = xstartTC2*sample_rate;
88 MeanPressure = mean(PT1(xstart1PT1:xstart2PT1))
89
90 % Standard deviation
91 Z = PT1(xstart1PT1:xstart2PT1);
92 Y = std(Z,1);
93
94 %Plotting burning pressure range
95 figure

```

```
96 plot(time(xstart1PT1:xstart2PT1),PT1(xstart1PT1:xstart2PT1))
97 grid
98 xlabel('Time [sec]')
99 ylabel('Pressure [MPa]')
100
101 % Burn Rate
102 BurnTime = xstartTC2-xstartTC1 % Time between T/C spikes [...
    sec]
103 L = 60.76; % Gauge length [mm]
104 r = L/BurnTime % Burn rate [mm/sec]
```

A.3 Combustion of sugar rocket propellant

```

1  %Estimation of specific heat capacities for phases of gas, ...
    condensed and
2  %mixtures
3  %Ideal Isp and Cstart calculated using the value of gamma
4
5  clear all
6  close all
7  clc
8
9  %KN-Sorbitol
10
11 %Thermodynamic constants
12 Tc = 1601; %Combustion temperature, K
13 R_gas = 8.314; %Universal gas constant, J/kmol K
14
15 %Forces and pressures
16 g = 9.806; %Gravitational constant
17 Pe = 1; %Exit pressure, atm
18 Pc = 68; %Ambient pressure, atm
19
20 %Number of gas moles per product
21 nH2O = 0.92723;
22 nN2 = 0.32131;
23 nCO = 0.47791;
24 nH2 = 0.41171;
25 nKOH = 0.01088;
26 nCO2 = 0.35899;
27
28 %Number of condensed moles
29 nK2CO3 = 0.31572;
30
31 MWK2CO3 = 138.21; %Molecular weight of potassium carbonate,...
    g/mol
32 m = 100; %Mass of propellant mix, g
33 ngas = nH2O+nN2+nCO+nH2+nKOH+nCO2; %Total number of gas ...
    moles
34 X = nK2CO3*MWK2CO3/100; %Mass fraction
35 M = m/ngas; %Effective molecular weight
36
37 %Specific heat capacity of the gas products using Shomate ...
    Equation
38 T = Tc/1000; %Temperature input for Shomate Equation
39
40 %H2O, range 500-1700
41 A = 30.09200;
42 B = 6.832514;
43 C = 6.793435;
44 D = -2.534480;
45 E = 0.082139;
46 Cp_H2O = A + B*T + C*T^2 + D*T^3 +E/T^2;

```

```

47
48 %N2, range 500-2000K
49 A = 19.50583;
50 B = 19.88705;
51 C = -8.598535;
52 D = 1.369784;
53 E = 0.527601;
54 Cp_N2 = A + B*T + C*T^2 + D*T^3 +E/T^2;
55
56 %CO, range 1300-6000K
57 A = 35.15070;
58 B = 1.300095;
59 C = -0.205921;
60 D = 0.013550;
61 E = -3.282780;
62 Cp_CO = A + B*T + C*T^2 + D*T^3 +E/T^2;
63
64 %H2, range 1000-2500
65 A = 18.563083;
66 B = 12.257357;
67 C = -2.859786;
68 D = 0.268238;
69 E = 1.977990;
70 Cp_H2 = A + B*T + C*T^2 + D*T^3 +E/T^2;
71
72 %KOH, range 2000-6000K
73 A = 49.48500;
74 B = 7.051337;
75 C = -1.412548;
76 D = 0.097243;
77 E = -0.245887;
78 Cp_KOH = A + B*T + C*T^2 + D*T^3 +E/T^2;
79
80 %CO2, range 1200-6000K
81 A = 58.16639;
82 B = 2.720074;
83 C = -0.492289;
84 D = 0.038844;
85 E =-6.447293;
86 Cp_CO2 = A + B*T + C*T^2 + D*T^3 +E/T^2;
87
88 %K2CO3, range 1300-2500, JANAF;
89 Cs_K2CO3 = 209.20;
90
91 %Specific heat capacity of gas phase at combustion ...
    temperature
92 Cpgas = 1/ngas *( (nH2O*Cp_H2O) + (nN2*Cp_N2) + (nCO*Cp_CO) ...
    + (nH2*Cp_H2) + (nKOH*Cp_KOH) + (nCO2*Cp_CO2));
93
94 %Specific heat capacity of gas phase + condensed phase at ...
    combustion temperature
95 Cpmix = 1/ngas *( (nH2O*Cp_H2O) + (nN2*Cp_N2) + (nCO*Cp_CO) ...
    + (nH2*Cp_H2) + (nKOH*Cp_KOH) + (nCO2*Cp_CO2) + nK2CO3*...
    Cs_K2CO3);

```

```
96
97 psi = X/(1-X);
98
99 %Specific heat ratio
100 gamma_gas = Cpgas / (Cpgas-R_gas); %gas phase
101 gamma_mix = Cpmix / (Cpmix-R_gas); %gas+condensed phase
102 gamma_2ph = gamma_gas * ( (1+psi*(Cs_K2CO3/Cpgas))/((1+...
    gamma_gas*psi*(Cs_K2CO3/Cpgas))) ); %Two phase flow
103
104 %ideal Isp
105 R_gas = R_gas*1000;
106 Isp = (1/g) * sqrt( (2*gamma_2ph)/(gamma_2ph-1) * (R_gas*Tc)...
    /(M) * (1-(Pe/Pc)^((gamma_2ph-1)/(gamma_2ph))) )
107
108 %Characteristic velocity
109 R = R_gas/M;
110 Cstar = sqrt((R*Tc)/(gamma_mix*(2/(gamma_mix+1))^((gamma_mix...
    +1)/(gamma_mix-1))))
111
112 %Exhaust velocity
113 ve = sqrt( ((2*gamma_2ph)/(gamma_2ph-1)) * ((R_gas*Tc)/(M)) ...
    * (1-(Pe/Pc)^((gamma_2ph-1)/gamma_2ph)))
```

A.4 Ideal performance calculations

```

1  %Motor performance estimation using known values of burn ...
   rate coefficient (a) and pressure exponent (n) of ...
   propellant to calculate the ideal chamber pressure, ...
   thrust and thus total impulse and specific impulse.
2  %This matlab script is based on Richard Nakka's SRM ...
   spreadsheet
3
4  clear all
5  close all
6  clc
7
8  %KN-Erythritol
9
10 %Thermodynamics parameters
11 gamma_gas = 1.2416; %Ratio of specific heat capacity, gas
12 gamma_mix = 1.1390; %Ratio of specific heat capacity, ...
   mixture
13 gamma_2ph = 1.0425; %Ratio of specific heat capacity, two ...
   phase flow
14 R_gas = 8314; %Universal gas constant, J/kmol K
15 M = 38.57; %Effective molecular weight of combustion ...
   products, kg/kmol
16 R = R_gas/M; %Specific gas constant, J/Kg K
17 T_0 = 1608; %Ideal combustion temperature, K
18
19 %Nozzle parameters
20 A_t = 15.3^2*pi/4*1E-6; %Nozzle throat cross-sectional area,...
   m^2
21 A_e = 39^2*pi/4*1E-6; %Nozzle exit cross-sectional area, m^2
22 N_exp = A_e/A_t; %Nozzle expansion ratio
23 P_e = 0.101; %Nozzle exit pressure, MPa
24 %P_e = 1; %Nozzle exit pressure, atm
25 C_f = 1.5; %Nozzle thrust coefficient
26
27 %Propellant parameters
28 rho_p = 1.730; %Propellant density, kg/L
29 a = 2.9025; %Burn rate coefficient, mm/s
30 n = 0.3952; %Pressure exponent
31
32 %Segment parameters
33 N = 9; %Number of segments
34 D = 50; %Segment outside diameter, mm
35 d_0 = 20.5; %Segment initial core diameter, mm
36 L_0 = 85; %Segment initial length, mm
37
38 %Chamber parameters
39 V_c = N*((pi/4) * D^2 * L_0); %Chamber volume (empty), mm^3
40
41 %Surface regression
42 %Row vector of 1000 linearly equally spaced points

```

```

43 s = linspace(0, ((D-d_0)/2), 1000);
44 inc=s(2)-s(1); %Surface regression, mm
45
46 %Burning area of bates segments, Ab(s)
47 d = d_0+2*s; %Instantaneous core diameter, mm
48 L = L_0-2*s; %Instantaneous length, mm
49 A_b = pi*N* (0.5* (D^2-d.^2) + L.*d); %Burning area, mm^2
50
51 %Initial chamber pressure, MPa
52 P_a = 0.101; %Ambient pressure, MPa
53 P_0(1)=P_a;
54
55 %Characteristic exhaust velocity, assuming combustion ...
    efficiency of 1, m/s
56 Cstar = sqrt((R*T_0)/(gamma_mix*(2/(gamma_mix+1))^(...
    gamma_mix+1)/(gamma_mix-1))))
57
58
59 %For statement to calculate the ideal steady-state chamber ...
    pressure
60 for i=1:length(s)
61     if i==1
62         r(i)=a*P_a^n; %Initial burn rate, mm/s
63         t(i)=0; %Initial time, sec
64     else
65         r(i)=a*P_0(i-1)^n; %Burn rate, mm/s
66         t(i)=(inc/r(i)) +t(i-1); %Burn time, sec
67     end
68     %Instantaneous volume of segments, m^3
69     V_seg(i) = N * pi/4 * (D^2-d(i).^2).*L(i).*1E-9;
70     V_free(i) = V_c*1E-9-V_seg(i); %Free volume in chamber,m...
        ^3
71     m_seg(i) = rho_p*V_seg(i)*1E3; %Mass of propellant ...
        segments, kg
72     if i==1;
73         m_gen(i)=0; %
74         m_noz(i)=0;
75     else
76         %Mass generation rate of combustion product, kg/s
77         m_gen(i) = (m_seg(i-1)-m_seg(i)) / (t(i)-t(i-1));
78         %Mass flow (through nozzle), Kg/s
79         m_noz(i) = (P_0(i-1)-P_a)*A_t*1E6 * sqrt(gamma_mix/(...
            R*T_0))*(2/(gamma_mix+1))^((gamma_mix+1)/(2*(...
            gamma_mix-1)));
80     end
81     %Mass storage rate of combustion products (in chamber), ...
        Kg/s
82     m_sto(i) = m_gen(i)-m_noz(i);
83     if i==1;
84         mass_sto(i)=0;
85     else
86         %Mass of combustion products stored in chamber, Kg
87         mass_sto(i) = m_sto(i)*(t(i)-t(i-1)) + mass_sto(i-1)...
            ;

```



```

88     end
89     %Density of combustion products in chamber, Kg/m^3
90     rho_prod(i) = mass_sto(i)/V_free(i);
91     %Steady-state chamber pressure, MPa
92     P_0(i)=(rho_prod(i)*R*T_0+P_a*1E6)*1E-6;
93 end
94
95
96 %Tail-off chamber pressure
97 Pbout = P_0(length(P_0));
98 t_to = [max(t):0.001:4];
99 Pc(1)=Pbout;
100 j=2;
101 while Pc(j-1)>0.01
102     Pc(j) = Pbout * exp((-R*T_0*A_t)/(V_c*Cstar)*(t_to(j)-...
103         max(t))*10E9 );
104     j=j+1;
105 end
106 t_to = t_to(1:length(Pc));
107 %Ideal thrust coefficient
108 C_F = sqrt( ((2.*gamma_2ph^2)./(gamma_2ph-1)) .* (2./(...
109     gamma_2ph+1)).^((gamma_2ph+1)./(gamma_2ph-1)) .* (1-(...
110     P_e./P_0).^((gamma_2ph-1)./(gamma_2ph))) + ((P_e./P_0)-(...
111     P_a./P_0)).*(A_e/A_t);
112
113 %Thrust
114 F = C_f*A_t*P_0*1E6;
115 Ftail = C_f*A_t*Pc*1E6;
116 samples=length(t);
117 time = max(t)
118 sample_rate = samples/time;
119 I_t = sum(F)*inv(sample_rate)
120 %I_sp = I_t/(m_seg(1)*9.81)
121 g=9.806;
122 I_sp = (1/g) * sqrt( ((2*gamma_2ph)/(gamma_2ph-1)) * ((R_gas...
123     *T_0)/(M)) * (1-(1./68).^((gamma_2ph-1)/gamma_2ph)))
124
125 %Burning surface are of propellant
126 figure
127 plot(t,A_b)
128 title('Surface area of propellant segments')
129 xlabel('Time [sec]')
130 ylabel('Surface area [mm^2]')
131
132 %Mass of propellant segments throughout the burn
133 figure
134 plot(t,m_seg)
135 title('Mass of propellant segments')
136 xlabel('Time [sec]')

```

```
137 ylabel('Propellant Mass [Kg]')
138
139 %Volume of propellant segments throughout the burn
140 figure
141 plot(t,V_seg)
142 title('Volume of propellant segments')
143 xlabel('Time [sec]')
144 ylabel('Propellant volume, m^3')
145
146
147 figure
148 plot(t,m_gen,t,m_noz)
149 title('m_gen and mnoz')
150 legend('m_{gen}', 'm_{noz}')
151 xlabel('Time [sec]')
152 ylabel('[Kg/s]')
153
154 figure
155 plot(t,m_sto)
156 title('Mass storage rate of combustion products in chamber')
157 xlabel('Time [sec]')
158 ylabel('m_{storage rate} [Kg/s]')
159
160 %Mass of combustion products in the chamber
161 figure
162 plot(t,mass_sto)
163 title('Mass of combustion products in chamber')
164 xlabel('Time [sec]')
165 ylabel('m_{product} [Kg]')
166
167 %Density of combustion products in the chamber
168 figure
169 plot(t,rho_prod)
170 title('Density of combustion products in chamber')
171 xlabel('Time [sec]')
172 ylabel('\rho_{product} [Kg/m^3]')
173
174 %Ideal thrust coefficient
175 figure
176 plot(t,C_F)
177 title('Ideal thrust coefficient, C_F')
178 xlabel('Time [sec]')
179 ylabel('Thrust coefficient')
180
181
182 %Ideal chamber pressure
183 figure
184 plot(t,P_0)
185 hold on
186 plot(t_to,Pc)
187 title('Ideal chamber pressure, P_c')
188 xlabel('Time [sec]')
189 ylabel('Chamber pressure [MPa]')
190
```

```
191 %Ideal thrust
192 figure
193 plot(t,F)
194 hold on
195 plot(t_to,Ftail)
196 title('Ideal thrust')
197 xlabel('Time [sec]')
198 ylabel('Newton [N]')
```

A.5 Pressure-time trace

```
1 clear all
2 close all
3 clc
4
5 %Pressure time trace method to estimate the burn rate ...
   behaviour of
6 %KN-Erythritol propellant using static test no. xxx of the ...
   Globos rocket
7
8 clear all
9 close all
10 clc
11
12 load PcGlobos.txt
13 load KNER.txt
14 load IdealPc.txt
15 load Idealtime.txt
16 load IdealPc_to.txt
17 load Idealtime_to.txt
18 Pc = (PcGlobos(:,1)-2.5635E-02)*2/10*40;
19 %Pc = (Pc(:,1))*2/10*40;
20 Pstrand = KNER(:,1);
21 rstrand = KNER(:,2);
22 PcIdeal = IdealPc(:,1);
23 timeIdeal = Idealtime(:,1);
24 time_toIdeal = Idealtime_to(:,1);
25 Pc_toIdeal = IdealPc_to(:,1);
26
27 sample_rate = 30; % Hertz
28 samples = length(Pc);
29 tot_time = samples/sample_rate; % seconds
30 time = linspace(1/sample_rate,tot_time,samples); % seconds
31
32 figure
33 plot(time, Pc, 'r')
34 grid
35 axis([0 4 0 4])
36 title('Recorded chamber pressure, KN-Erythritol Globos motor...
   firing')
37 xlabel('Time [sec]')
38 ylabel('Chamber pressure [MPa]')
39 print -depsc -tiff -r300 GlobosChamberPressure
40
41
42
43 figure
44 plot(time,Pc,'r')
45 hold on
46 plot(timeIdeal, PcIdeal,'b')
47 hold on
```

```

48 plot(time_toIdeal, Pc_toIdeal, 'b')
49 grid
50 axis([0 max(time) 0 4])
51 legend('Motor firing', 'Ideal')
52 title('Comparison of motor firing and ideal chamber pressure...
      ')
53 xlabel('Time [sec]')
54 ylabel('Pressure [MPa]')
55 print -depsc -tiff -r300 ComparisonGlobosIdeal
56
57 %Cstar
58 At = 15.3^2*pi/4; %Nozzle throat cross-sectional area
59 mp = 2.057; %Mass of propellant
60 cstar = At/mp * inv(sample_rate)*(sum(Pc))% m/sec
61 %cstar = At/mp * 1/sample_rate*trapz(Pc(1:124))% m/sec
62
63 %Defining the region of steady state pressure
64 Pc = Pc(20:82);
65
66 %New time
67 sample_rate = 30; % Hertz
68 samples = length(Pc);
69 tot_time = samples/sample_rate; % seconds
70 time = linspace(1/sample_rate, tot_time, samples); % seconds
71 dt = time(2)-time(1);
72
73 figure
74 plot(time, Pc)
75 grid
76 axis([0 max(time) 0 4])
77
78
79
80 N = 9;
81 D = 50;
82 dint = 20.5;
83 Lint = 85;
84 rhoP = 1.73;
85
86 %cstar = 900
87 %Pressure time trace
88 for i = 1:length(Pc)
89     if i==1;
90         s(i) = 3.375; % Initial guess, mm
91     else
92         s(i) = s(i-1) + ds(i-1);
93     end
94     d(i) = dint+2*s(i); %Instantaneous core diameter, mm
95     L(i) = Lint-2*s(i); %Instantaneous length, mm
96     Ab(i) = pi*N*(0.5 * (D^2-d(i)^2) + (L(i) * d(i)));
97     ds(i) = (At/Ab(i)) * (Pc(i)*1E6/(rhoP*cstar))*dt;
98     r(i) = ds(i)/dt;
99 end
100

```

```
101 figure
102 plot(time,r, 'x')
103 grid
104 title('Pressure time trace')
105 xlabel('time [sec]')
106 ylabel('Burning rate [mm/sec]')
107
108
109 figure
110 plot(Pc,r,'xr')
111 %axis([0 10 0 10])
112 grid
113 title('Burn rate, KN-Erythritol Globos motor firing')
114 xlabel('Pressure [MPa]')
115 ylabel('Burning rate [mm/sec]')
116 print -depsc -tiff -r300 GlobosBurnRate
117
118
119 figure
120 plot(Pc,r,'xr')
121 hold on
122 plot(Pstrand,rstrand,'xg')
123 axis([0 10 0 10])
124 legend('Motor firing','Strand burner')
125 grid
126 title('Comparison of burn rate for KN-Erythritol propellant'...
127 )
128 xlabel('Pressure [MPa]')
129 ylabel('Burning rate [mm/sec]')
130 print -depsc -tiff -r300 ComparisonBurnRate
```

APPENDIX B

Particle distribution

Particle distribution of potassium nitrate (Riedel.de Haen, puriss p.a. Reag. ACS) is given in Table B.1 where the mass percent of retained and passed particles are shown.

Particle distribution curve is shown in Figure B.1 as a line plot and as a log plot in Figure B.2.

Screen size		
Passed	Retained	Mass [%]
1180	600	9.8
600	300	43.6
300	150	37.6
150	125	2.90
125	100	3.26
100	53	2.89

Table B.1: Particle distribution of potassium nitrate.

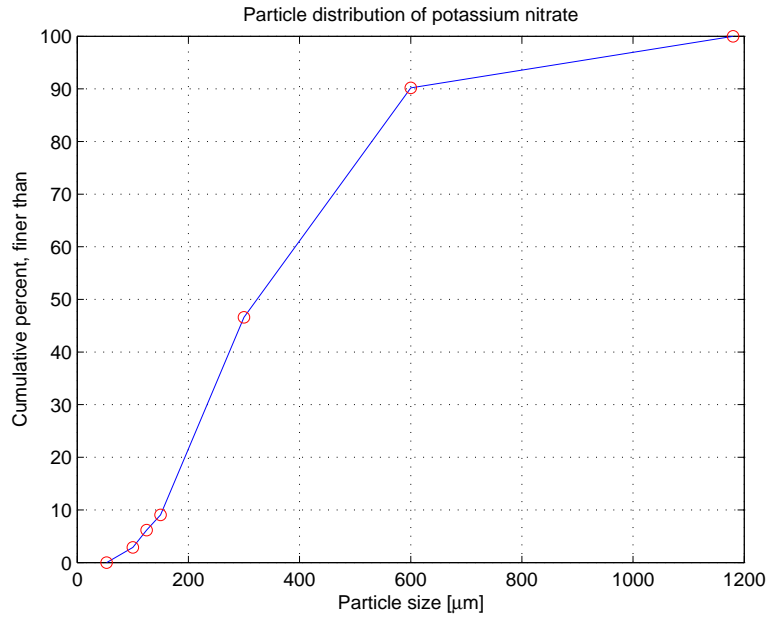


Figure B.1: Particle distribution of potassium nitrate

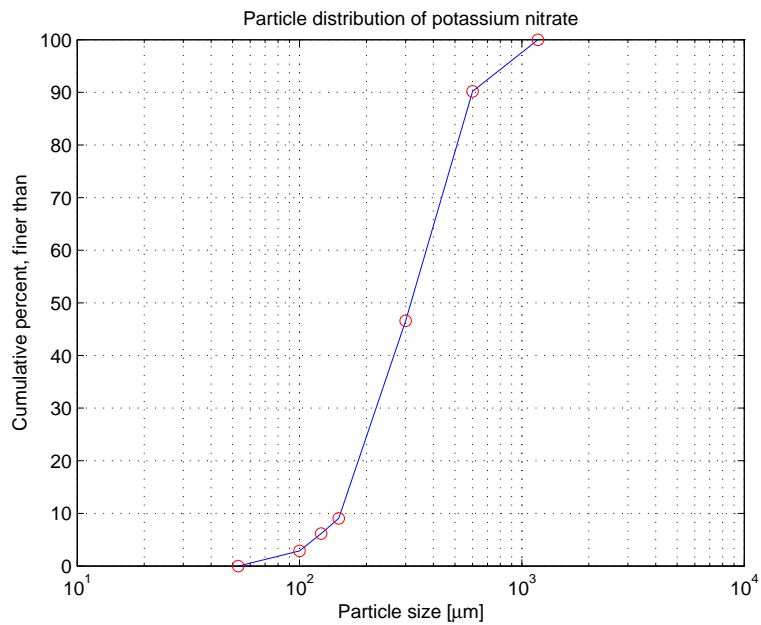


Figure B.2: Particle distribution of potassium nitrate where particle size is shown as the log of the particle size.

APPENDIX C

Propellant batches

C.1 KN-Sorbitol propellant batches

KN-Sorbitol		
Batch no.	Slurry temp. [°C]	Mold temp [°C].
001	115	101
002	115	89
003	110	100
004	117	105
005	110	90

Table C.1: Slurry and mold temperature of casting batches of KN-Sorbitol.

C.2 KN-Erythritol propellant batches

KN-Erythritol		
Batch no.	Slurry temp. [°C]	Mold temp [°C].
001	147	111
002	145	105
003	145	103
004	145	102

Table C.2: Slurry and mold temperature of casting batches of KN-Erythritol.

C.3 KN-Mannitol propellant batches

KN-Mannitol		
Batch no.	Slurry temp. [°C]	Mold temp [°C].
001	172	140
002	171	131
003	171	140
004	175	137
005	175	138

Table C.3: Slurry and mold temperature of casting batches of KN-Mannitol.

APPENDIX D

Propellant Density

The ideal density of a two component propellant mix is expressed as

$$\rho_p = \frac{1}{\frac{f_{ox}}{\rho_{ox}} + \frac{f_{fuel}}{\rho_{fuel}}} \quad (\text{D.1})$$

where ρ_p is the ideal density of the propellant mix, f_{ox} and f_{fuel} is the mass fraction of oxidizer and fuel, ρ_{ox} and ρ_{fuel} is the density of the oxidizer and fuel.

Ideal densities for KN-Sorbitol, KN-Erythritol and KN-Mannitol propellants are compared to recorded mean densities and shown in Table [D.1](#).

Propellant type	Ideal Density	Recorded Density	
KN-Sorbitol	1.841	1.803	[g/cm ³]
KN-Erythritol	1.820	1.770	[g/cm ³]
KN-Mannitol	1.841	1.766	[g/cm ³]

Table D.1: Ideal and recorded densities of 65/35 O/F ratio for KN-Sorbitol, KN-Erythritol and KN-Mannitol propellants

D.1 Example

For a sorbitol propellant mix of 65/35 oxidizer/fuel ratio the ideal density is

$$\rho_p = \frac{1}{\frac{0.65}{2.109g/cm^3} + \frac{0.35}{1.489g/cm^3}} = 1.841g/cm^3 \quad (D.2)$$

APPENDIX E

Ideal performance calculations using PROPEP

E.1 PROPEP results

E.1.1 KN-Sorbitol ideal performance calculations

```

KNS0          Run using June 1988 Version of PEP,
Case 1 of 1   3 Aug 2010 at 0:24:16.89 am

CODE          WEIGHT   D-H   DENS      COMPOSITION
 896 POTASSIUM NITRATE   65.000 -1169 0.07620   1N 30 1K
1180 Sorbitol          35.000 -1775 0.05380   6C 14H 6O

THE PROPELLANT DENSITY IS 0.06651 LB/CU-IN OR 1.8409 GM/CC
THE TOTAL PROPELLANT WEIGHT IS 100.0000 GRAMS

NUMBER OF GRAM ATOMS OF EACH ELEMENT PRESENT IN INGREDIENTS

 2.689677 H    1.152719 C    0.642877 N    3.081349 O
 0.642877 K

*****CHAMBER RESULTS FOLLOW *****

  T(K)  T(F)  P(ATM)  P(PST)  ENTHALPY  ENTROPY  CP/CV   GAS  RT/V
1601. 2422.  68.02  1000.00 -138.11  168.61  1.1362  2.509 27.113

SPECIFIC HEAT (MOLAR) OF GAS AND TOTAL= 10.301 14.720
NUMBER MOLS GAS AND CONDENSED= 2.5089 0.3157

 0.92733 H2O    0.47805 CO    0.41157 H2    0.35889 CO2
 0.32131 N2    0.31568 K2CO3* 0.01097 KH0   0.00041 K
1.92E-04 NH3   6.07E-05 K2H2O2 3.54E-05 CH4   6.77E-06 H
5.72E-06 KCN   4.14E-06 CH2O  3.72E-06 CNH   3.38E-06 KH
1.00E-06 NO2

THE MOLECULAR WEIGHT OF THE MIXTURE IS 35.403

*****EXHAUST RESULTS FOLLOW *****

  T(K)  T(F)  P(ATM)  P(PST)  ENTHALPY  ENTROPY  CP/CV   GAS  RT/V
1033. 1400.  1.00   14.70  -165.13  168.61  1.1485  2.497 0.400

SPECIFIC HEAT (MOLAR) OF GAS AND TOTAL= 9.463 13.617
NUMBER MOLS GAS AND CONDENSED= 2.4971 0.3214

 0.76623 H2O    0.57809 H2    0.51974 CO2    0.32141 K2CO3&
 0.32139 N2    0.31132 CO    0.00020 CH4    0.00005 NH3
3.68E-05 KH0   1.00E-06 NO2

THE MOLECULAR WEIGHT OF THE MIXTURE IS 35.479

*****PERFORMANCE: FROZEN ON FIRST LINE, SHIFTING ON SECOND LINE*****

IMPULSE  IS EX    T*    P*    C*    ISP*  OPT-EX  D-ISP    A*M    EX-T
 151.3  1.1418  1495.  39.19 2972.0  10.01  278.5  0.09239  948.
 153.4  1.1287  1506.  39.37 2992.8  114.5  282.3  0.09304  1033.

```

Figure E.1: Propep results for KN-Sorbitol propellant.

E.1.2 KN-Erythritol ideal performance calculations

```

KNER                      Run using June 1988 Version of PEP,
Case 1 of 1              28 Jul 2010 at 3:23:19.11 pm

CODE                      WEIGHT   D-H   DENS      COMPOSITION
 896 POTASSIUM NITRATE    65.000 -1169 0.07620   1N 30 1K
1181 Erythritol          35.000 -1732 0.05240   4C 10H 40

THE PROPELLANT DENSITY IS 0.06575 LB/CU-IN OR 1.8199 GM/CC
THE TOTAL PROPELLANT WEIGHT IS 100.0000 GRAMS

NUMBER OF GRAM ATOMS OF EACH ELEMENT PRESENT IN INGREDIENTS

 2.865940 H    1.146376 C    0.642877 N    3.075006 O
 0.642877 K

*****CHAMBER RESULTS FOLLOW *****

T(K)  T(F)  P(ATM)  P(PST)  ENTHALPY  ENTROPY  CP/CV    GAS  RT/V
1608. 2434.  68.02  1000.00 -136.60   172.00   1.1392  2.593 26.238

SPECIFIC HEAT (MOLAR) OF GAS AND TOTAL= 10.213 14.503
NUMBER MOLS GAS AND CONDENSED= 2.5926 0.3147

 0.95371 H2O    0.49891 CO    0.47234 H2    0.33263 CO2
 0.32130 N2    0.31471 K2CO3* 0.01275 KH0   0.00051 K
 2.24E-04 NH3  7.49E-05 K2H2O2 4.74E-05 CH4   7.90E-06 H
 7.63E-06 KCN  4.78E-06 CH2O  4.53E-06 KH    4.48E-06 CNH

THE MOLECULAR WEIGHT OF THE MIXTURE IS 34.396

*****EXHAUST RESULTS FOLLOW *****

T(K)  T(F)  P(ATM)  P(PST)  ENTHALPY  ENTROPY  CP/CV    GAS  RT/V
1029. 1394.  1.00   14.70  -164.54   172.00   1.1518  2.579 0.388

SPECIFIC HEAT (MOLAR) OF GAS AND TOTAL= 9.367 13.405
NUMBER MOLS GAS AND CONDENSED= 2.5787 0.3214

 0.78480 H2O    0.64744 H2    0.50126 CO2    0.32336 CO
 0.32141 K2CO3& 0.32139 N2    0.00030 CH4    0.00006 NH3
 3.50E-05 KH0

THE MOLECULAR WEIGHT OF THE MIXTURE IS 34.481

*****PERFORMANCE: FROZEN ON FIRST LINE, SHIFTING ON SECOND LINE*****

IMPULSE  IS EX    T*    P*    C*    ISP*  OPT-EX  D-ISP    A*M  EX-T
 153.7  1.1451  1499. 39.14 3024.0  116.5  9.94  279.8  0.09401  942.
 155.9  1.1310  1510. 39.34 3045.9  116.5  10.58 283.8  0.09469  1029.

```

Figure E.2: Propep results for KN-Erythritol propellant.

E.1.3 KN-Mannitol ideal performance calculations

```

KNMN                Run using June 1988 Version of PEP,
Case 1 of 1         4 Aug 2010 at 4:29: 3.59 pm

CODE                WEIGHT   D-H   DENS      COMPOSITION
 896 POTASSIUM NITRATE 65.000 -1169 0.07620   1N 30 1K
1182 Mannitol        35.000 -1723 0.05380   6C 14H 6O

THE PROPELLANT DENSITY IS 0.06651 LB/CU-IN OR 1.8409 GM/CC
THE TOTAL PROPELLANT WEIGHT IS 100.0000 GRAMS

NUMBER OF GRAM ATOMS OF EACH ELEMENT PRESENT IN INGREDIENTS

 2.689677 H      1.152719 C      0.642877 N      3.081349 O
 0.642877 K

*****CHAMBER RESULTS FOLLOW *****

  T(K)  T(F)  P(ATM)  P(PST)  ENTHALPY  ENTROPY  CP/CV  GAS  RT/V
1637. 2487.  68.02  1000.00 -136.29   169.74  1.1364  2.514 27.056

SPECIFIC HEAT (MOLAR) OF GAS AND TOTAL=  10.351  14.723
NUMBER MOLS GAS AND CONDENSED=  2.5142  0.3131

 0.93189 H2O      0.48496 CO      0.40461 H2      0.35457 CO2
 0.32132 N2      0.31310 K2CO3*  0.01581 KHO     0.00065 K
1.70E-04 NH3     9.16E-05 K2H2O2 2.32E-05 CH4     9.77E-06 H
7.12E-06 KCN     5.66E-06 KH     4.04E-06 CH2O    3.63E-06 CNH
1.00E-06 HO      1.00E-06 NO2

THE MOLECULAR WEIGHT OF THE MIXTURE IS  35.369

*****EXHAUST RESULTS FOLLOW *****

  T(K)  T(F)  P(ATM)  P(PST)  ENTHALPY  ENTROPY  CP/CV  GAS  RT/V
1061. 1450.  1.00   14.70  -163.95   169.74  1.1471  2.497 0.400

SPECIFIC HEAT (MOLAR) OF GAS AND TOTAL=  9.506  13.725
NUMBER MOLS GAS AND CONDENSED=  2.4974  0.3214

 0.77895 H2O      0.56557 H2      0.50691 CO2     0.32427 CO
 0.32139 N2      0.32139 K2CO3&  0.00010 CH4     0.00008 KHO
3.86E-05 NH3     2.26E-06 K      1.00E-06 NO2

THE MOLECULAR WEIGHT OF THE MIXTURE IS  35.476

*****PERFORMANCE: FROZEN ON FIRST LINE, SHIFTING ON SECOND LINE*****

IMPULSE  IS EX    T*    P*    C*    ISP*  OPT-EX  D-ISP  A*M  EX-T
 153.1  1.1419  1529.  39.18 3008.4  116.2  10.01  281.9  0.09353  969.
 155.2  1.1127  1551.  39.59 3071.1  116.2  10.52  285.6  0.09548  1061.

```

Figure E.3: Propep results for KN-Mannitol propellant.

APPENDIX F

Propellant strand burns

F.1 Analysis of KN-Sorbitol strand burns

KN-Sorbitol 65/35 O/F ratio	
Test no.	KNSO100barH3001
Batch no.	KNSO-002
Relative humidity	46 %
Ambient temperature	23.6 °C
Mean pressure	10.08 MPa
T/C 1 spike start point	5.80 sec
T/C 2 spike start point	13.19 sec
Gauge length	65.62 mm
Burn time	7.39 sec
Burn rate, r	8.87 mm/sec

Table F.1: KN-Sorbitol. Set pressure 10 MPa.

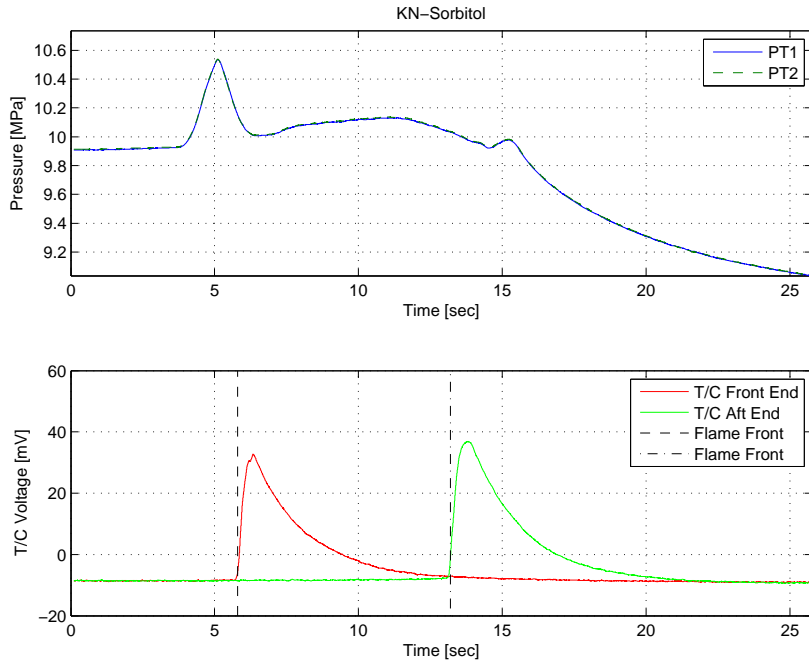


Figure F.1: KN-Sorbitol. Set pressure 10 MPa.

KN-Sorbitol 65/35 O/F ratio	
Test no.	KNSO100barH3002
Batch no.	KNSO-002
Relative humidity	45 %
Ambient temperature	23.8 °C
Mean pressure	10.28 MPa
T/C 1 spike start point	4.90 sec
T/C 2 spike start point	12.39 sec
Gauge length	65.70 mm
Burn time	7.49 sec
Burn rate, r	8.76 mm/sec

Table F.2: KN-Sorbitol. Set pressure 10 MPa.

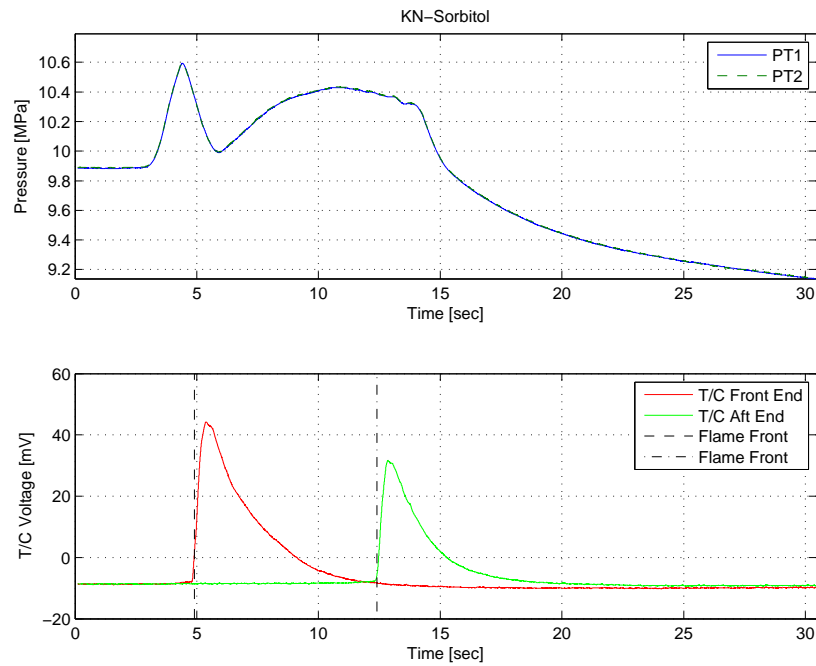


Figure F.2: KN-Sorbitol. Set pressure 10 MPa.

KN-Sorbitol 65/35 O/F ratio	
Test no.	KNSO90barH3001
Batch no.	KNSO-002
Relative humidity	43 %
Ambient temperature	24.1 °C
Mean pressure	9.05 MPa
T/C 1 spike start point	4.00 sec
T/C 2 spike start point	11.59 sec
Gauge length	65.09 mm
Burn time	7.59 sec
Burn rate, r	8.56 mm/sec

Table F.3: KN-Sorbitol. Set pressure 9 MPa.

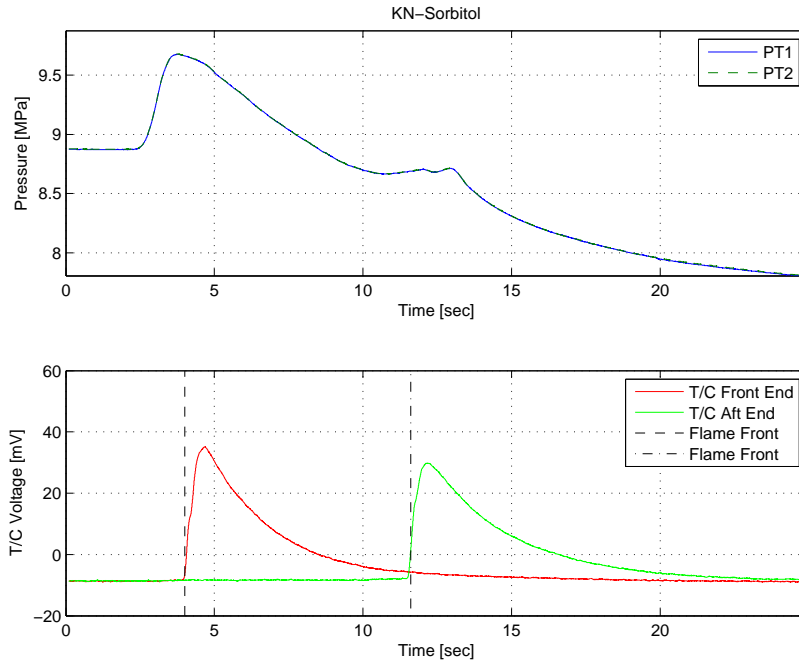


Figure F.3: KN-Sorbitol. Set pressure 9 MPa.

KN-Sorbitol 65/35 O/F ratio	
Test no.	KNSO90barH3002
Batch no.	KNSO-002
Relative humidity	43 %
Ambient temperature	24.4 °C
Mean pressure	9.65 MPa
T/C 1 spike start point	4.10 sec
T/C 2 spike start point	11.89 sec
Gauge length	65.59 mm
Burn time	7.79 sec
Burn rate, r	8.41 mm/sec

Table F.4: KN-Sorbitol. Set pressure 9 MPa.

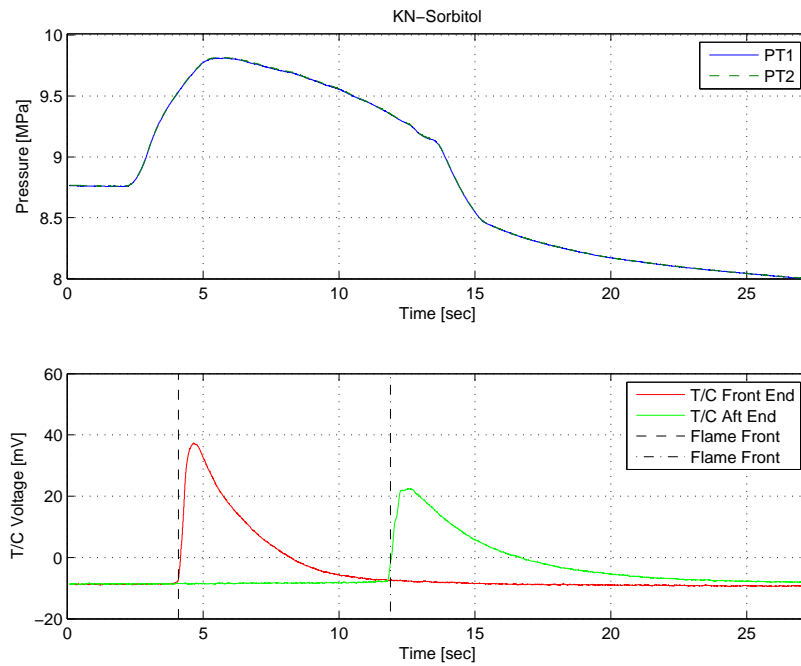


Figure F.4: KN-Sorbitol. Set pressure 9 MPa.

Remarks:

- Pressure relief valve opened at higher pressure than expected, thus the mean pressure is higher.

KN-Sorbitol 65/35 O/F ratio	
Test no.	KNSO90barH3003
Batch no.	KNSO-002
Relative humidity	43 %
Ambient temperature	24.5 °C
Mean pressure	9.59 MPa
T/C 1 spike start point	3.30 sec
T/C 2 spike start point	10.69 sec
Gauge length	64.79 mm
Burn time	7.39 sec
Burn rate, r	8.76 mm/sec

Table F.5: KN-Sorbitol. Set pressure 9 MPa.

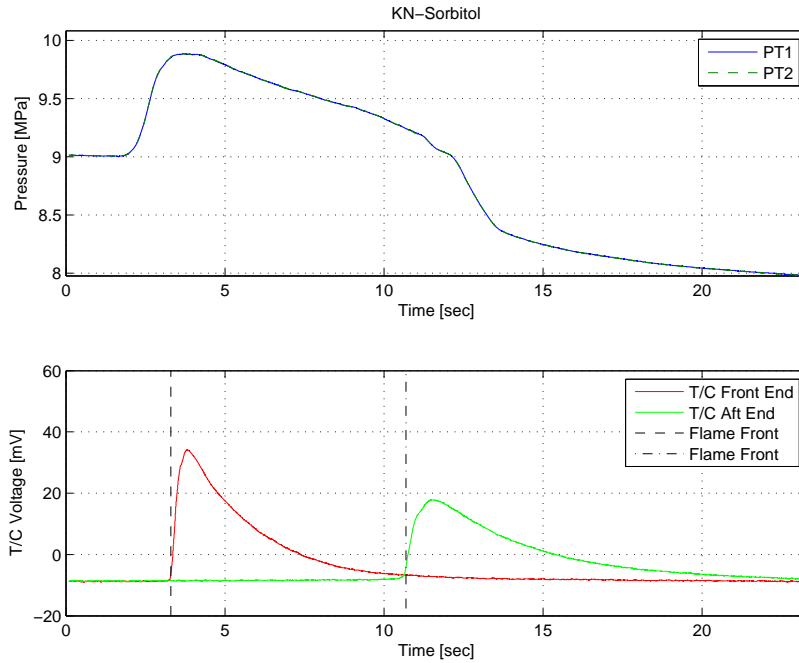


Figure F.5: KN-Sorbitol. Set pressure 9 MPa.

Remarks:

- Pressure relief valve opened at higher pressure than expected, thus the mean pressure is higher.

KN-Sorbitol 65/35 O/F ratio	
Test no.	KNSO90barH3004
Batch no.	KNSO-002
Relative humidity	44 %
Ambient temperature	24.4 °C
Mean pressure	9.07 MPa
T/C 1 spike start point	3.70 sec
T/C 2 spike start point	10.69 sec
Gauge length	60.76 mm
Burn time	6.99 sec
Burn rate, r	8.68 mm/sec

Table F.6: KN-Sorbitol. Set pressure 9 MPa.

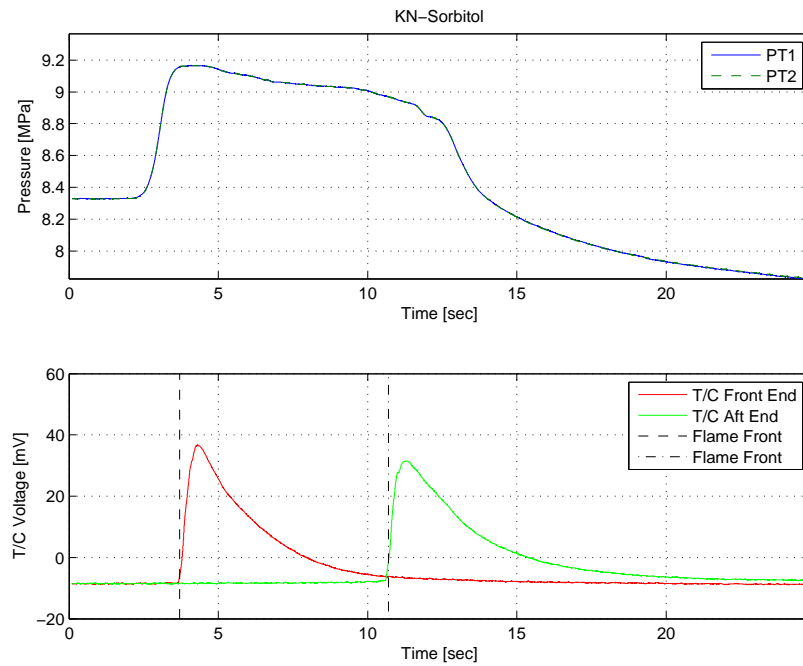


Figure F.6: KN-Sorbitol. Set pressure 9 MPa.

KN-Sorbitol 65/35 O/F ratio	
Test no.	KNSO80barH3001
Batch no.	KNSO-002
Relative humidity	44 %
Ambient temperature	24.8 °C
Mean pressure	7.78 MPa
T/C 1 spike start point	4.40 sec
T/C 2 spike start point	12.29 sec
Gauge length	65.30 mm
Burn time	7.89 sec
Burn rate, r	8.27 mm/sec

Table F.7: KN-Sorbitol. Set pressure 8 MPa.

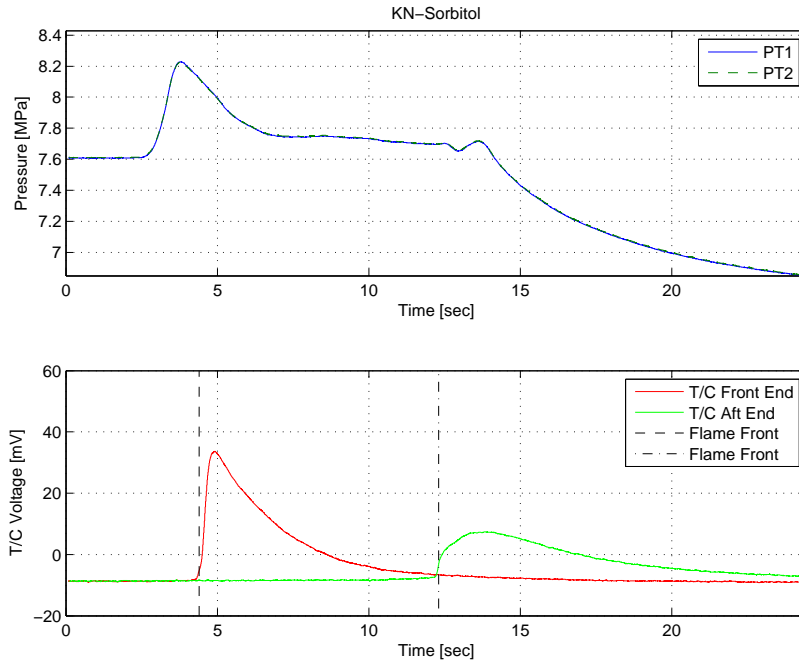


Figure F.7: KN-Sorbitol. Set pressure 8 MPa.

Remarks:

- T/C aft end has a relatively lower steepness than T/C front end.

KN-Sorbitol 65/35 O/F ratio	
Test no.	KNSO80barH3002
Batch no.	KNSO-002
Relative humidity	43 %
Ambient temperature	24.7 °C
Mean pressure	7.83 MPa
T/C 1 spike start point	5.30 sec
T/C 2 spike start point	13.39 sec
Gauge length	64.77 mm
Burn time	8.09 sec
Burn rate, r	7.99 mm/sec

Table F.8: KN-Sorbitol. Set pressure 8 MPa.

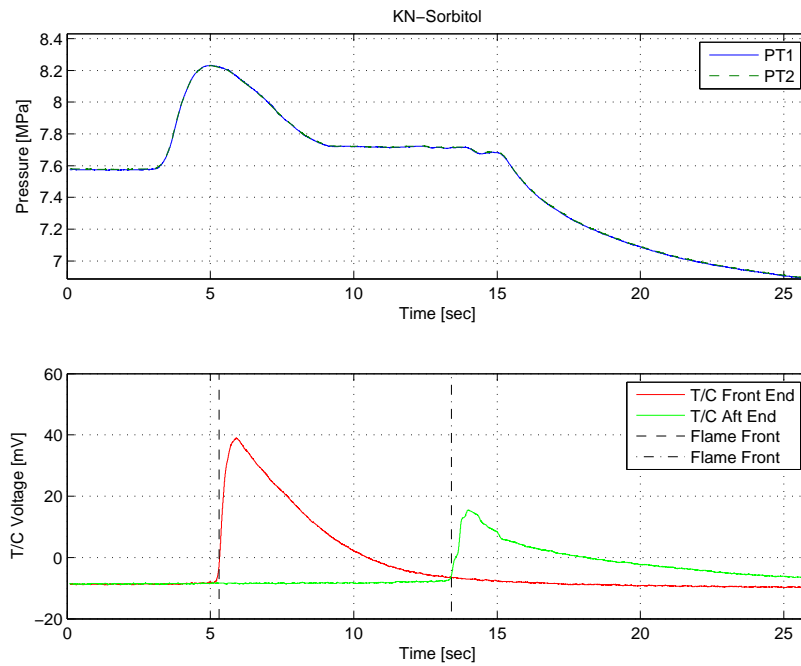


Figure F.8: KN-Sorbitol. Set pressure 8 MPa.

KN-Sorbitol 65/35 O/F ratio	
Test no.	KNSO70barH3001
Batch no.	KNSO-002
Relative humidity	40 %
Ambient temperature	25.1 °C
Mean pressure	7.05 MPa
T/C 1 spike start point	4.80 sec
T/C 2 spike start point	13.40 sec
Gauge length	67.66 mm
Burn time	8.60 sec
Burn rate, r	7.87 mm/sec

Table F.9: KN-Sorbitol. Set pressure 7 MPa.

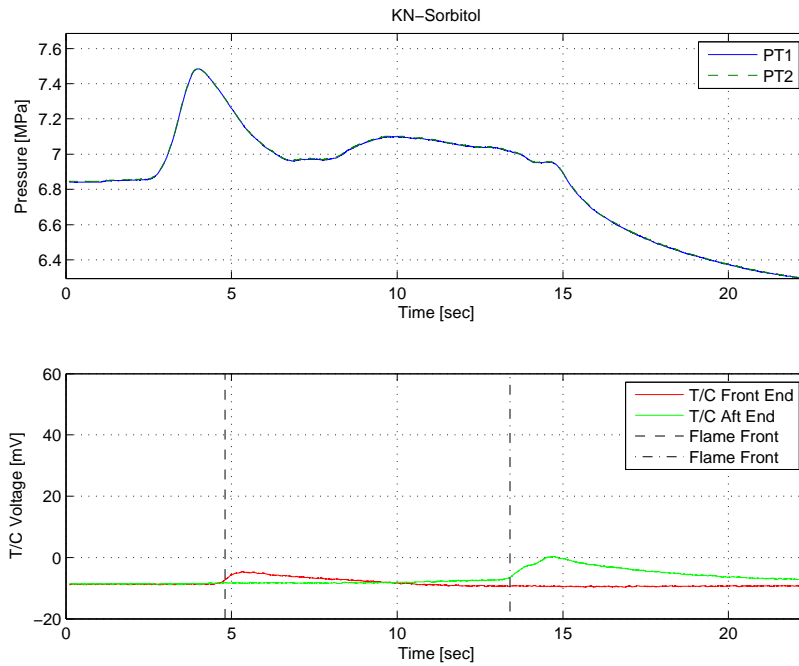


Figure F.9: KN-Sorbitol. Set pressure 7 MPa.

Remarks:

- Recorded value of both T/C to low.

KN-Sorbitol 65/35 O/F ratio	
Test no.	KNSO70barH3002
Batch no.	KNSO-002
Relative humidity	40 %
Ambient temperature	25.1 °C
Mean pressure	7.02 MPa
T/C 1 spike start point	4.10 sec
T/C 2 spike start point	12.60 sec
Gauge length	61.35 mm
Burn time	8.50 sec
Burn rate, r	7.22 mm/sec

Table F.10: KN-Sorbitol. Set pressure 7 MPa.

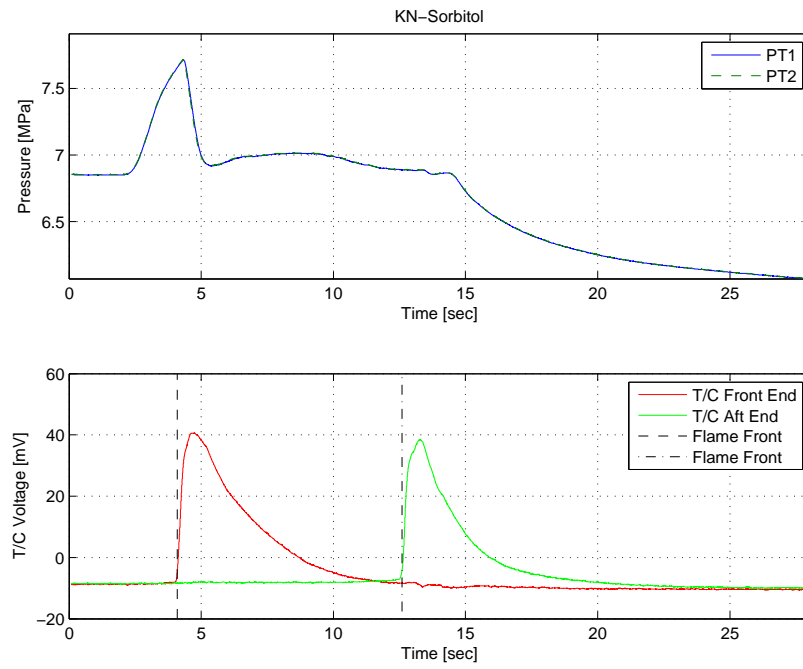


Figure F.10: KN-Sorbitol. Set pressure 7 MPa.

KN-Sorbitol 65/35 O/F ratio	
Test no.	KNSO60barH3001
Batch no.	KNSO-003
Relative humidity	44 %
Ambient temperature	23.0 °C
Mean pressure	5.89 MPa
T/C 1 spike start point	3.70 sec
T/C 2 spike start point	12.00 sec
Gauge length	68.78 mm
Burn time	9.30 sec
Burn rate, r	7.40 mm/sec

Table F.11: KN-Sorbitol. Set pressure 6 MPa.

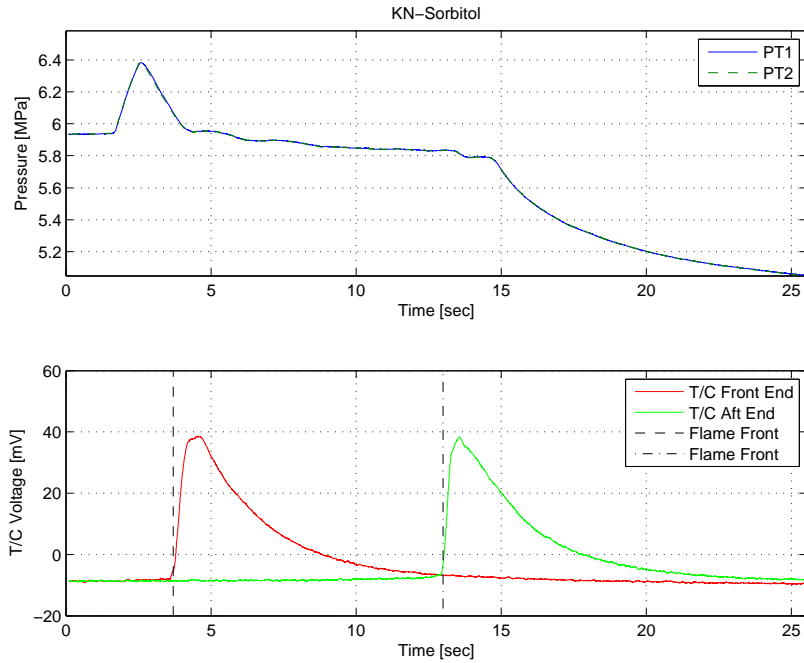


Figure F.11: KN-Sorbitol. Set pressure 6 MPa

KN-Sorbitol 65/35 O/F ratio	
Test no.	KNSO60barH3002
Batch no.	KNSO-003
Relative humidity	44 %
Ambient temperature	23.1 °C
Mean pressure	6.01 MPa
T/C 1 spike start point	3.80 sec
T/C 2 spike start point	12.70 sec
Gauge length	68.87 mm
Burn time	8.90 sec
Burn rate, r	7.74 mm/sec

Table F.12: KN-Sorbitol. Set pressure 6 MPa.

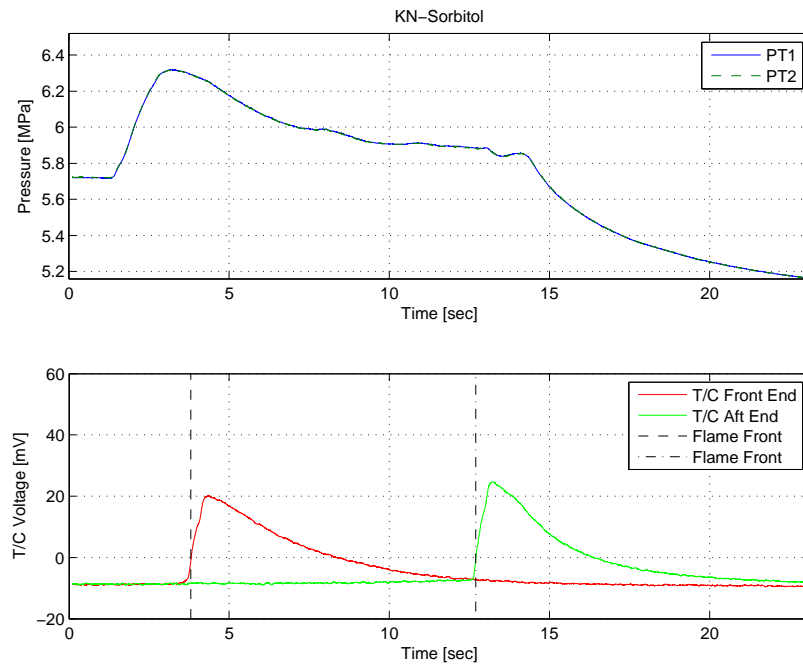


Figure F.12: KN-Sorbitol. Set pressure 6 MPa.

KN-Sorbitol 65/35 O/F ratio	
Test no.	KNSO50barH3001
Batch no.	KNSO-003
Relative humidity	44 %
Ambient temperature	23.4 °C
Mean pressure	5.00 MPa
T/C 1 spike start point	3.70 sec
T/C 2 spike start point	13.20 sec
Gauge length	68.89 mm
Burn time	9.50 sec
Burn rate, r	7.25 mm/sec

Table F.13: KN-Sorbitol. Set pressure 5 MPa.

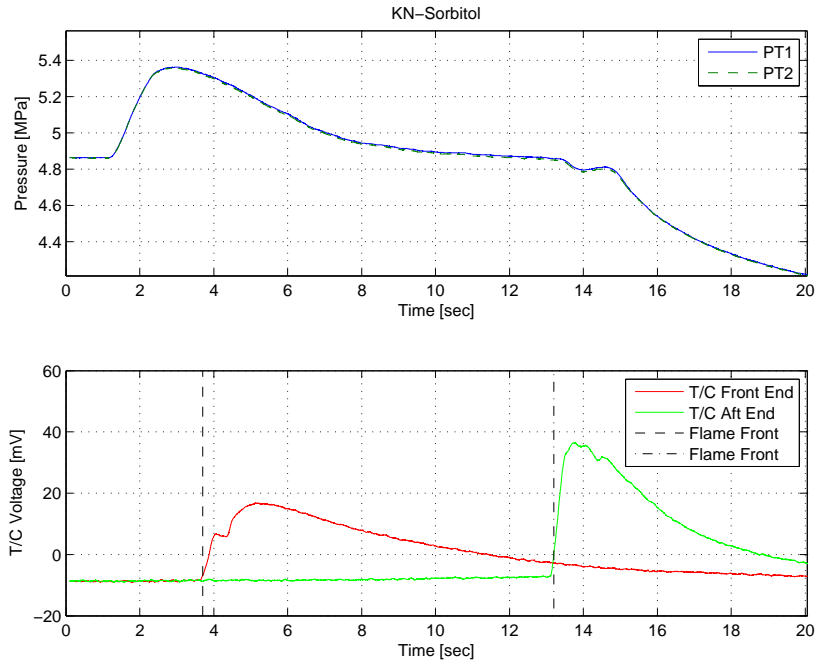


Figure F.13: KN-Sorbitol. Set pressure 5 MPa.

KN-Sorbitol 65/35 O/F ratio	
Test no.	KNSO50barH3002
Batch no.	KNSO-003
Relative humidity	44 %
Ambient temperature	23.5 °C
Mean pressure	5.02 MPa
T/C 1 spike start point	4.90 sec
T/C 2 spike start point	14.00 sec
Gauge length	69.49 mm
Burn time	9.10 sec
Burn rate, r	7.64 mm/sec

Table F.14: KN-Sorbitol. Set pressure 5 MPa.

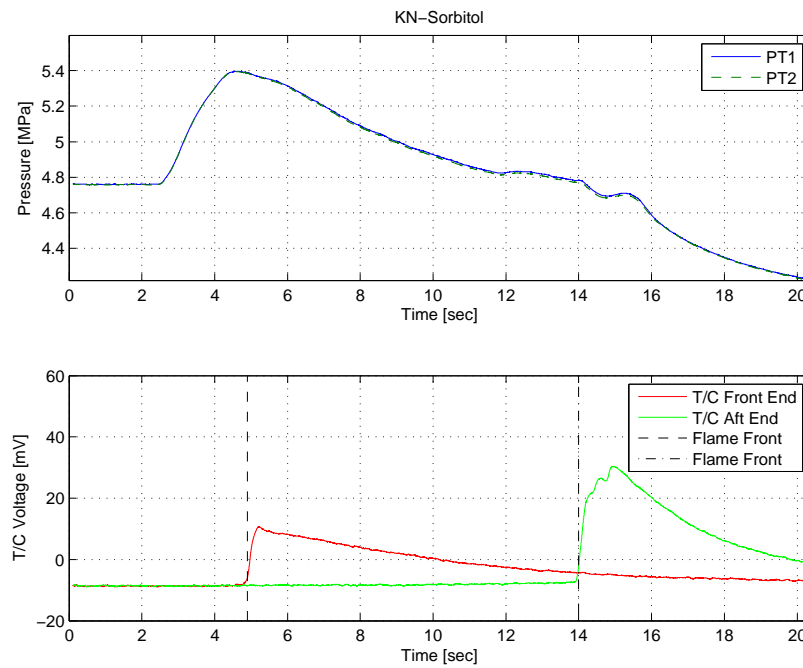


Figure F.14: KN-Sorbitol. Set pressure 5 MPa.

Remarks:

- Lower recorded value of T/C 1 than expected.

KN-Sorbitol 65/35 O/F ratio	
Test no.	KNSO40barH3001
Batch no.	KNSO-003
Relative humidity	44 %
Ambient temperature	23.6 °C
Mean pressure	3.87 MPa
T/C 1 spike start point	3.80 sec
T/C 2 spike start point	12.90 sec
Gauge length	67.19 mm
Burn time	10.10 sec
Burn rate, r	6.65 mm/sec

Table F.15: KN-Sorbitol. Set pressure 4 MPa.

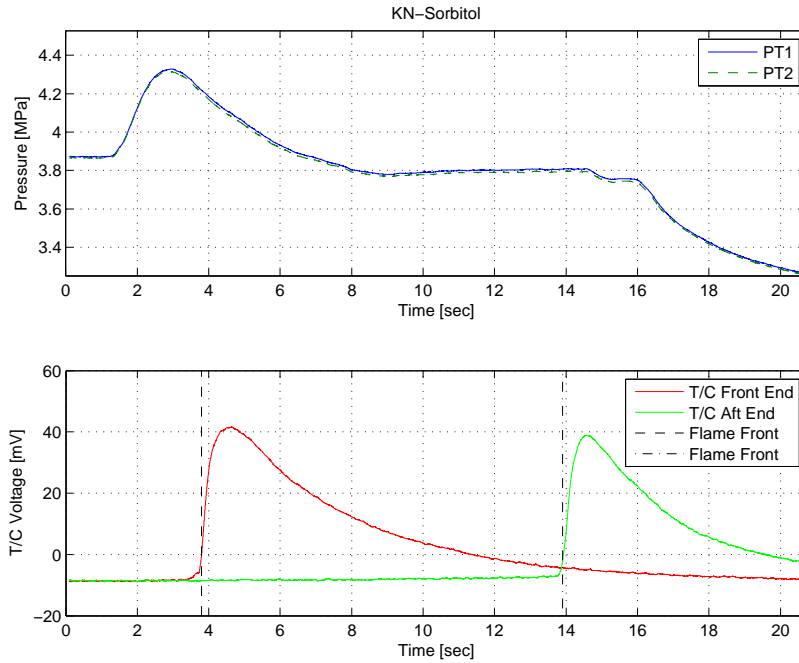


Figure F.15: KN-Sorbitol. Set pressure 4 MPa.

KN-Sorbitol 65/35 O/F ratio	
Test no.	KNSO40barH3002
Batch no.	KNSO-003
Relative humidity	43 %
Ambient temperature	23.8 °C
Mean pressure	3.95 MPa
T/C 1 spike start point	4.00 sec
T/C 2 spike start point	14.20 sec
Gauge length	67.90 mm
Burn time	10.20 sec
Burn rate, r	6.66 mm/sec

Table F.16: KN-Sorbitol. Set pressure 4 MPa.

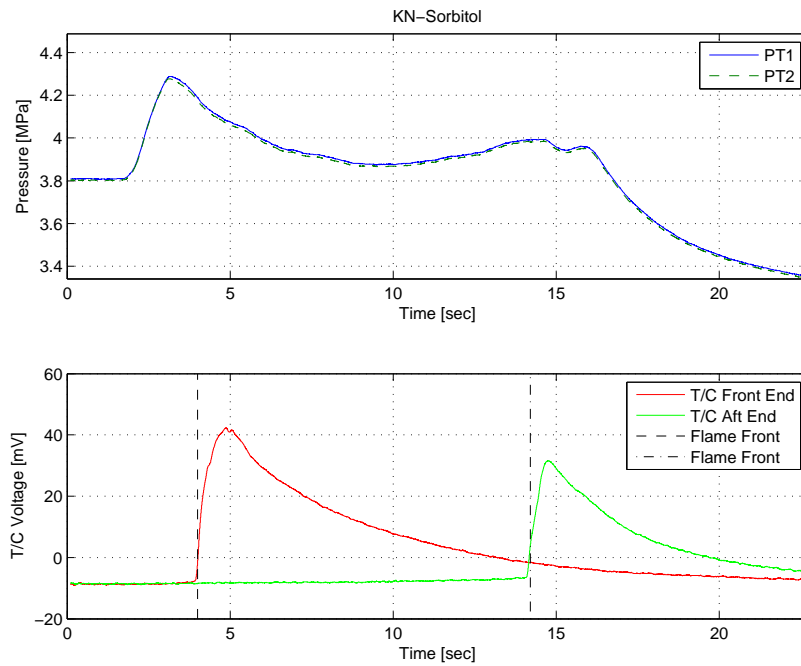


Figure F.16: KN-Sorbitol. Set pressure 4 MPa.

KN-Sorbitol 65/35 O/F ratio	
Test no.	KNSO30barH3001
Batch no.	KNSO-303
Relative humidity	43 %
Ambient temperature	23.7 °C
Mean pressure	2.85 MPa
T/C 1 spike start point	4.20 sec
T/C 2 spike start point	15.00 sec
Gauge length	68.23 mm
Burn time	10.80 sec
Burn rate, r	6.32 mm/sec

Table F.17: KN-Sorbitol. Set pressure 3 MPa.

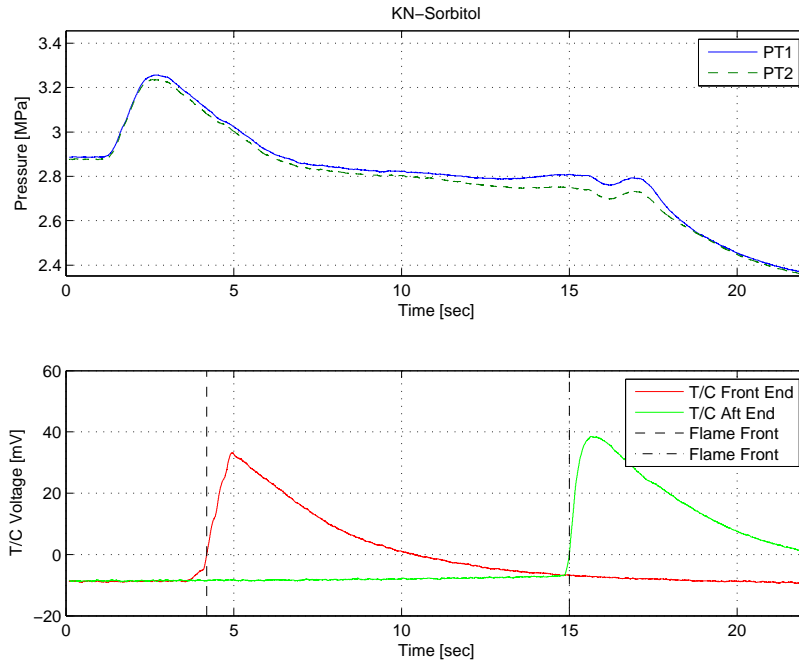


Figure F.17: KN-Sorbitol. Set pressure 3 MPa.

Remarks:

- Slight pressure drop noticed.

KN-Sorbitol 65/35 O/F ratio	
Test no.	KNSO30barH3002
Batch no.	KNSO-003
Relative humidity	43 %
Ambient temperature	24.1 °C
Mean pressure	2.96 MPa
T/C 1 spike start point	4.20 sec
T/C 2 spike start point	14.70 sec
Gauge length	70.11 mm
Burn time	11.50 sec
Burn rate, r	6.10 mm/sec

Table F.18: KN-Sorbitol. Set pressure 3 MPa.

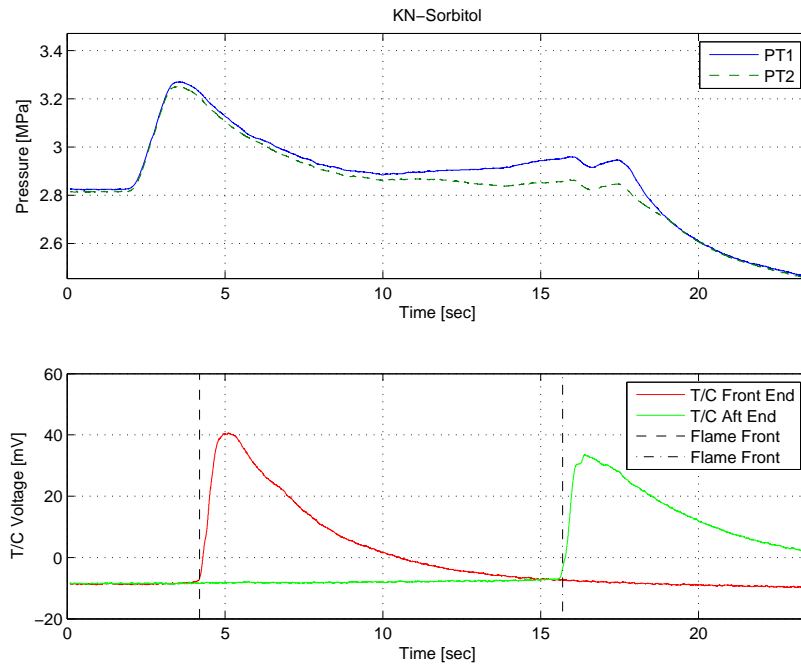


Figure F.18: KN-Sorbitol. Set pressure 3 MPa.

Remarks:

- Pressure drop noticed.

KN-Sorbitol 65/35 O/F ratio	
Test no.	KNSO20barH3001
Batch no.	KNSO-003
Relative humidity	43 %
Ambient temperature	24.1 °C
Mean pressure	1.89 MPa
T/C 1 spike start point	4.80 sec
T/C 2 spike start point	16.70 sec
Gauge length	68.70 mm
Burn time	11.90 sec
Burn rate, r	5.77 mm/sec

Table F.19: KN-Sorbitol. Set pressure 2 MPa.

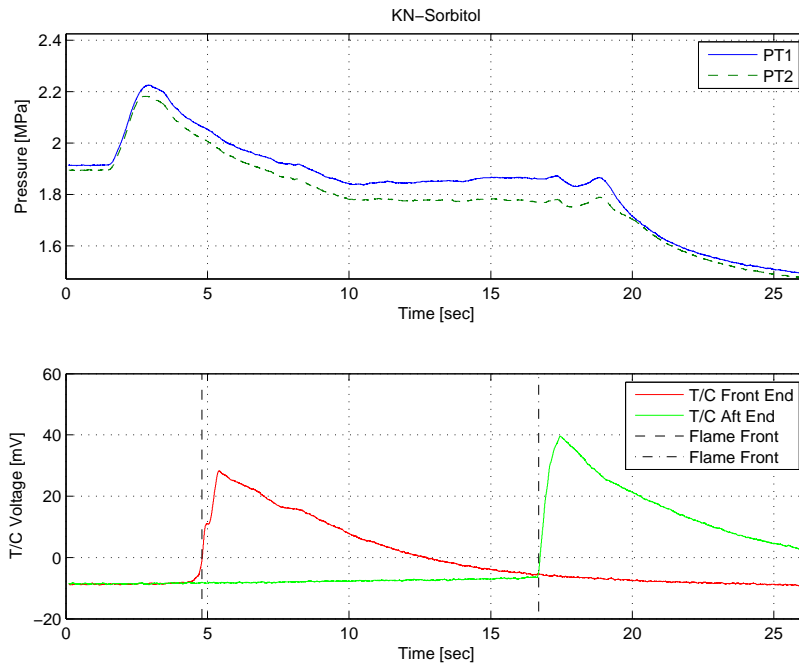


Figure F.19: KN-Sorbitol. Set pressure 2 MPa.

Remarks:

- Pressure drop throughout the burn.

KN-Sorbitol 65/35 O/F ratio	
Test no.	KNSO20barH3002
Batch no.	KNSO-003
Relative humidity	43 %
Ambient temperature	24.0 °C
Mean pressure	2.05 MPa
T/C 1 spike start point	5.80 sec
T/C 2 spike start point	17.60 sec
Gauge length	68.05 mm
Burn time	11.80 sec
Burn rate, r	5.77 mm/sec

Table F.20: KN-Sorbitol. Set pressure 2 MPa.

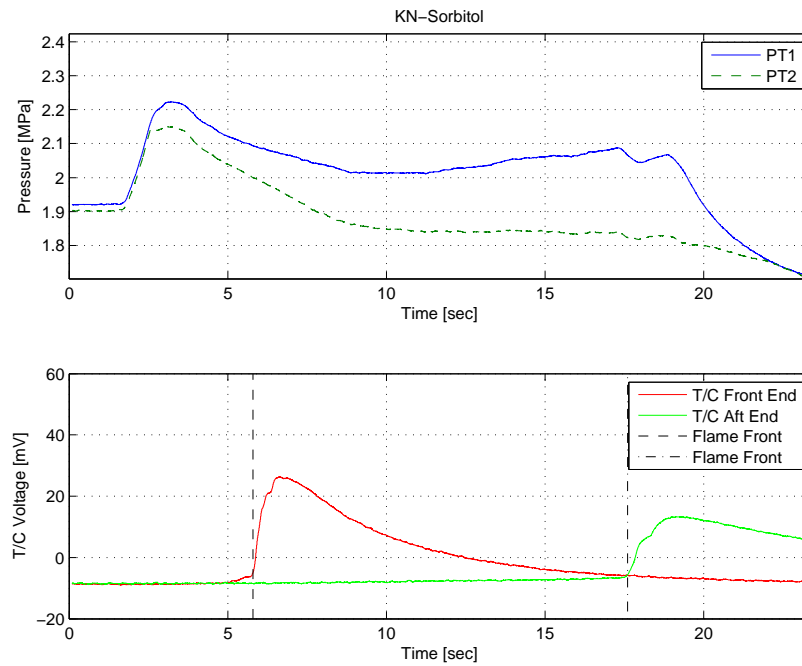


Figure F.20: KN-Sorbitol. Set pressure 2 MPa.

Remarks:

- Major pressure drop.
- T/C aft end has a relatively lower steepness than T/C front end.

KN-Sorbitol 65/35 O/F ratio	
Test no.	KNSO10barH3001
Batch no.	KNSO-003
Relative humidity	44 %
Ambient temperature	23.7 °C
Mean pressure	0.90 MPa
T/C 1 spike start point	5.00 sec
T/C 2 spike start point	17.00 sec
Gauge length	68.77 mm
Burn time	12.00 sec
Burn rate, r	5.73 mm/sec

Table F.21: KN-Sorbitol. Set pressure 1 MPa.

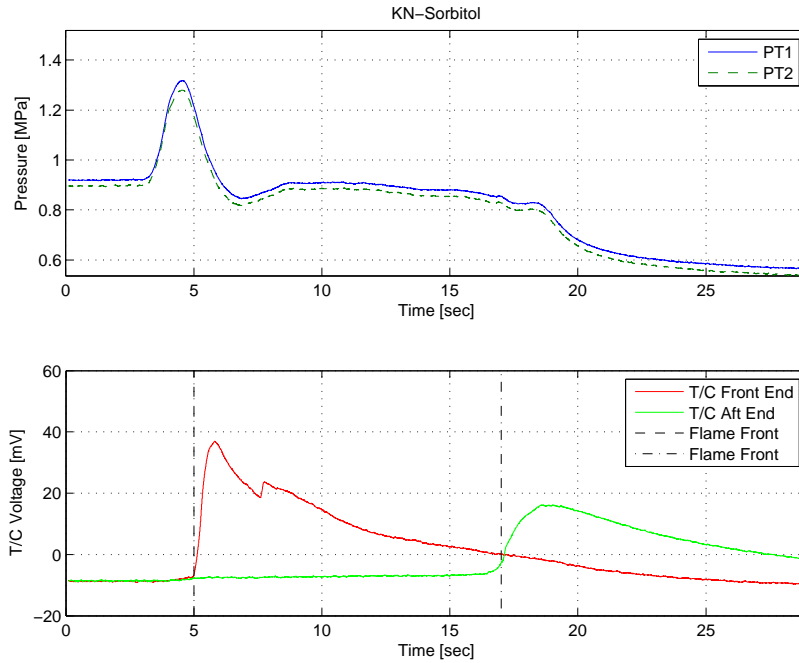


Figure F.21: KN-Sorbitol. Set pressure 1 MPa.

Remarks:

- Recorded pressure value of PT2 is about 2-3 % lower than the PT1 value.
- T/C aft end has a relatively lower steepness than T/C front end.

KN-Sorbitol 65/35 O/F ratio	
Test no.	KNSO10barH3002
Batch no.	KNSO-003
Relative humidity	44 %
Ambient temperature	23.8 °C
Mean pressure	0.88 MPa
T/C 1 spike start point	5.40 sec
T/C 2 spike start point	18.50 sec
Gauge length	70.29 mm
Burn time	13.10 sec
Burn rate, r	5.37 mm/sec

Table F.22: KN-Sorbitol. Set pressure 1 MPa.

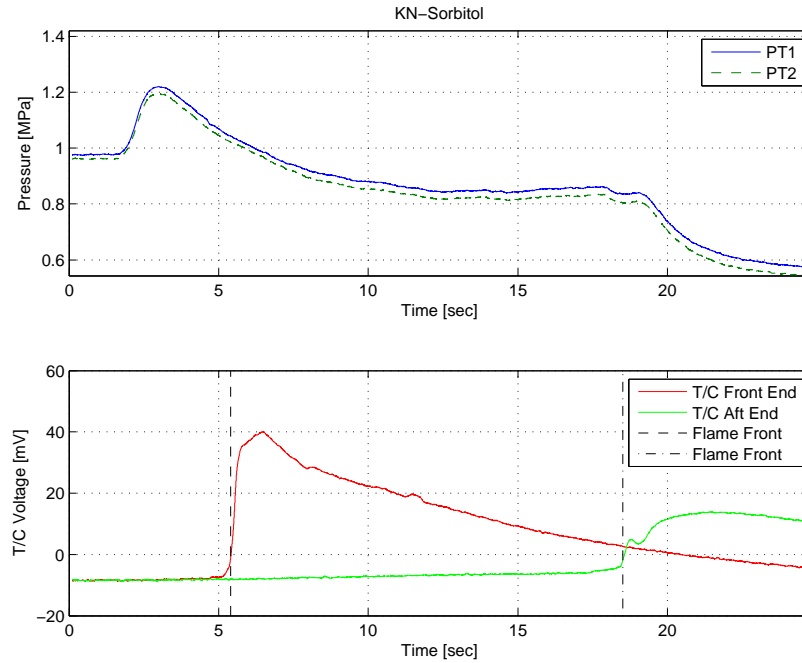


Figure F.22: KN-Sorbitol. Set pressure 1 MPa.

Remarks:

- Recorded pressure value of PT2 is about 2-3 % lower than the PT1 value.
- T/C aft end has a relatively lower steepness than T/C front end.

KN-Sorbitol 65/35 O/F ratio			
Test no.	KNSO0barH3001		
Batch no.	KNSO-005		
Relative humidity	47	%	
Ambient temperature	24.3	°C	
Mean pressure	0.0	MPa	
T/C 1 spike start point	7.00	sec	
T/C 2 spike start point	30.00	sec	
Gauge length	70.73	mm	
Burn time	23.00	sec	
Burn rate, r	3.08	mm/sec	

Table F.23: KN-Sorbitol. Atmospheric pressure

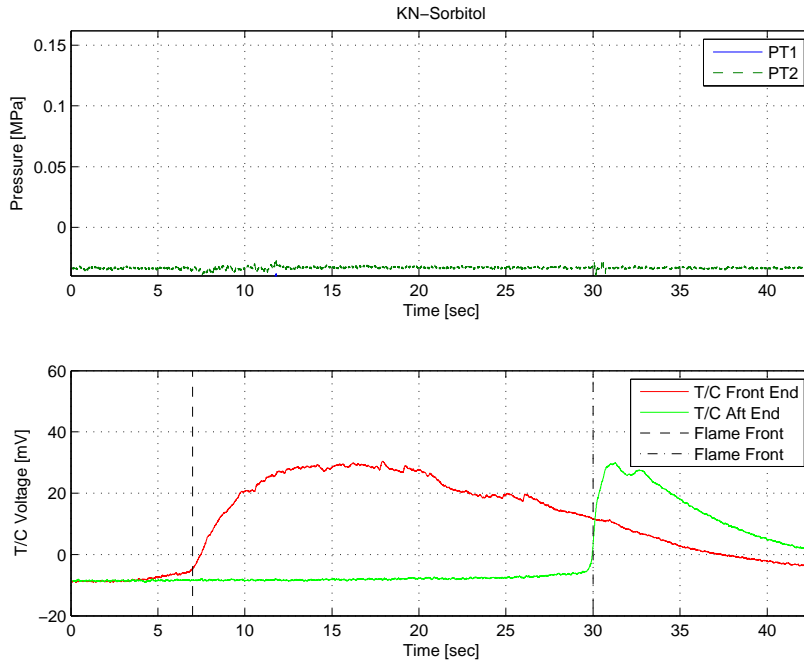


Figure F.23: KN-Sorbitol. Atmospheric pressure

Remarks:

- T/C front end has a relatively lower steepness than T/C aft end.

F.2 Analysis of KN-Erythritol strand burns

KN-Erythritol 65/35 O/F ratio	
Test no.	KNER100barH3001
Batch no.	KNER-003
Relative humidity	44 %
Ambient temperature	24.1 °C
Mean pressure	9.98 MPa
T/C 1 spike start point	3.50 sec
T/C 2 spike start point	12.40 sec
Gauge length	64.98 mm
Burn time	8.90 sec
Burn rate, r	7.30 mm/sec

Table F.24: KN-Erythritol. Set pressure 10 MPa.

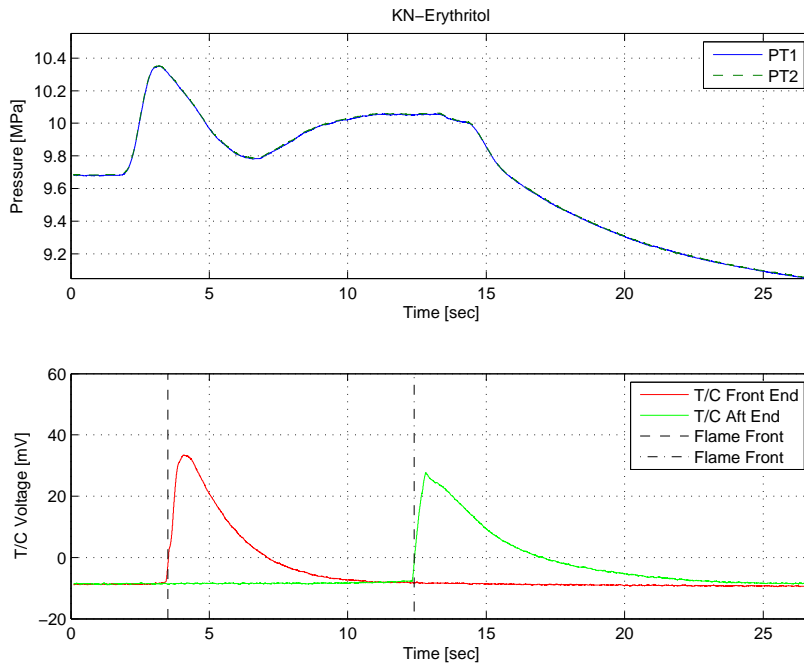


Figure F.24: KN-Erythritol. Set pressure 10 MPa.

KN-Erythritol 65/35 O/F ratio	
Test no.	KNER100barH3002
Batch no.	KNER-003
Relative humidity	44 %
Ambient temperature	24.1 °C
Mean pressure	10.05 MPa
T/C 1 spike start point	3.70 sec
T/C 2 spike start point	12.70 sec
Gauge length	64.98 mm
Burn time	9.00 sec
Burn rate, r	7.22 mm/sec

Table F.25: KN-Erythritol. Set pressure 10 MPa.

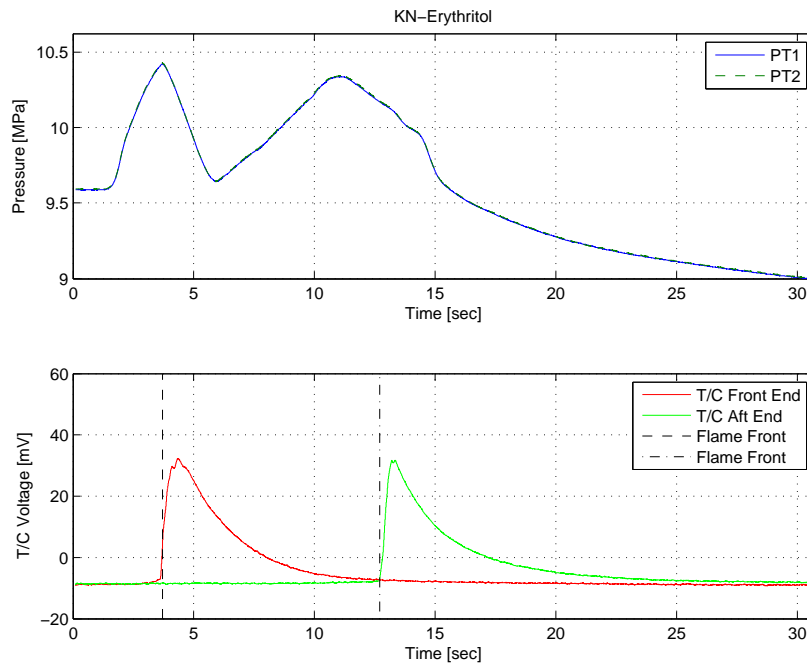


Figure F.25: KN-Erythritol. Set pressure 10 MPa.

KN-Erythritol 65/35 O/F ratio	
Test no.	KNER90barH3001
Batch no.	KNER-003
Relative humidity	45 %
Ambient temperature	24.1 °C
Mean pressure	9.16 MPa
T/C 1 spike start point	3.40 sec
T/C 2 spike start point	11.90 sec
Gauge length	63.48 mm
Burn time	8.50 sec
Burn rate, r	7.47 mm/sec

Table F.26: KN-Erythritol. Set pressure 9 MPa.

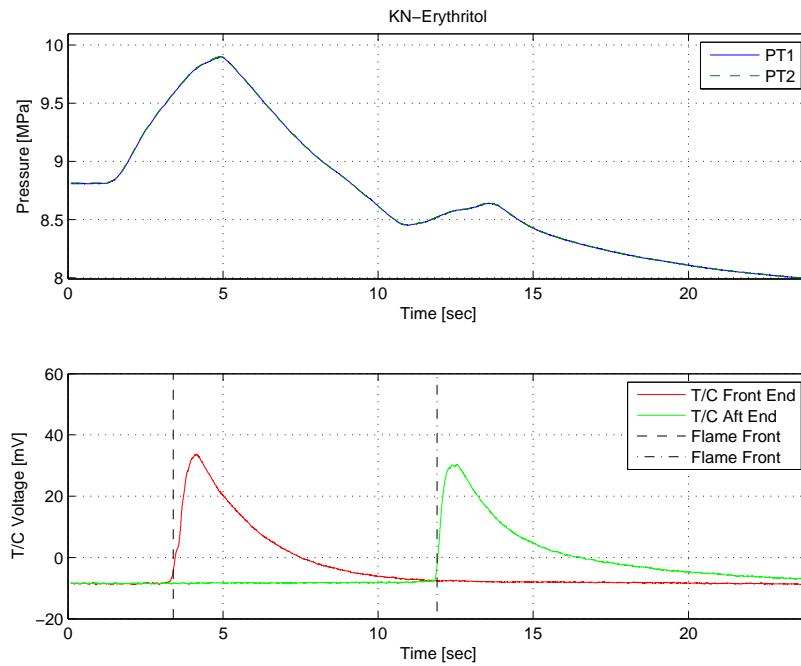


Figure F.26: KN-Erythritol. Set pressure 9 MPa.

KN-Erythritol 65/35 O/F ratio	
Test no.	KNER90barH3002
Batch no.	KNER-003
Relative humidity	45 %
Ambient temperature	24.1 °C
Mean pressure	9.66 MPa
T/C 1 spike start point	4.60 sec
T/C 2 spike start point	13.60 sec
Gauge length	62.48 mm
Burn time	9.00 sec
Burn rate, r	6.94 mm/sec

Table F.27: KN-Erythritol. Set pressure 9 MPa.

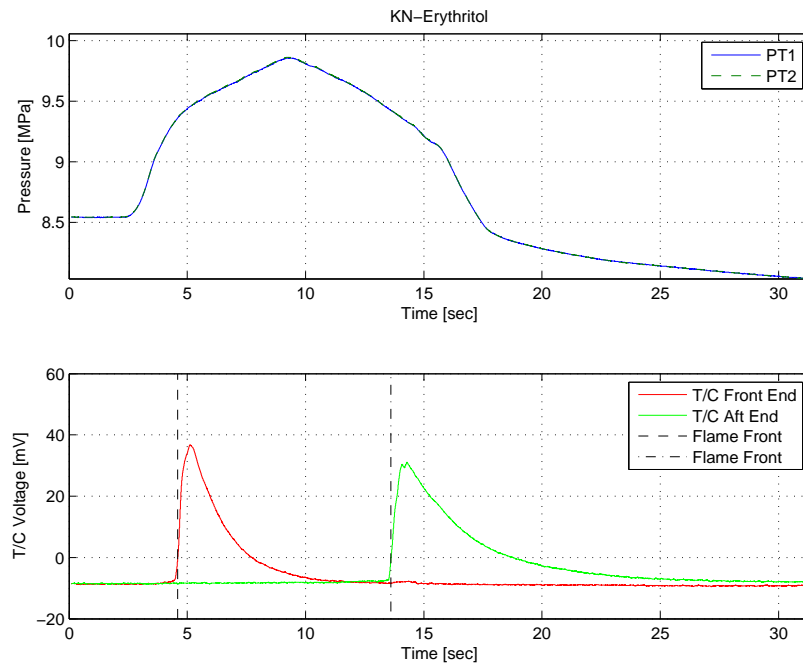


Figure F.27: KN-Erythritol. Set pressure 9 MPa.

KN-Erythritol 65/35 O/F ratio	
Test no.	KNER90barH3003
Batch no.	KNER-003
Relative humidity	46 %
Ambient temperature	23.6 °C
Mean pressure	8.73 MPa
T/C 1 spike start point	4.00 sec
T/C 2 spike start point	13.60 sec
Gauge length	64.56 mm
Burn time	9.60 sec
Burn rate, r	6.73 mm/sec

Table F.28: KN-Erythritol. Set pressure 9 MPa.

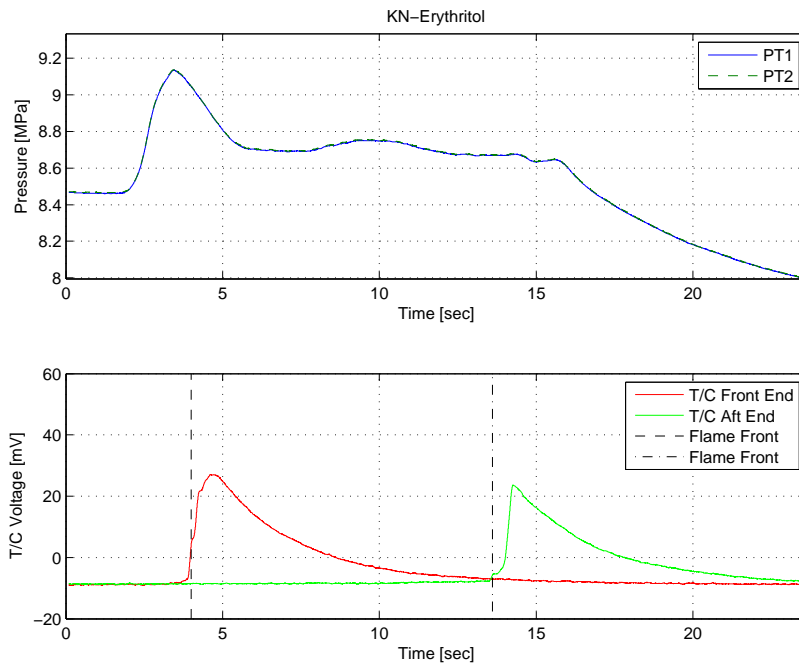


Figure F.28: KN-Erythritol. Set pressure 9 MPa.

KN-Erythritol 65/35 O/F ratio	
Test no.	KNER80barH3001
Batch no.	KNER-003
Relative humidity	46 %
Ambient temperature	23.5 °C
Mean pressure	7.88 MPa
T/C 1 spike start point	3.30 sec
T/C 2 spike start point	13.80 sec
Gauge length	64.94 mm
Burn time	10.50 sec
Burn rate, r	6.19 mm/sec

Table F.29: KN-Erythritol. Set pressure 8 MPa.

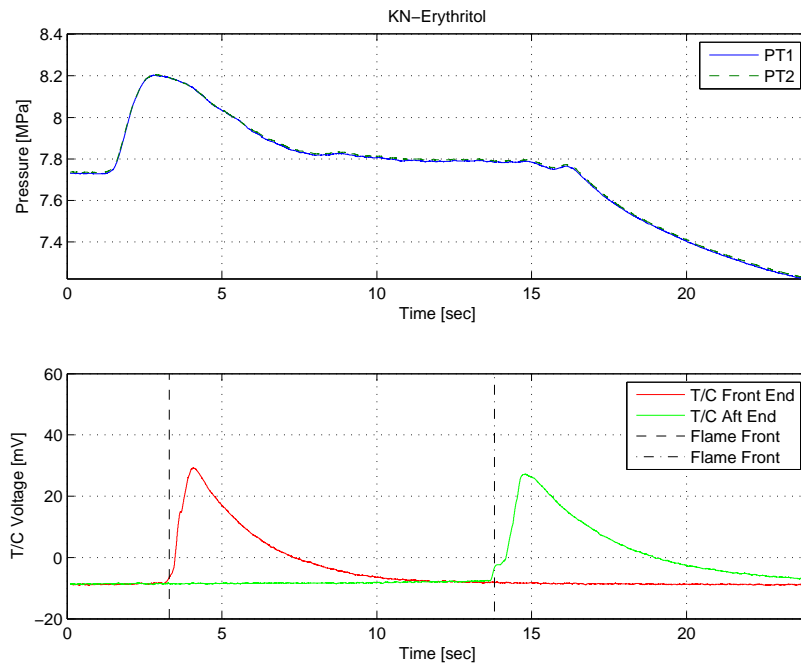


Figure F.29: KN-Erythritol. Set pressure 8 MPa.

KN-Erythritol 65/35 O/F ratio	
Test no.	KNER80barH3002
Batch no.	KNER-003
Relative humidity	46 %
Ambient temperature	23.5 °C
Mean pressure	7.87 MPa
T/C 1 spike start point	3.20 sec
T/C 2 spike start point	12.90 sec
Gauge length	63.71 mm
Burn time	9.70 sec
Burn rate, r	6.57 mm/sec

Table F.30: KN-Erythritol. Set pressure 8 MPa.

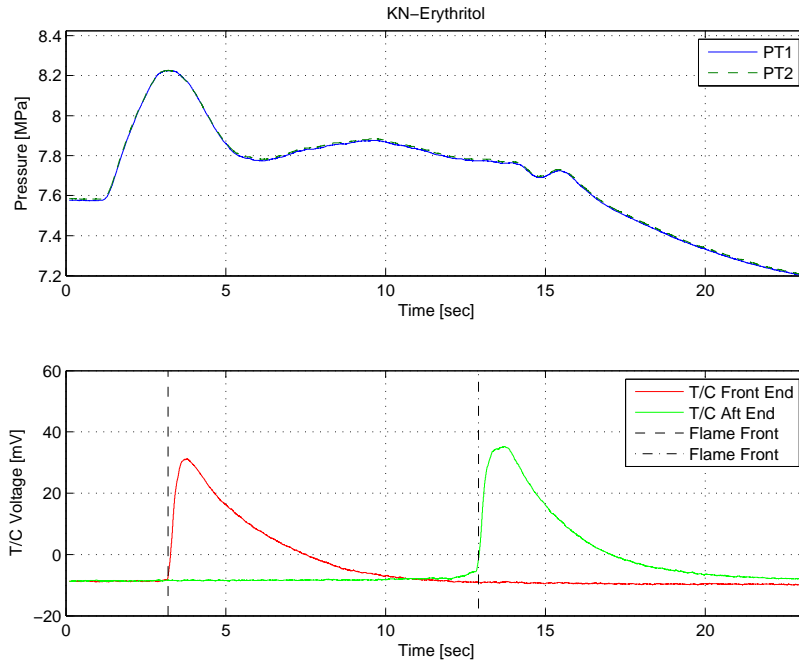


Figure F.30: KN-Erythritol. Set pressure 8 MPa.

KN-Erythritol 65/35 O/F ratio	
Test no.	KNER70barH3001
Batch no.	KNER-001
Relative humidity	41 %
Ambient temperature	25.1 °C
Mean pressure	6.90 MPa
T/C 1 spike start point	4.10 sec
T/C 2 spike start point	15.50 sec
Gauge length	66.34 mm
Burn time	11.40 sec
Burn rate, r	5.82 mm/sec

Table F.31: KN-Erythritol. Set pressure 7 MPa.

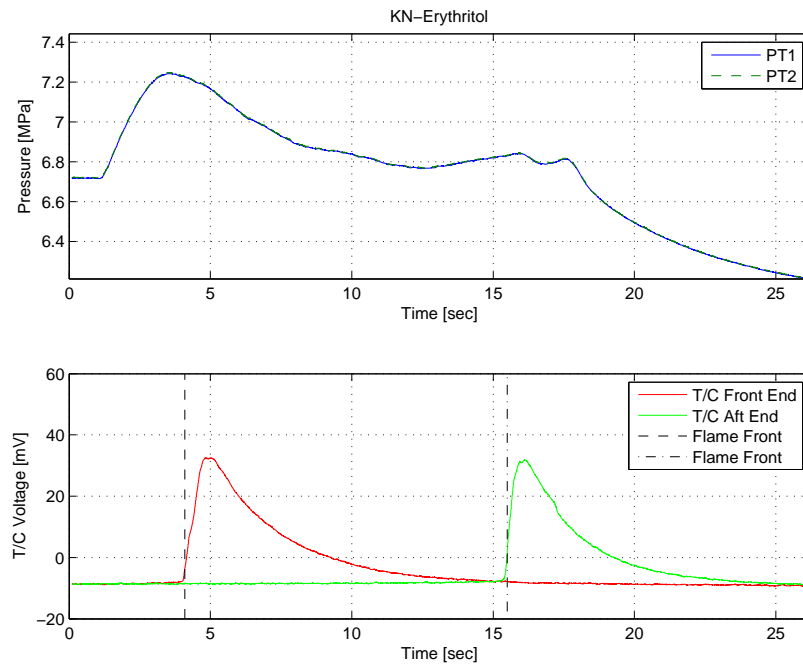


Figure F.31: KN-Erythritol. Set pressure 7 MPa.

KN-Erythritol 65/35 O/F ratio	
Test no.	KNER70barH3002
Batch no.	KNER-001
Relative humidity	41 %
Ambient temperature	25.1 °C
Mean pressure	6.87 MPa
T/C 1 spike start point	3.80 sec
T/C 2 spike start point	14.90 sec
Gauge length	67.50 mm
Burn time	11.10 sec
Burn rate, r	6.08 mm/sec

Table F.32: KN-Erythritol. Set pressure 7 MPa.

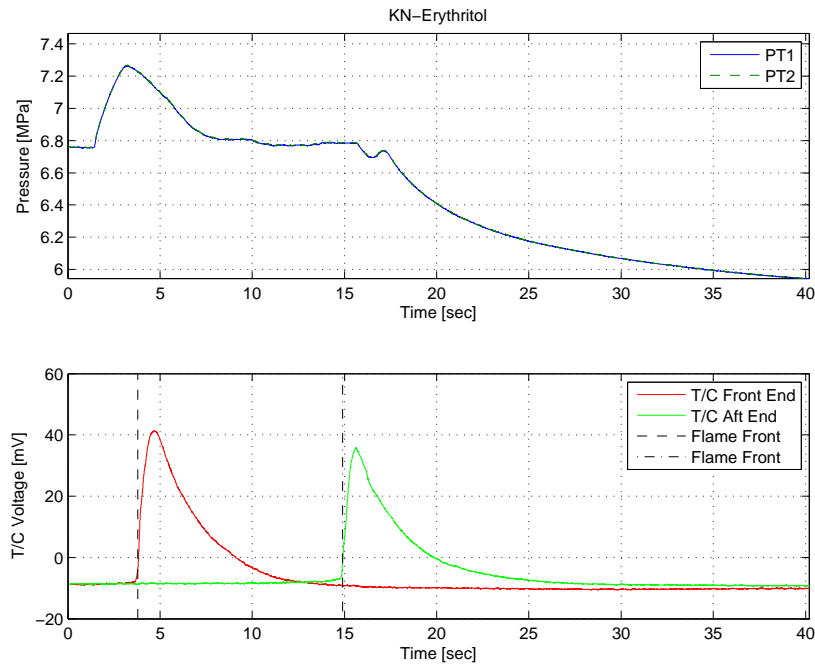


Figure F.32: KN-Erythritol. Set pressure 7 MPa.

KN-Erythritol 65/35 O/F ratio	
Test no.	KNER60barH3001
Batch no.	KNER-001
Relative humidity	41 %
Ambient temperature	25.1 °C
Mean pressure	5.92 MPa
T/C 1 spike start point	4.30 sec
T/C 2 spike start point	15.80 sec
Gauge length	69.27 mm
Burn time	11.50 sec
Burn rate, r	6.02 mm/sec

Table F.33: KN-Erythritol. Set pressure 6 MPa.

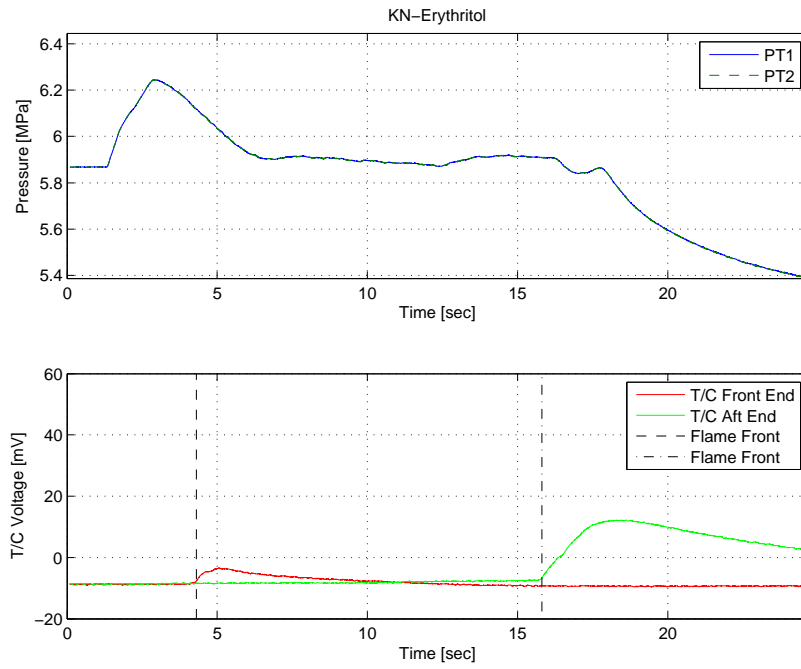


Figure F.33: KN-Erythritol. Set pressure 6 MPa

KN-Erythritol 65/35 O/F ratio	
Test no.	KNER60barH3002
Batch no.	KNER-001
Relative humidity	41 %
Ambient temperature	25.1 °C
Mean pressure	5.88 MPa
T/C 1 spike start point	4.20 sec
T/C 2 spike start point	16.60 sec
Gauge length	68.08 mm
Burn time	12.40 sec
Burn rate, r	5.49 mm/sec

Table F.34: KN-Erythritol. Set pressure 6 MPa.

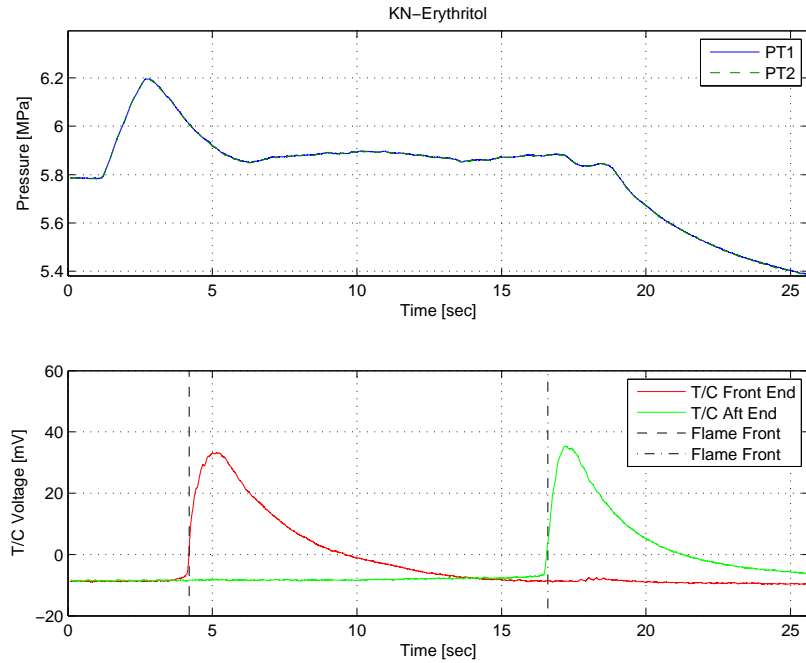


Figure F.34: KN-Erythritol. Set pressure 6 MPa.

KN-Erythritol 65/35 O/F ratio	
Test no.	KNER50barH3001
Batch no.	KNER-003
Relative humidity	44 %
Ambient temperature	23.6 °C
Mean pressure	5.01 MPa
T/C 1 spike start point	3.70 sec
T/C 2 spike start point	15.50 sec
Gauge length	67.52 mm
Burn time	11.80 sec
Burn rate, r	5.72 mm/sec

Table F.35: KN-Erythritol. Set pressure 5 MPa.

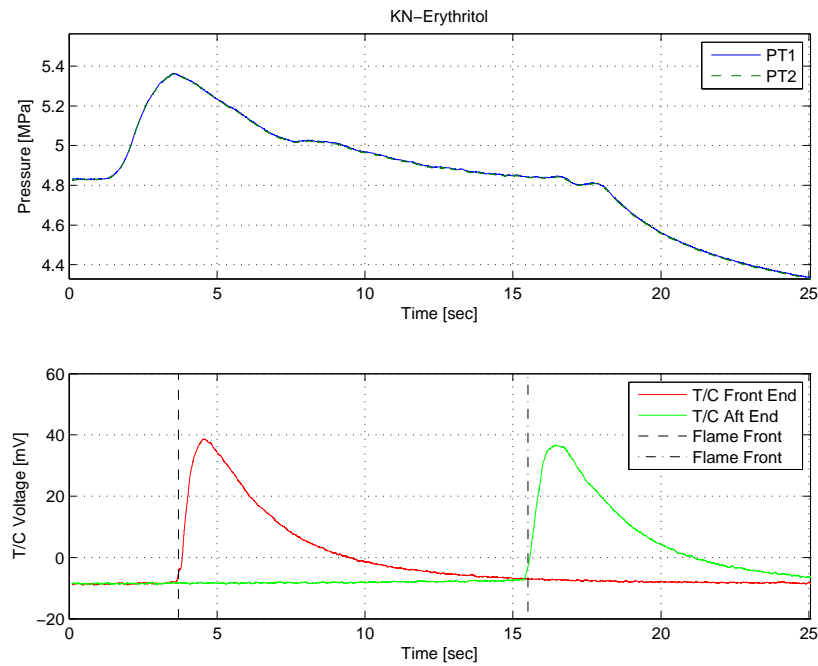


Figure F.35: KN-Erythritol. Set pressure 5 MPa.

KN-Erythritol 65/35 O/F ratio	
Test no.	KNER50barH3002
Batch no.	KNER-003
Relative humidity	44 %
Ambient temperature	23.5 °C
Mean pressure	5.09 MPa
T/C 1 spike start point	4.20 sec
T/C 2 spike start point	15.10 sec
Gauge length	68.34 mm
Burn time	10.90 sec
Burn rate, r	6.27 mm/sec

Table F.36: KN-Erythritol. Set pressure 5 MPa.

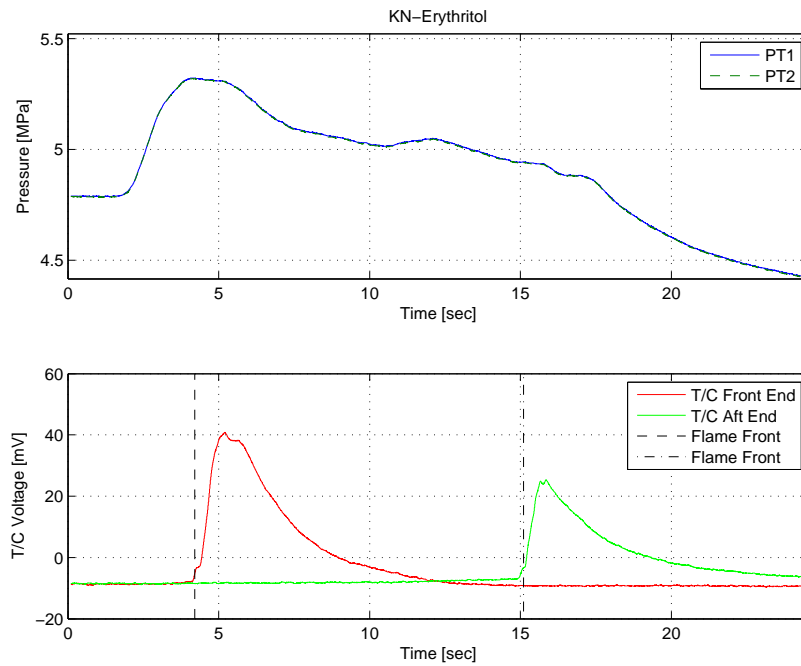


Figure F.36: KN-Erythritol. Set pressure 5 MPa.

KN-Erythritol 65/35 O/F ratio	
Test no.	KNER40barH3001
Batch no.	KNER-003
Relative humidity	44 %
Ambient temperature	23.9 °C
Mean pressure	3.93 MPa
T/C 1 spike start point	4.10 sec
T/C 2 spike start point	17.80 sec
Gauge length	67.76 mm
Burn time	13.7 sec
Burn rate, r	4.95 mm/sec

Table F.37: KN-Erythritol. Set pressure 4 MPa.

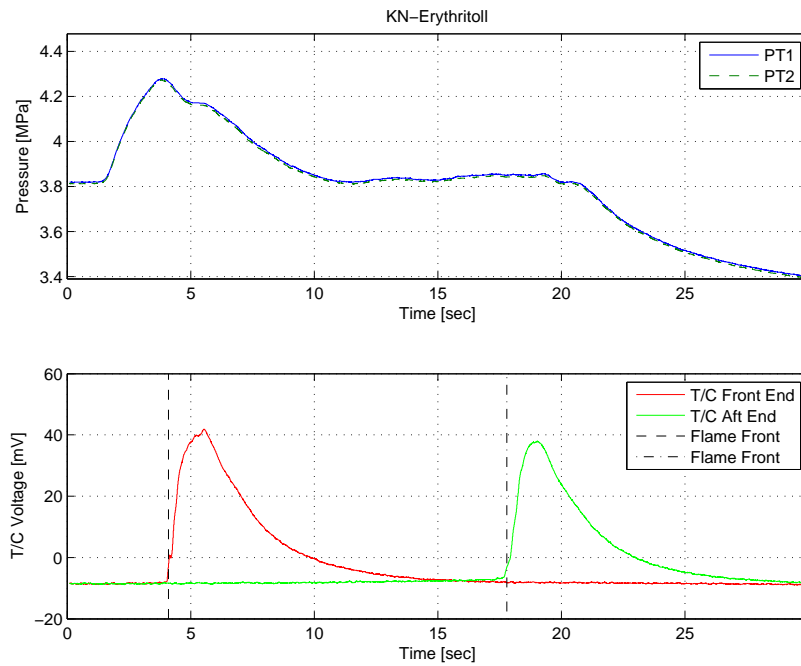


Figure F.37: KN-Erythritol. Set pressure 4 MPa.

KN-Erythritol 65/35 O/F ratio	
Test no.	KNER40barH3002
Batch no.	KNER-003
Relative humidity	44 %
Ambient temperature	23.8 °C
Mean pressure	3.80 MPa
T/C 1 spike start point	4.20 sec
T/C 2 spike start point	17.70 sec
Gauge length	67.80 mm
Burn time	13.50 sec
Burn rate, r	5.02 mm/sec

Table F.38: KN-Erythritol. Set pressure 4 MPa.

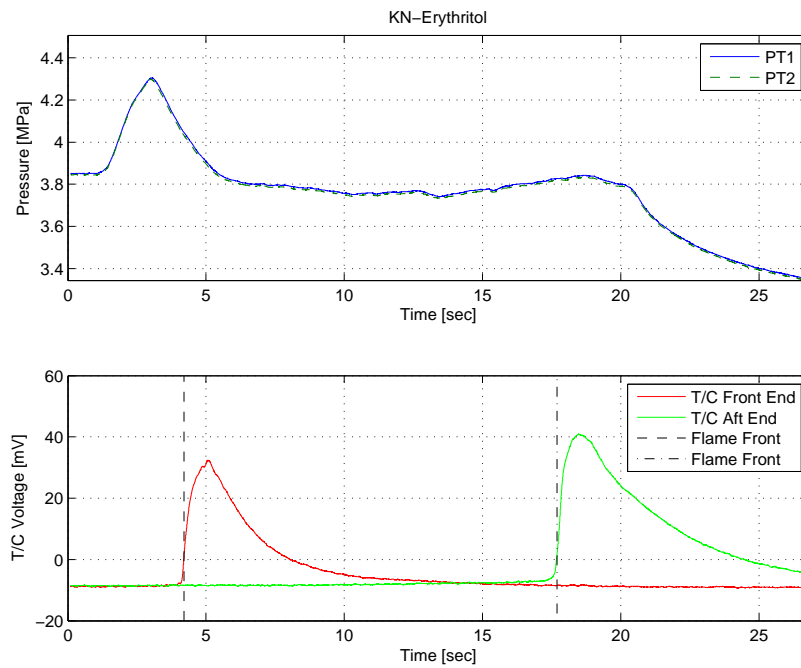


Figure F.38: KN-Erythritol. Set pressure 4 MPa.

KN-Erythritol 65/35 O/F ratio	
Test no.	KNER30barH3001
Batch no.	KNER-303
Relative humidity	43 %
Ambient temperature	24.0 °C
Mean pressure	2.92 MPa
T/C 1 spike start point	5.40 sec
T/C 2 spike start point	21.20 sec
Gauge length	69.30 mm
Burn time	15.80 sec
Burn rate, r	4.39 mm/sec

Table F.39: KN-Erythritol. Set pressure 3 MPa.

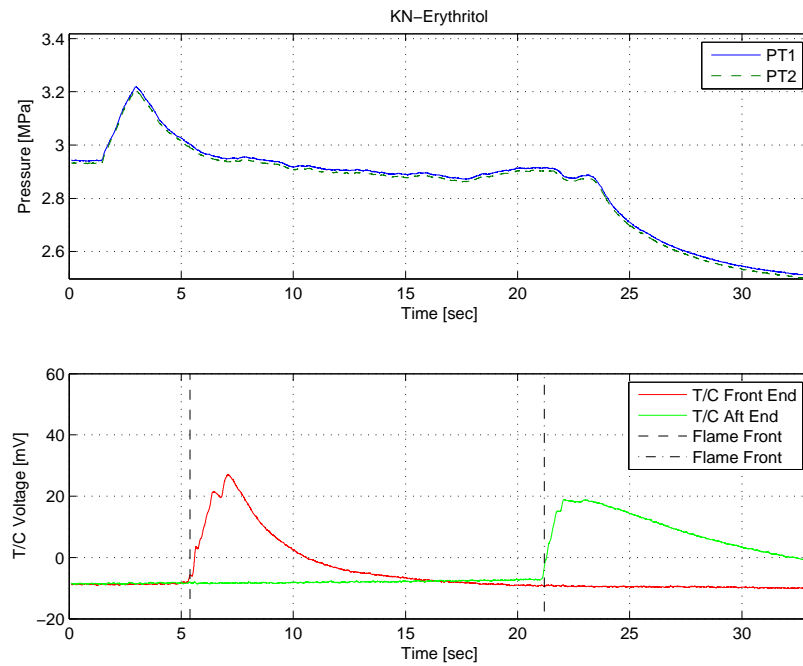


Figure F.39: KN-Erythritol. Set pressure 3 MPa.

KN-Erythritol 65/35 O/F ratio	
Test no.	KNER30barH3002
Batch no.	KNER-003
Relative humidity	43 %
Ambient temperature	24.1 °C
Mean pressure	2.99 MPa
T/C 1 spike start point	5.00 sec
T/C 2 spike start point	21.00 sec
Gauge length	68.40 mm
Burn time	15.60 sec
Burn rate, r	4.38 mm/sec

Table F.40: KN-Erythritol. Set pressure 3 MPa.

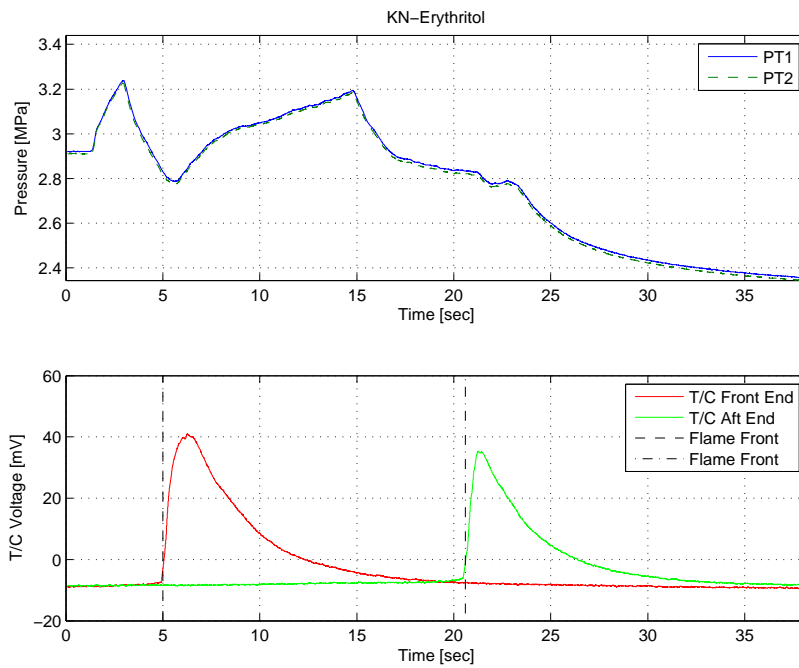


Figure F.40: KN-Erythritol. Set pressure 3 MPa.

Remarks:

- Pressure drop noticed.

KN-Erythritol 65/35 O/F ratio	
Test no.	KNER20barH3001
Batch no.	KNER-001
Relative humidity	48 %
Ambient temperature	25.1 °C
Mean pressure	2.30 MPa
T/C 1 spike start point	6.50 sec
T/C 2 spike start point	24.00 sec
Gauge length	70.59 mm
Burn time	17.50 sec
Burn rate, r	4.04 mm/sec

Table F.41: KN-Erythritol. Set pressure 2 MPa.

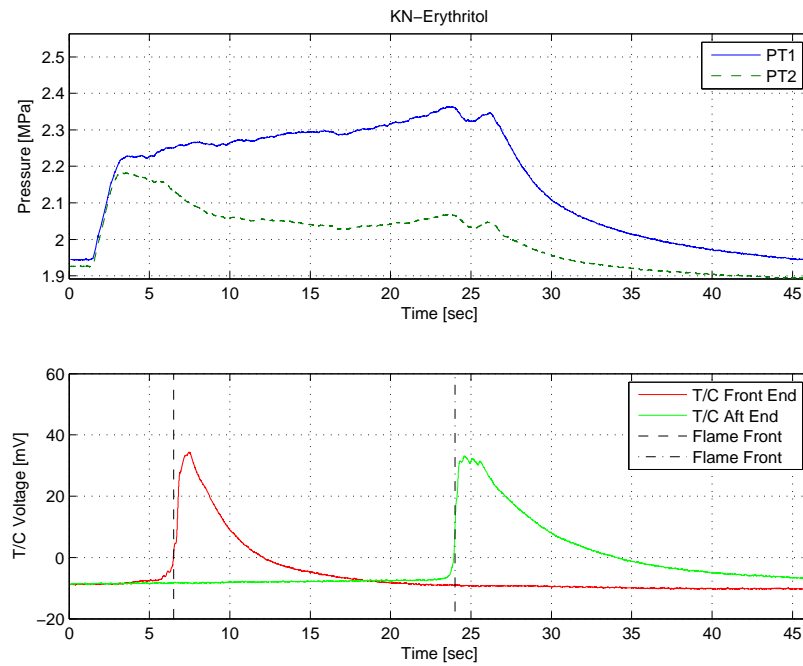


Figure F.41: KN-Erythritol. Set pressure 2 MPa.

KN-Erythritol 65/35 O/F ratio	
Test no.	KNER20barH3002
Batch no.	KNER-001
Relative humidity	47 %
Ambient temperature	25.1 °C
Mean pressure	2.14 MPa
T/C 1 spike start point	5.40 sec
T/C 2 spike start point	23.10 sec
Gauge length	68.65 mm
Burn time	17.70 sec
Burn rate, r	3.88 mm/sec

Table F.42: KN-Erythritol. Set pressure 2 MPa.

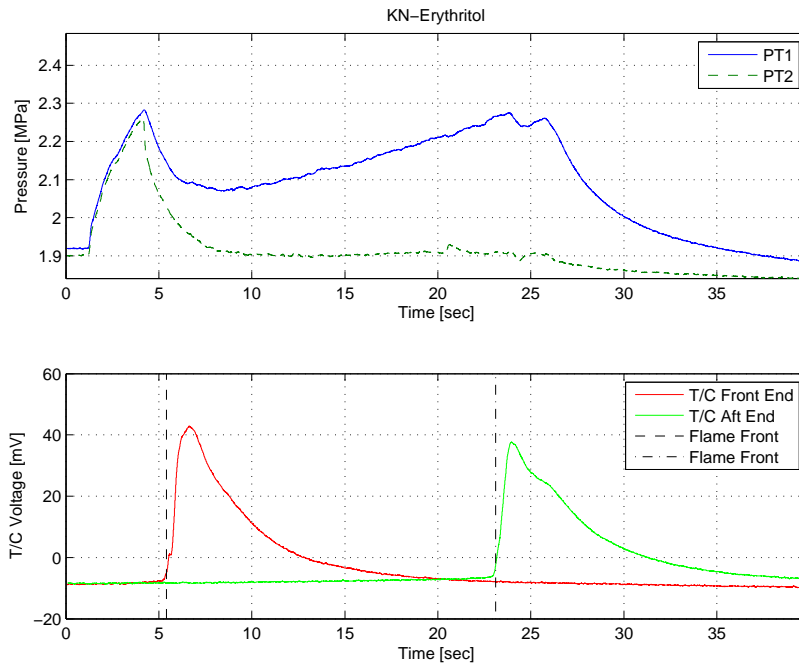


Figure F.42: KN-Erythritol. Set pressure 2 MPa.

KN-Erythritol 65/35 O/F ratio	
Test no.	KNER10barH3001
Batch no.	KNER-004
Relative humidity	43 %
Ambient temperature	26.6 °C
Mean pressure	1.28 MPa
T/C 1 spike start point	8.80 sec
T/C 2 spike start point	30.50 sec
Gauge length	70.25 mm
Burn time	21.70 sec
Burn rate, r	3.24 mm/sec

Table F.43: KN-Erythritol. Set pressure 1 MPa.

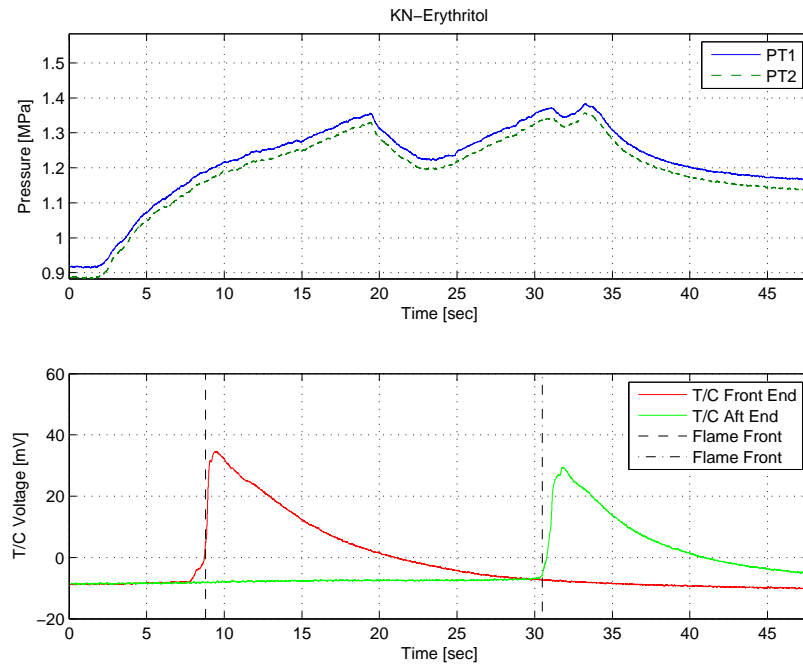


Figure F.43: KN-Erythritol. Set pressure 1 MPa.

KN-Erythritol 65/35 O/F ratio	
Test no.	KNER10barH3002
Batch no.	KNER-004
Relative humidity	41 %
Ambient temperature	26.6 °C
Mean pressure	1.16 MPa
T/C 1 spike start point	7.70 sec
T/C 2 spike start point	30.00 sec
Gauge length	65.05 mm
Burn time	22.30 sec
Burn rate, r	2.92 mm/sec

Table F.44: KN-Erythritol. Set pressure 1 MPa.

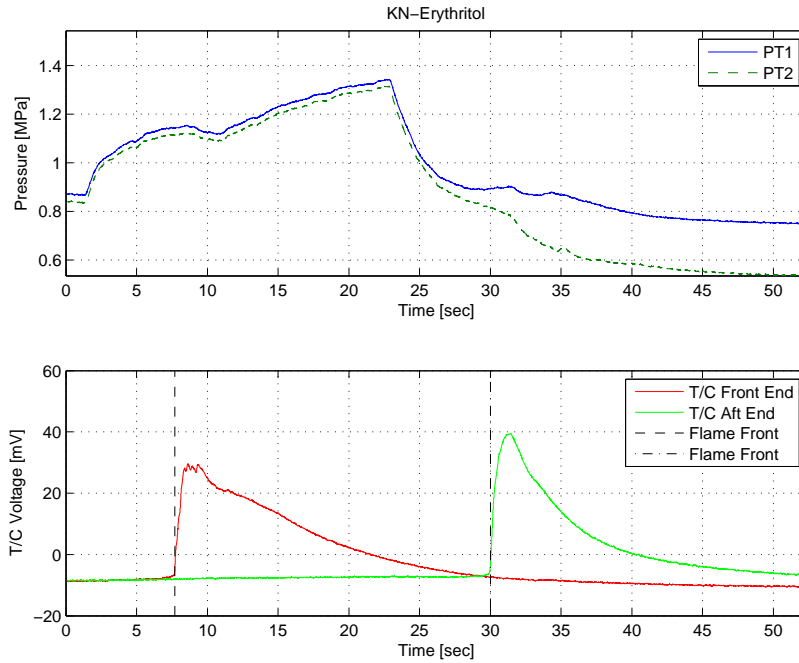


Figure F.44: KN-Erythritol. Set pressure 1 MPa.

KN-Erythritol 65/35 O/F ratio			
Test no.	KNER0barH3001		
Batch no.	KNER-004		
Relative humidity	45	%	
Ambient temperature	27.1	°C	
Mean pressure	0.0	MPa	
T/C 1 spike start point	NA	sec	
T/C 2 spike start point	NA	sec	
Gauge length	69.13	mm	
Burn time	NA	sec	
Burn rate, r	NA	mm/sec	

Table F.45: KN-Erythritol. Atmospheric pressure

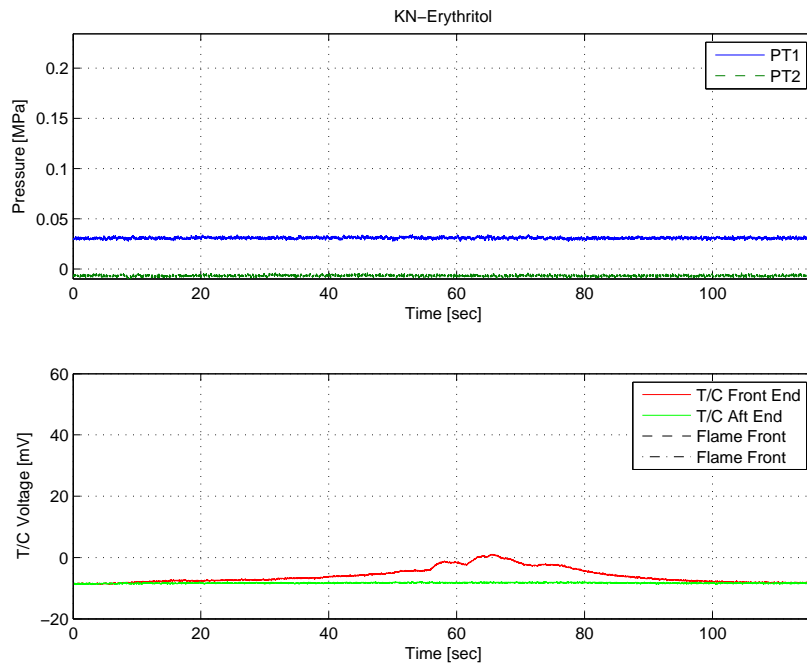


Figure F.45: KN-Erythritol. Atmospheric pressure

Remarks:

- Combustion failure. Propellant strand extinguished.

F.3 Analysis of KN-Mannitol strand burns

KN-Mannitol 65/35 O/F ratio	
Test no.	KNMN100barH3003
Batch no.	KNMN-003
Relative humidity	46 %
Ambient temperature	22.5 °C
Mean pressure	10.19 MPa
T/C 1 spike start point	4.30 sec
T/C 2 spike start point	11.10 sec
Gauge length	60.70 mm
Burn time	6.80 sec
Burn rate, r	8.93 mm/sec

Table F.46: KN-Mannitol. Set pressure 10 MPa.

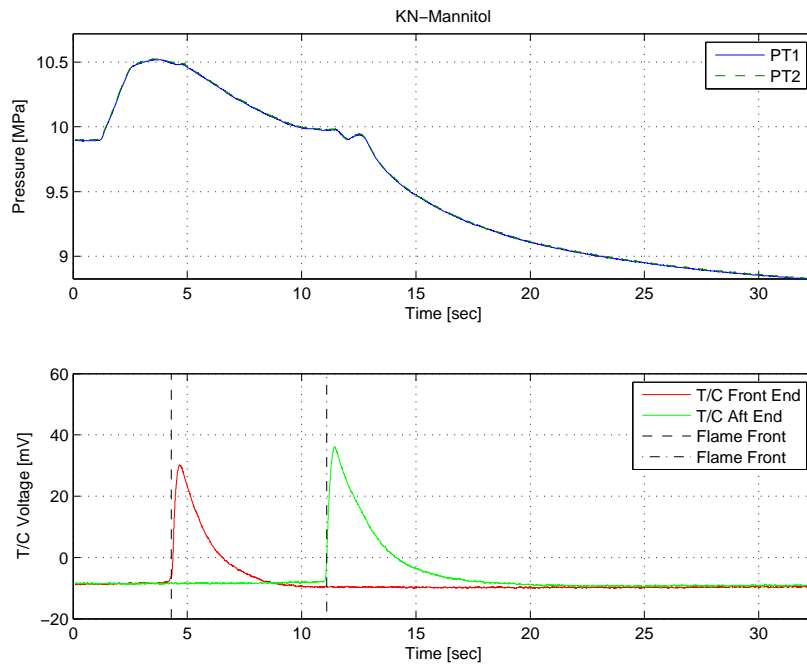


Figure F.46: KN-Mannitol. Set pressure 10 MPa.

KN-Mannitol 65/35 O/F ratio			
Test no.	KNMN100barH3004		
Batch no.	KNMN-003		
Relative humidity	46	%	
Ambient temperature	22.8	°C	
Mean pressure	10.18	MPa	
T/C 1 spike start point	3.60	sec	
T/C 2 spike start point	11.90	sec	
Gauge length	71.40	mm	
Burn time	8.30	sec	
Burn rate, r	8.60	mm/sec	

Table F.47: KN-Mannitol. Set pressure 10 MPa.

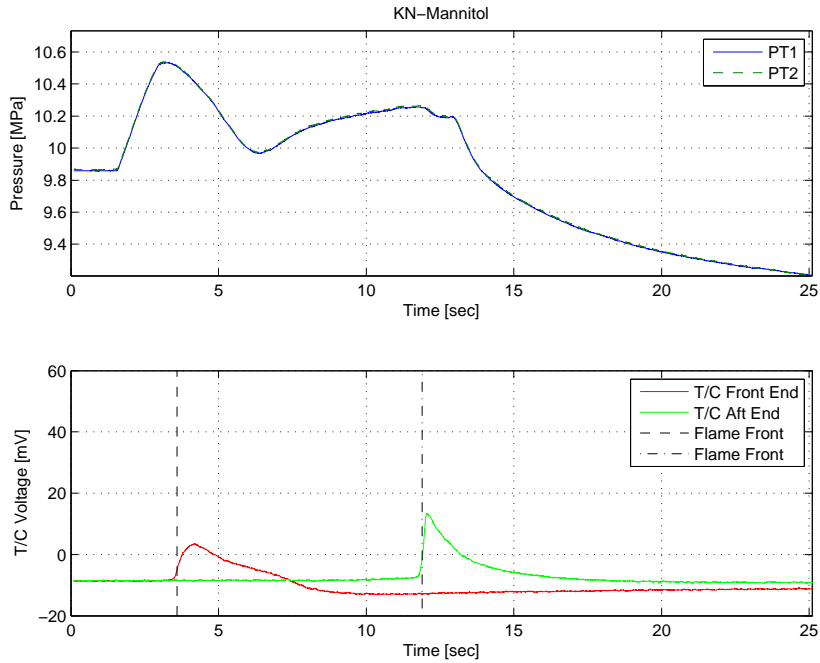


Figure F.47: KN-Mannitol. Set pressure 10 MPa.

KN-Mannitol 65/35 O/F ratio	
Test no.	KNMN90barH3001
Batch no.	KNMN-003
Relative humidity	41 %
Ambient temperature	24.1 °C
Mean pressure	9.01 MPa
T/C 1 spike start point	4.10 sec
T/C 2 spike start point	11.50 sec
Gauge length	65.50 mm
Burn time	7.40 sec
Burn rate, r	8.85 mm/sec

Table F.48: KN-Mannitol. Set pressure 9 MPa.

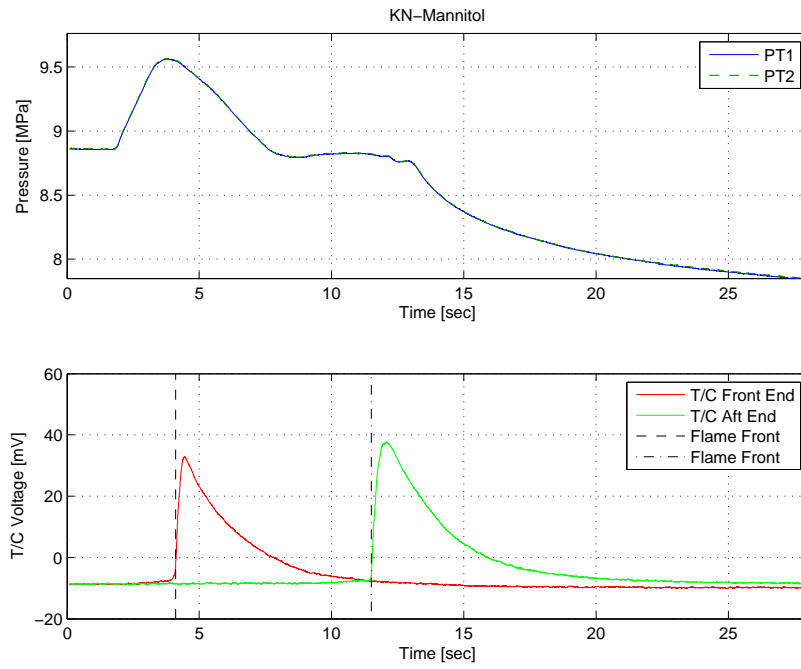


Figure F.48: KN-Mannitol. Set pressure 9 MPa.

KN-Mannitol 65/35 O/F ratio	
Test no.	KNMN90barH3002
Batch no.	KNMN-003
Relative humidity	40 %
Ambient temperature	24.4 °C
Mean pressure	8.98 MPa
T/C 1 spike start point	4.10 sec
T/C 2 spike start point	11.70 sec
Gauge length	65.41 mm
Burn time	7.60 sec
Burn rate, r	8.61 mm/sec

Table F.49: KN-Mannitol. Set pressure 9 MPa.

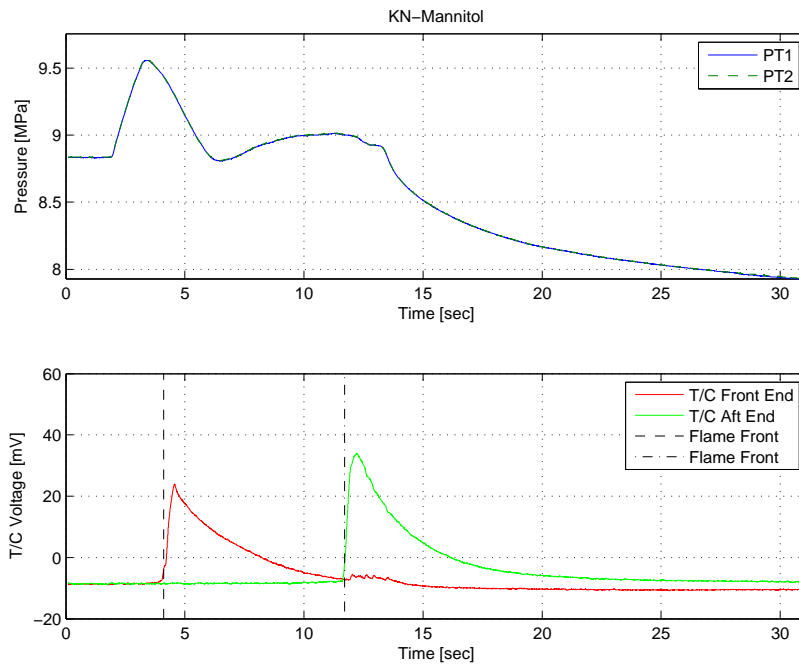


Figure F.49: KN-Mannitol. Set pressure 9 MPa.

KN-Mannitol 65/35 O/F ratio	
Test no.	KNMN80barH3001
Batch no.	KNMN-004
Relative humidity	45 %
Ambient temperature	24.0 °C
Mean pressure	7.74 MPa
T/C 1 spike start point	4.10 sec
T/C 2 spike start point	12.10 sec
Gauge length	63.64 mm
Burn time	8.00 sec
Burn rate, r	7.96 mm/sec

Table F.50: KN-Mannitol. Set pressure 8 MPa.

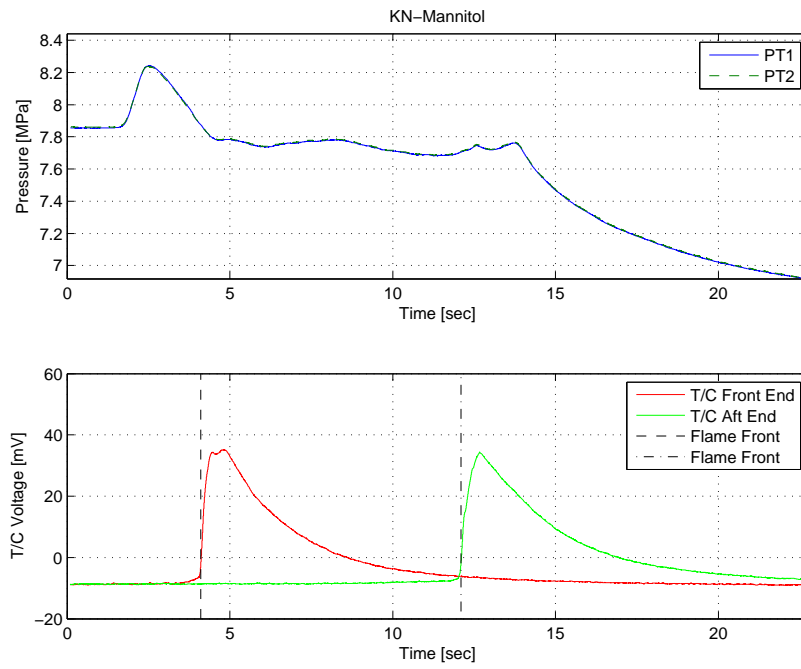


Figure F.50: KN-Mannitol. Set pressure 8 MPa.

KN-Mannitol 65/35 O/F ratio	
Test no.	KNMN80barH3002
Batch no.	KNMN-004
Relative humidity	45 %
Ambient temperature	24.4 °C
Mean pressure	7.78 MPa
T/C 1 spike start point	4.00 sec
T/C 2 spike start point	12.10 sec
Gauge length	66.83 mm
Burn time	8.10 sec
Burn rate, r	8.25 mm/sec

Table F.51: KN-Mannitol. Set pressure 8 MPa.

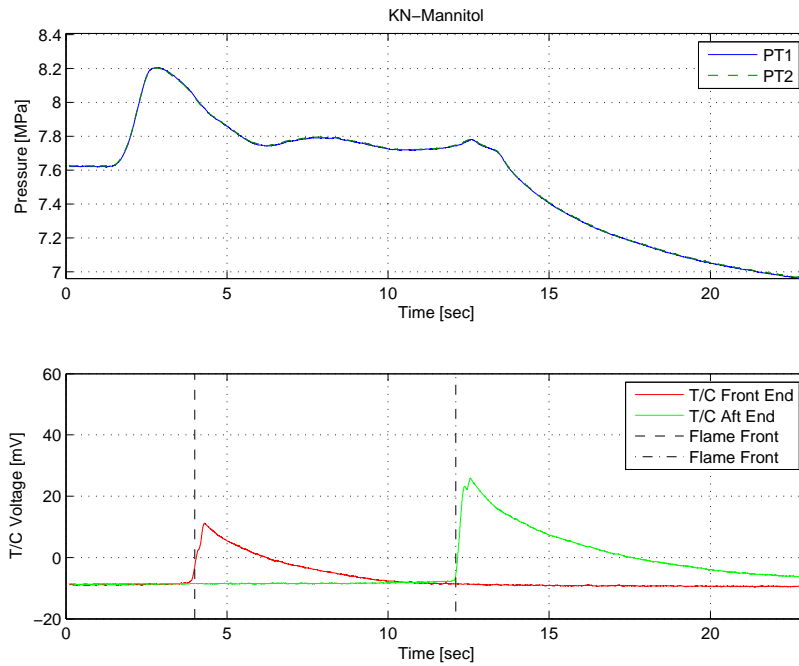


Figure F.51: KN-Mannitol. Set pressure 8 MPa.

KN-Mannitol 65/35 O/F ratio	
Test no.	KNMN70barH3002
Batch no.	KNMN-004
Relative humidity	44 %
Ambient temperature	25.1 °C
Mean pressure	6.91 MPa
T/C 1 spike start point	3.80 sec
T/C 2 spike start point	11.80 sec
Gauge length	64.86 mm
Burn time	8.00 sec
Burn rate, r	8.11 mm/sec

Table F.52: KN-Mannitol. Set pressure 7 MPa.

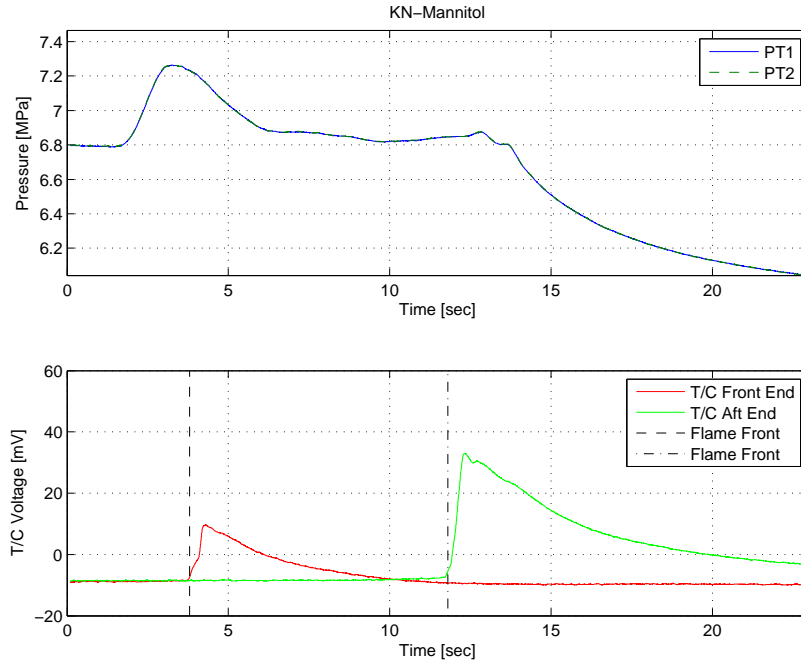


Figure F.52: KN-Mannitol. Set pressure 7 MPa.

KN-Mannitol 65/35 O/F ratio	
Test no.	KNMN70barH3003
Batch no.	KNMN-004
Relative humidity	44 %
Ambient temperature	25.1 °C
Mean pressure	6.88 MPa
T/C 1 spike start point	3.70 sec
T/C 2 spike start point	11.80 sec
Gauge length	67.25 mm
Burn time	8.10 sec
Burn rate, r	8.30 mm/sec

Table F.53: KN-Mannitol. Set pressure 7 MPa.

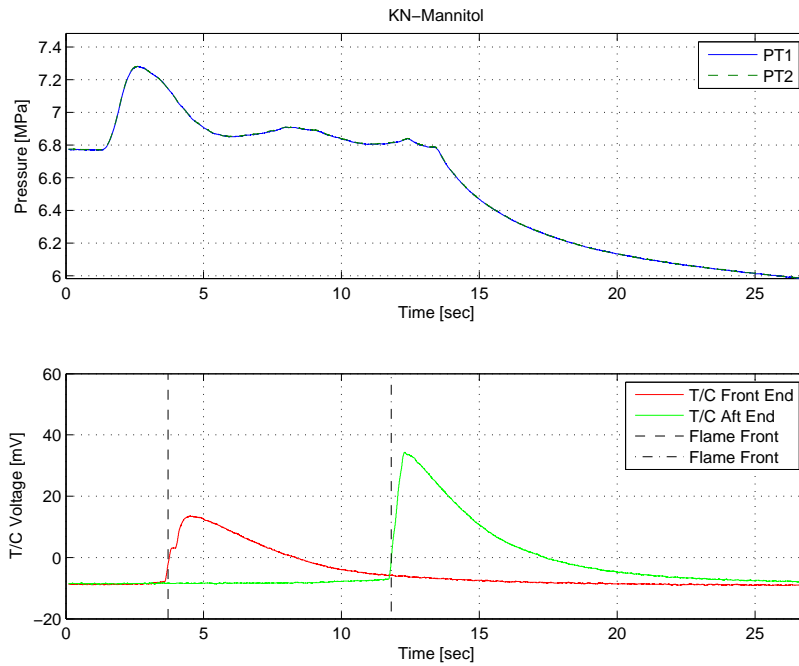


Figure F.53: KN-Mannitol. Set pressure 7 MPa.

KN-Mannitol 65/35 O/F ratio	
Test no.	KNMN70barH3004
Batch no.	KNMN-004
Relative humidity	42 %
Ambient temperature	25.1 °C
Mean pressure	6.88 MPa
T/C 1 spike start point	4.00 sec
T/C 2 spike start point	13.25 sec
Gauge length	68.82 mm
Burn time	9.25 sec
Burn rate, r	7.44 mm/sec

Table F.54: KN-Mannitol. Set pressure 7 MPa.

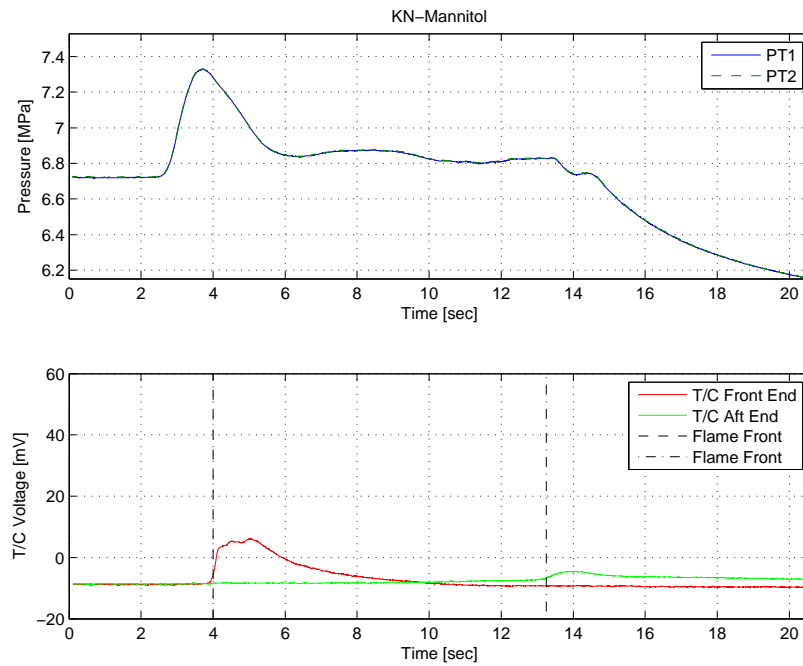


Figure F.54: KN-Mannitol. Set pressure 7 MPa.

KN-Mannitol 65/35 O/F ratio	
Test no.	KNMN60barH3001
Batch no.	KNMN-004
Relative humidity	41 %
Ambient temperature	25.1 °C
Mean pressure	5.97 MPa
T/C 1 spike start point	3.90 sec
T/C 2 spike start point	12.60 sec
Gauge length	66.17 mm
Burn time	8.70 sec
Burn rate, r	7.61 mm/sec

Table F.55: KN-Mannitol. Set pressure 6 MPa.

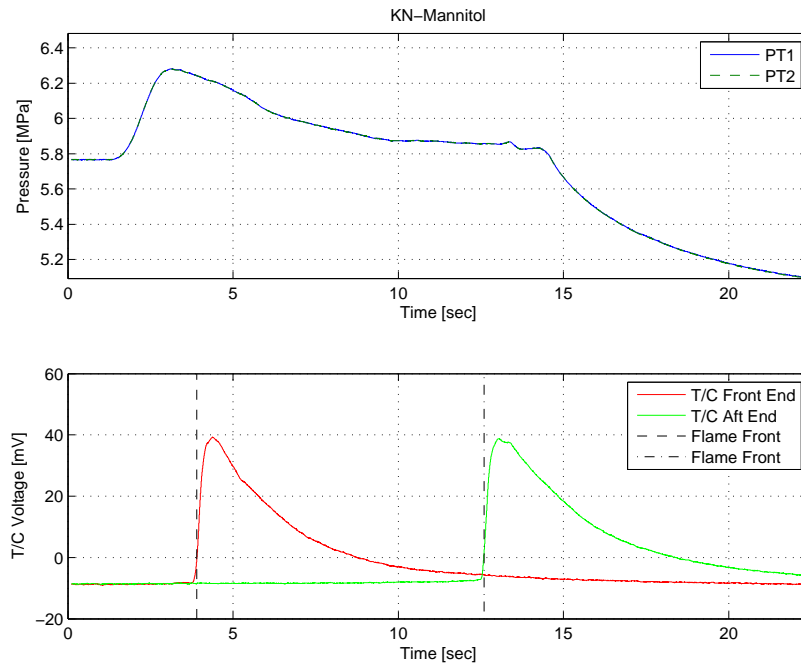


Figure F.55: KN-Mannitol. Set pressure 6 MPa

KN-Mannitol 65/35 O/F ratio	
Test no.	KNMN60barH3002
Batch no.	KNMN-004
Relative humidity	40 %
Ambient temperature	25.1 °C
Mean pressure	5.87 MPa
T/C 1 spike start point	6.80 sec
T/C 2 spike start point	15.70 sec
Gauge length	66.61 mm
Burn time	8.90 sec
Burn rate, r	7.48 mm/sec

Table F.56: KN-Mannitol. Set pressure 6 MPa.

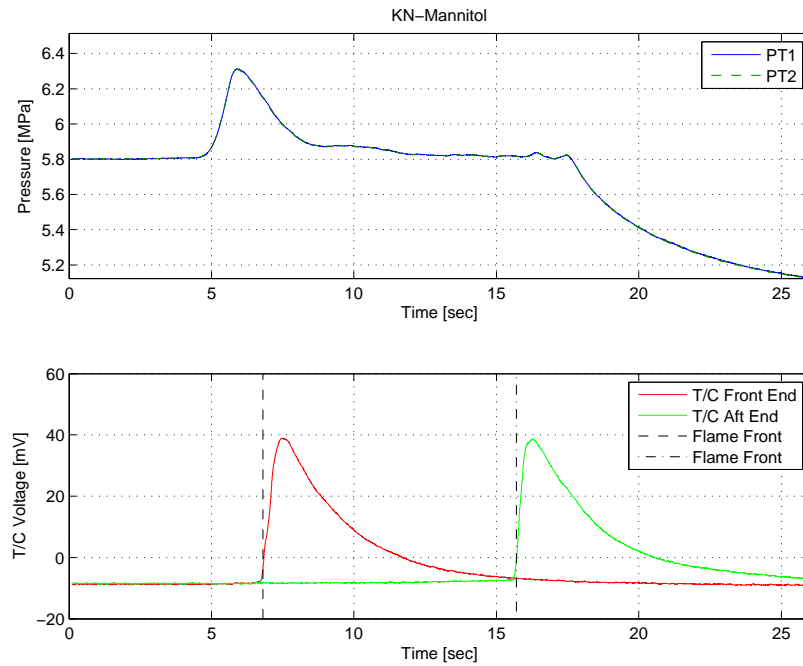


Figure F.56: KN-Mannitol. Set pressure 6 MPa.

KN-Mannitol 65/35 O/F ratio	
Test no.	KNMN50barH3001
Batch no.	KNMN-004
Relative humidity	40 %
Ambient temperature	25.1 °C
Mean pressure	4.77 MPa
T/C 1 spike start point	4.30 sec
T/C 2 spike start point	13.90 sec
Gauge length	64.35 mm
Burn time	9.60 sec
Burn rate, r	6.70 mm/sec

Table F.57: KN-Mannitol. Set pressure 5 MPa.

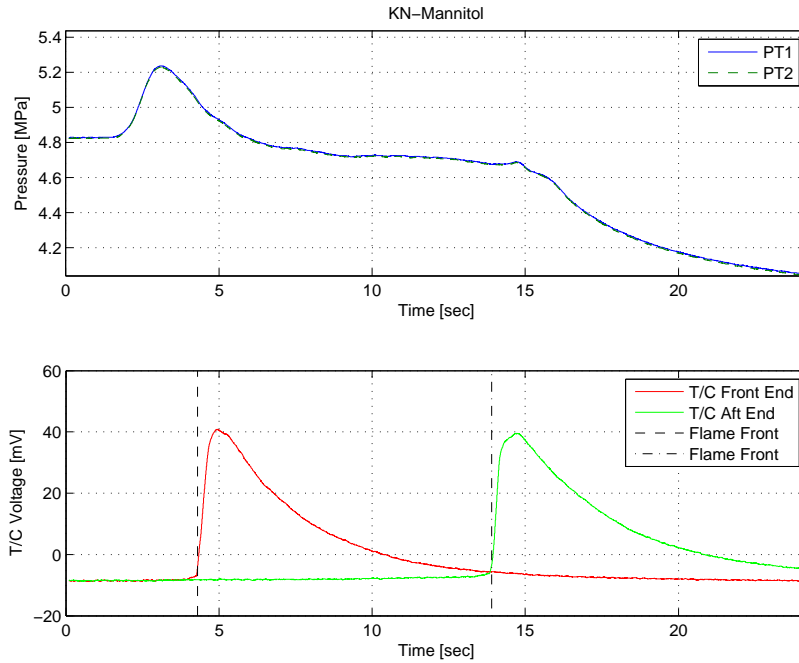


Figure F.57: KN-Mannitol. Set pressure 5 MPa.

KN-Mannitol 65/35 O/F ratio	
Test no.	KNMN50barH3002
Batch no.	KNMN-004
Relative humidity	40 %
Ambient temperature	25.1 °C
Mean pressure	4.69 MPa
T/C 1 spike start point	3.90 sec
T/C 2 spike start point	12.90 sec
Gauge length	66.01 mm
Burn time	9.00 sec
Burn rate, r	7.33 mm/sec

Table F.58: KN-Mannitol. Set pressure 5 MPa.

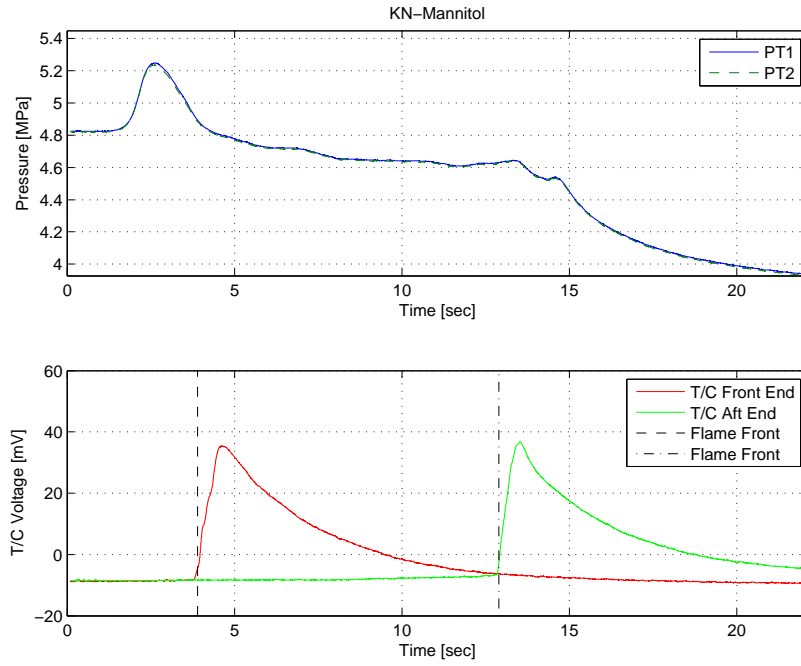


Figure F.58: KN-Mannitol. Set pressure 5 MPa.

KN-Mannitol 65/35 O/F ratio	
Test no.	KNMN40barH3001
Batch no.	KNMN-002
Relative humidity	42 %
Ambient temperature	24.0 °C
Mean pressure	3.85 MPa
T/C 1 spike start point	3.40 sec
T/C 2 spike start point	13.30 sec
Gauge length	69.26 mm
Burn time	9.90 sec
Burn rate, r	7.00 mm/sec

Table F.59: KN-Mannitol. Set pressure 4 MPa.

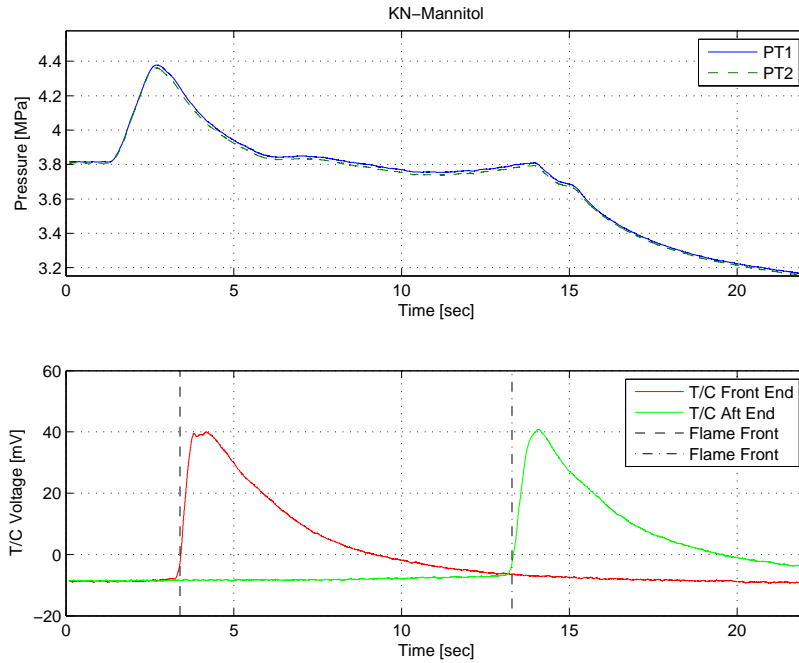


Figure F.59: KN-Mannitol. Set pressure 4 MPa.

KN-Mannitol 65/35 O/F ratio	
Test no.	KNMN40barH3002
Batch no.	KNMN-003
Relative humidity	42 %
Ambient temperature	23.8 °C
Mean pressure	3.83 MPa
T/C 1 spike start point	3.70 sec
T/C 2 spike start point	14.30 sec
Gauge length	66.63 mm
Burn time	10.60 sec
Burn rate, r	6.29 mm/sec

Table F.60: KN-Mannitol. Set pressure 4 MPa.

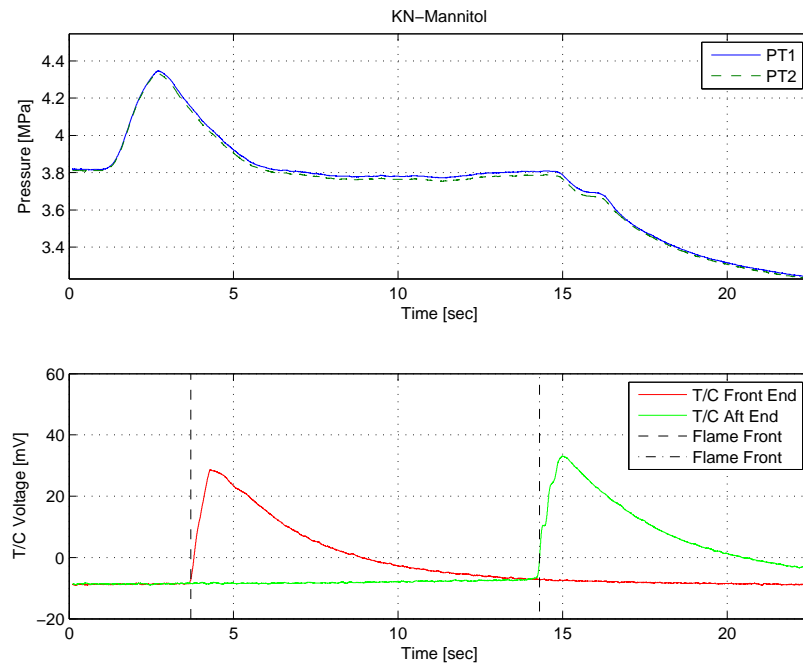


Figure F.60: KN-Mannitol. Set pressure 4 MPa.

KN-Mannitol 65/35 O/F ratio	
Test no.	KNMN30barH3001
Batch no.	KNMN-302
Relative humidity	43 %
Ambient temperature	24.2 °C
Mean pressure	2.92 MPa
T/C 1 spike start point	4.20 sec
T/C 2 spike start point	15.50 sec
Gauge length	68.56 mm
Burn time	11.30 sec
Burn rate, r	6.07 mm/sec

Table F.61: KN-Mannitol. Set pressure 3 MPa.

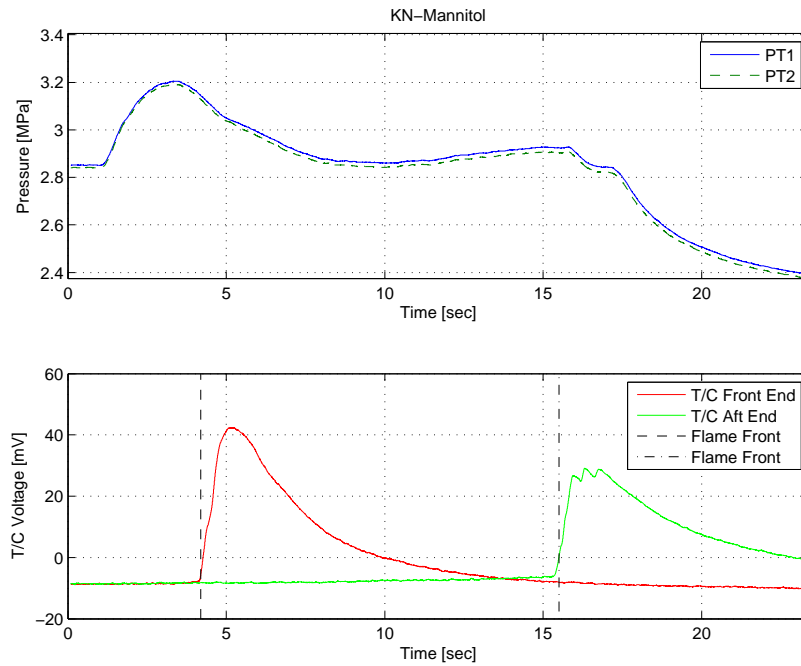


Figure F.61: KN-Mannitol. Set pressure 3 MPa.

KN-Mannitol 65/35 O/F ratio	
Test no.	KNMN30barH3002
Batch no.	KNMN-002
Relative humidity	43 %
Ambient temperature	24.2 °C
Mean pressure	2.99 MPa
T/C 1 spike start point	4.40 sec
T/C 2 spike start point	15.40 sec
Gauge length	67.35 mm
Burn time	11.00 sec
Burn rate, r	6.12 mm/sec

Table F.62: KN-Mannitol. Set pressure 3 MPa.

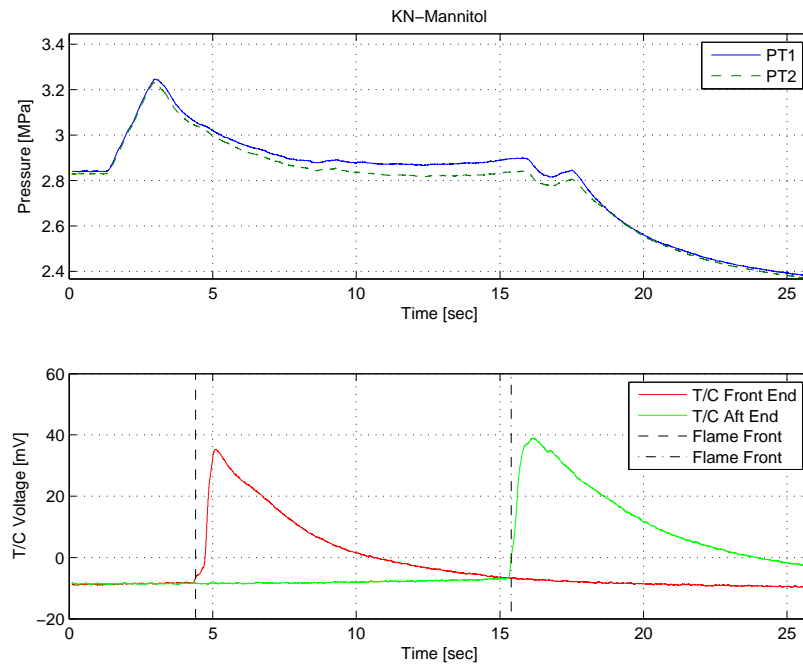


Figure F.62: KN-Mannitol. Set pressure 3 MPa.

KN-Mannitol 65/35 O/F ratio	
Test no.	KNMN20barH3001
Batch no.	KNMN-002
Relative humidity	45 %
Ambient temperature	25.3 °C
Mean pressure	1.93 MPa
T/C 1 spike start point	4.60 sec
T/C 2 spike start point	17.10 sec
Gauge length	69.47 mm
Burn time	12.50 sec
Burn rate, r	5.56 mm/sec

Table F.63: KN-Mannitol. Set pressure 2 MPa.

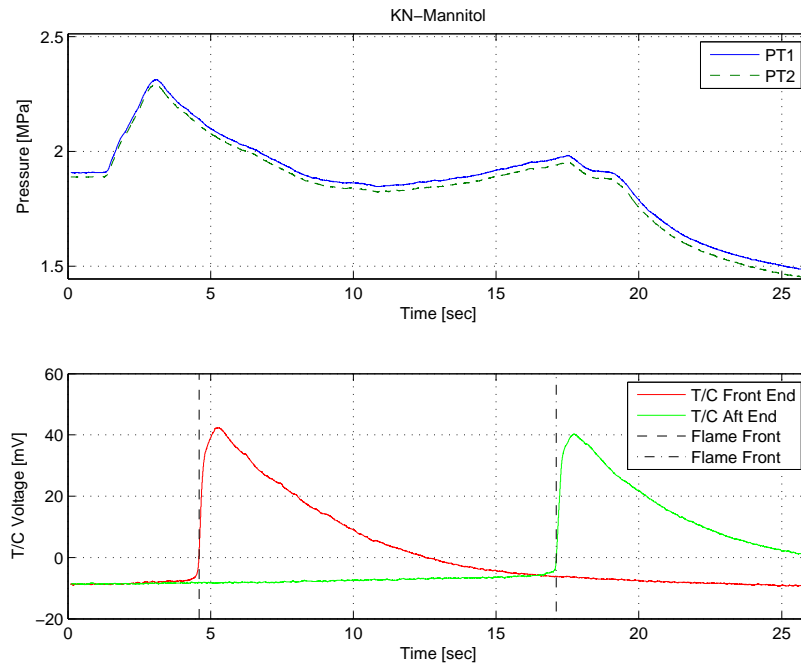


Figure F.63: KN-Mannitol. Set pressure 2 MPa.

KN-Mannitol 65/35 O/F ratio	
Test no.	KNMN20barH3002
Batch no.	KNMN-002
Relative humidity	45 %
Ambient temperature	25.4 °C
Mean pressure	2.07 MPa
T/C 1 spike start point	5.00 sec
T/C 2 spike start point	17.15 sec
Gauge length	70.15 mm
Burn time	12.15 sec
Burn rate, r	5.77 mm/sec

Table F.64: KN-Mannitol. Set pressure 2 MPa.

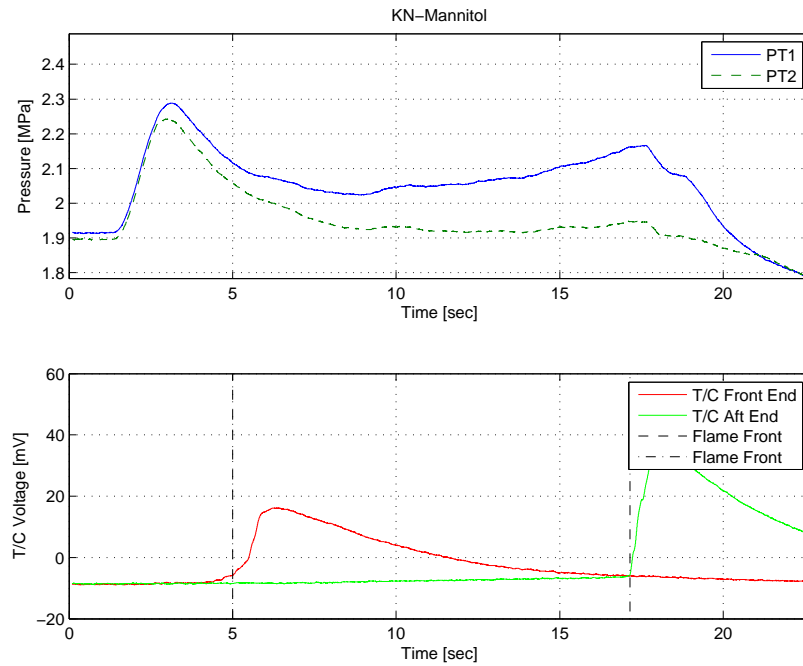


Figure F.64: KN-Mannitol. Set pressure 2 MPa.

KN-Mannitol 65/35 O/F ratio	
Test no.	KNMN10barH3001
Batch no.	KNMN-005
Relative humidity	54 %
Ambient temperature	28.0 °C
Mean pressure	0.99 MPa
T/C 1 spike start point	4.90 sec
T/C 2 spike start point	17.40 sec
Gauge length	68.36 mm
Burn time	12.50 sec
Burn rate, r	5.47 mm/sec

Table F.65: KN-Mannitol. Set pressure 1 MPa.

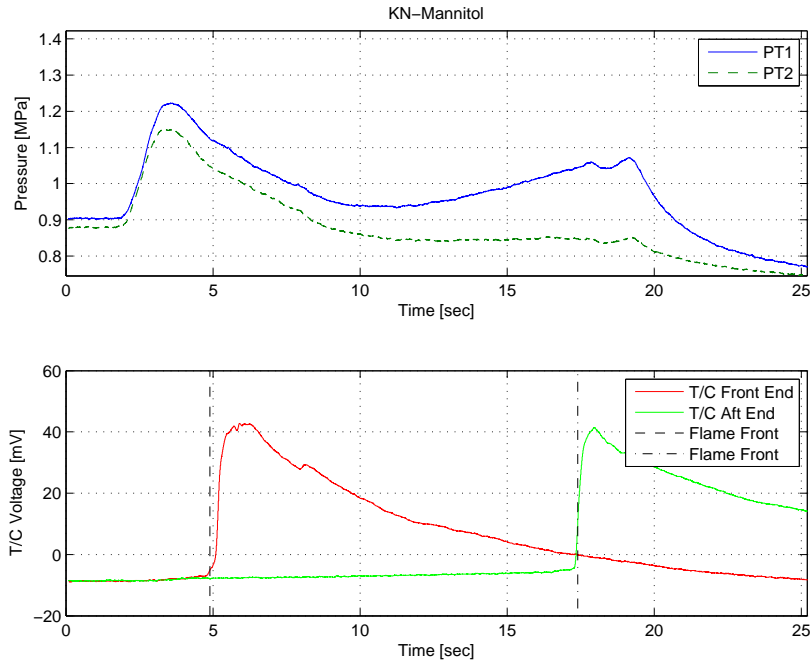


Figure F.65: KN-Mannitol. Set pressure 1 MPa.

KN-Mannitol 65/35 O/F ratio	
Test no.	KNMN10barH3002
Batch no.	KNMN-005
Relative humidity	56 %
Ambient temperature	26.2 °C
Mean pressure	1.41 MPa
T/C 1 spike start point	4.20 sec
T/C 2 spike start point	16.60 sec
Gauge length	68.95 mm
Burn time	12.40 sec
Burn rate, r	5.56 mm/sec

Table F.66: KN-Mannitol. Set pressure 1 MPa.

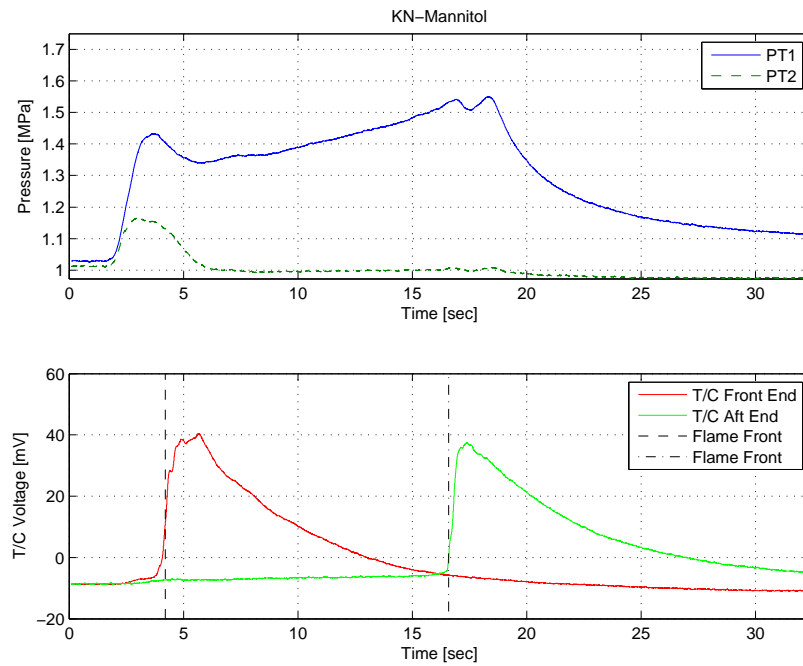


Figure F.66: KN-Mannitol. Set pressure 1 MPa.

KN-Mannitol 65/35 O/F ratio	
Test no.	KNMN10barH3003
Batch no.	KNMN-005
Relative humidity	51 %
Ambient temperature	27.0 °C
Mean pressure	0.94 MPa
T/C 1 spike start point	5.40 sec
T/C 2 spike start point	17.40 sec
Gauge length	67.11 mm
Burn time	12.00 sec
Burn rate, r	5.60 mm/sec

Table F.67: KN-Mannitol. Set pressure 1 MPa.

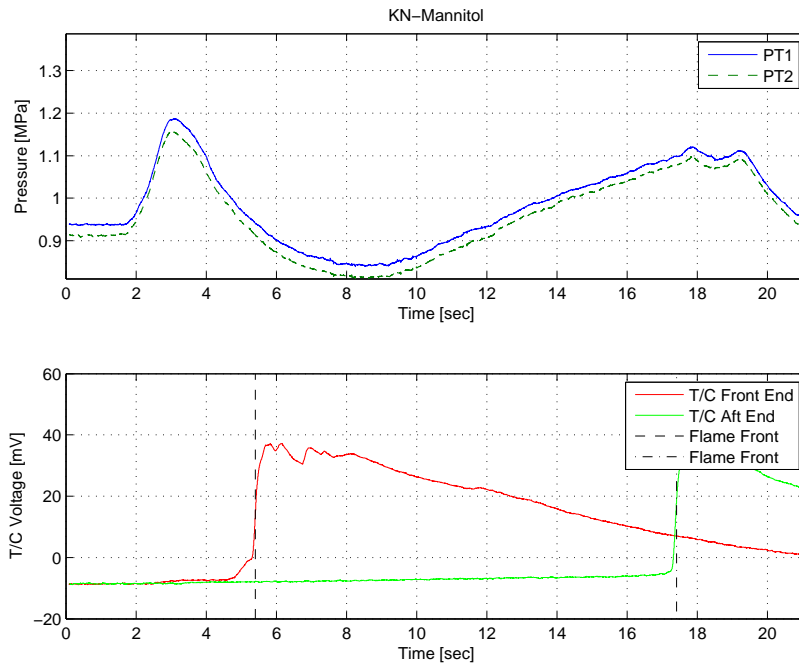


Figure F.67: KN-Mannitol. Set pressure 1 MPa.

KN-Mannitol 65/35 O/F ratio	
Test no.	KNMN10barH3004
Batch no.	KNMN-005
Relative humidity	48 %
Ambient temperature	26.7 °C
Mean pressure	0.87 MPa
T/C 1 spike start point	5.70 sec
T/C 2 spike start point	18.30 sec
Gauge length	70.76 mm
Burn time	12.60 sec
Burn rate, r	5.62 mm/sec

Table F.68: KN-Mannitol. Set pressure 1 MPa.

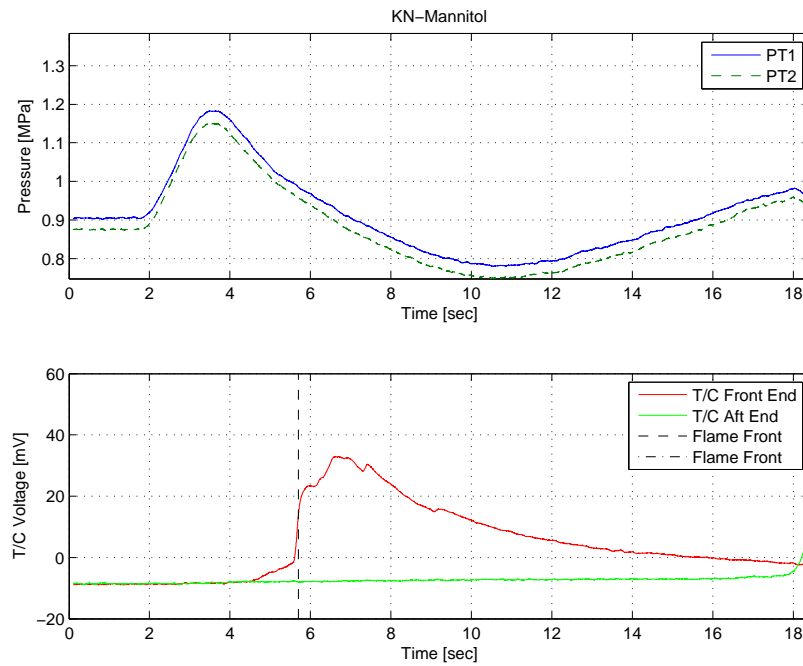


Figure F.68: KN-Mannitol. Set pressure 1 MPa.

KN-Mannitol 65/35 O/F ratio	
Test no.	KNMN0barH3001
Batch no.	KNMN-005
Relative humidity	47 %
Ambient temperature	27.0 °C
Mean pressure	0.0 MPa
T/C 1 spike start point	11.8 sec
T/C 2 spike start point	33.00 sec
Gauge length	67.33 mm
Burn time	21.2 sec
Burn rate, r	3.18 mm/sec

Table F.69: KN-Mannitol. Atmospheric pressure

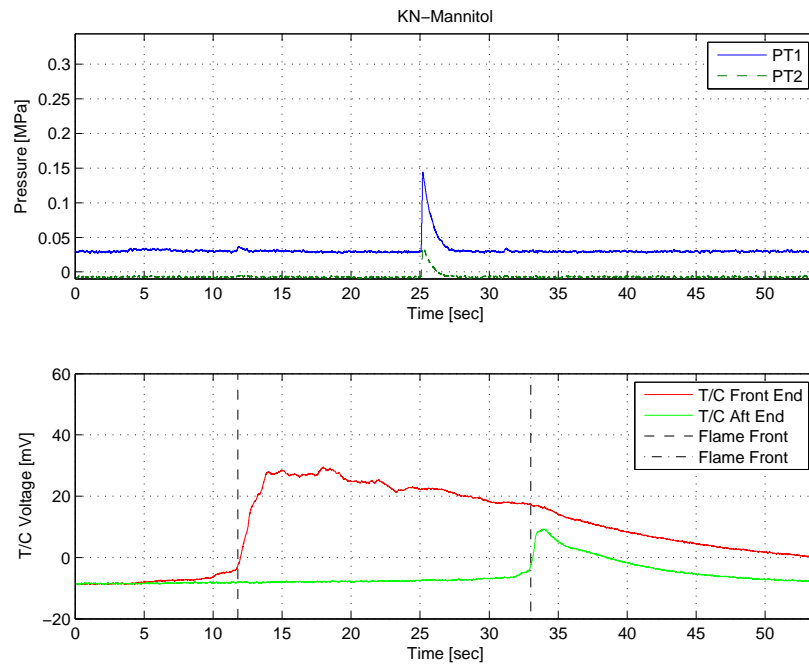


Figure F.69: KN-Mannitol. Atmospheric pressure

www.kemi.dtu.dk

Department of Chemistry
Kemitorvet
Technical University of Denmark
Building 207
DK-2800 Kgs. Lyngby
Denmark
Tel: (+45) 45 25 24 19
Fax: (+45) 45 93 31 36
4
Email: isc@kemi.dtu.dk